PRDW
Consulting Port and Coastal Engineers

SAMPLING AND ANALYSIS OF THE CITY OF CAPE TOWN'S MARINE OUTFALLS AT GREEN POINT, CAMPS BAY AND HOUT BAY

Final Report on Dispersion Model Calibration and Results for Green Point

REV.00

01 October 2020

Lwandle Technologies (Pty) Ltd / City of Cape Town
Cape Town, South Africa

lwandle
MARINE ENVIRONMENTAL SERVICES

CITY OF CAPE TOWN
ISIXEKO SASEKAPA
STAD KAAPSTAD

PRDW
Consulting Port and Coastal Engineers

SAMPLING AND ANALYSIS OF THE CITY OF CAPE TOWN'S MARINE OUTFALLS AT GREEN POINT, CAMPS BAY AND HOUT BAY

Final Report on Dispersion Model Calibration and Results for Green Point

S2101-RP-CE-007-R0

01 October 2020

REV.	TYPE	DATE	EXECUTED	CHECK	APPROVED	CLIENT	DESCRIPTION / COMMENTS
0	C	1/10/2020	SAL/SK/SRW	SAL	[signature]		For approval

TYPE OF ISSUE: (A) Draft (B) To bid or proposal (C) For Approval (D) Approved (E) Void

Lwandle Technologies (Pty) Ltd / City of Cape Town
Cape Town, South Africa

lwandle MARINE ENVIRONMENTAL SERVICES

CITY OF CAPE TOWN
ISIXEKO SASEKAPA
STAD KAAPSTAD

PRDW South Africa (Pty) Ltd
5th Floor, Nedbank Building, Clock Tower Precinct, Victoria & Alfred Waterfront
Cape Town, South Africa | PO Box 50023, Waterfront 8002
T: +27 21 418 3830
www.prdw.com

Cape Town, South Africa
Santiago, Chile
Perth, Australia
Seattle, USA
Vitoria, Brazil
Panama City, Panama

PRDW
Consulting Port and Coastal Engineers

TABLE OF CONTENTS	Page N°

TABLES — Page N°

FIGURES — Page N°

1. INTRODUCTION

1.1 Background

The City of Cape Town (CoCT) has appointed Lwandle Technologies (Pty) Ltd (Lwandle) to perform sampling and analysis of the CoCT's marine outfalls at Green Point, Camps Bay and Hout Bay for a period of three years (Tender 124s/2018/19). Lwandle has sub-contracted PRDW South Africa (Pty) Ltd (PRDW) to undertake dispersion modelling for the three outfalls.

1.2 Scope and objectives

The scope of the study is to perform three-dimensional (3D) hydrodynamic and dispersion modelling for the Green Point, Camps Bay and Hout Bay marine outfalls operated by the CoCT. The objectives of the study are as follows:

- Provide imagery and animations of the effluent plume suitable for overlaying the sampling and monitoring data.
- Determine the dilutions achieved in the near- and far-field for a conservative tracer representing dissolved constituents in the effluent such as nutrients, etc. This includes a probabilistic description of the Zone of Initial Dilution (ZID) taking into account variations in metocean conditions and variations in effluent flows and/or concentrations.
- Determine the probability of the plume reaching the shoreline and the concentrations of faecal indicator bacteria (enterococci and E.coli) during these events.
- Determine the concentrations of discharged Total Suspended Solids (TSS) in the water column and where these are deposited on the seabed. This is a proxy for the fate of pollutants that adsorb to solid particles, e.g. heavy metals.

The model results can be used by Lwandle and the CoCT for the following:

- To refine the location of sampling stations (for the second year of sampling).
- To assist interpretation of sampling results, e.g. are observed concentrations likely to have had an outfall as a source or rather stormwater or other sources.
- To predict the metocean conditions when plume may impact bathers.
- To define the size of the ZID and the spatial extent of particulate deposition zones for the Coastal Waters Discharge Permit application.
- To determine how many dilutions are achieved by the time that the plume reaches desalination plant intakes.

Future applications of the models (outside the scope of this study) could include:

- Testing the impacts of changes in flow rates, effluent density (e.g. due to the addition of desalination brine) and effluent concentrations on the dispersion.
- Test options to improve the dispersion, e.g. modifications to the diffuser, lengthening of the pipeline, etc.
- The models could also be operationalised to provide forecasts of bathing water quality as is done in Denmark, Sweden and New Zealand, e.g. http://newkbh.badevand.dk. The concept is that if the effluent from the outfalls is impacting bathing beaches a limited number of times per year, then a forecast may be the best short- to medium-term approach to mitigate the associated risk.

1.3 Deliverables

PRDW's deliverables comprise the following:

- Deliverable 1: Progress report on model setup (one report for each outfall).
- Deliverable 2: Progress report on model calibration for winter/spring (August – September 2019) and preliminary results (one report for each outfall).
- Deliverable 3: Final report including model calibration for summer/autumn (February – April 2020) and final results (one report for each outfall).

This report is Deliverable 3 for Green Point. This report supersedes the Deliverable 1 and Deliverable 2 reports as all the information contained in the previous reports is included and updated here. Similar reports are provided for Camps Bay and Hout Bay.

1.4 Report structure

Section 2 presents a description of the models, which include a hydrodynamic, water quality, suspended sediment and wave model. Section 3 presents the discharge characterisation which describes the diffuser, effluent and water quality guidelines. Section 4 describes the model setup which includes the mesh, bathymetry, wind, boundary conditions and model settings. The model calibration is presented in Section 5 followed by the model results in Section 6. Conclusions and recommendations are provided in Sections 7 and Section 8.

2. DESCRIPTION OF THE MODELS

2.1 Overview

The modelling was undertaken using the MIKE modelling system developed by DHI in Denmark. PRDW has 15 years of experience in applying these models. The MIKE system is widely used by international engineering consultancies and includes a number of features that makes it an appropriate model for this application, including:

- A dynamic coupling of a near-field jet model within the 3D far-field hydrodynamic model;
- the ability to dynamically couple different sub-models to include all the relevant physical and biogeochemical processes; and
- the use of a flexible mesh which allows refinement around the outfalls.

The following four sub-models were used:

- Hydrodynamic model: 3D hydrodynamics including tides, wind, waves, temperature and salinity. Includes an integral jet model for each port with dynamic two-way coupling of near- and far-field dispersion.
- Water quality model: 3D water quality model for modelling the far-field advection-dispersion of:
  - a conservative tracer representing dissolved constituents in the effluent such as nutrients, etc
  - Faecal indicator bacteria (E.coli and enterococci) including die-off.
- Suspended sediment model: 3D model for modelling Total Suspended Solids (TSS) - advection-dispersion-settling-deposition-resuspension based on combined current-wave bed stresses.
- Spectral wave model: wave refraction and breaking to generate wave-driven currents and wave bed stresses.

2.2 Hydrodynamic model

2.2.1 General description

The three-dimensional MIKE 3 Flow Flexible Mesh Model was used for the hydrodynamic modelling. The application of the model is described in the User Manual (DHI, 2020a), while full details of the physical processes being simulated and the numerical solution techniques are described in the Scientific Documentation (DHI, 2020b).

The model is based on the numerical solution of the three-dimensional incompressible Reynolds averaged Navier-Stokes equations invoking the assumptions of Boussinesq and of hydrostatic pressure. The model consists of the continuity, momentum, temperature, salinity and density equations and is closed by a k-ε vertical turbulence closure scheme. Horizontal eddy viscosity is modelled with the Smagorinsky formulation.

The time integration of the shallow water equations and the transport equations is performed using a semi-implicit scheme, where the horizontal terms are treated explicitly and the vertical terms are treated implicitly. In the vertical direction a structured mesh, based on a sigma-coordinate transformation is used, while the geometrical flexibility of the unstructured flexible mesh comprising triangles or quadrangles is utilised in the horizontal plane.

The model includes the following physical phenomena:

- Currents due to tides;
- Currents due to wind stress on the water surface;
- Currents due to density gradients;
- Currents due to waves; the second order stresses due to breaking of short period waves are included using the radiation stresses computed in the Spectral Wave model;
- Coriolis forcing;
- Bottom friction;
- Flooding and drying;
- Sources and sinks including dynamic near and far-field coupling; and
- Heat exchange.

2.2.2 Near and far-field coupling

An important feature of the model is a dynamic coupling of a near-field jet model and the 3D far-field hydrodynamic model. The near-field solution based on the integral jet model equations by Jirka (2004). Entrainment into the jet is using Distributed Entrainment Sink Approach by Choi and Lee (2007). At the end of the near-field the diluted discharge is released into far-field model as a source, as shown in Figure 2-1.

In order to determine, when the jet/plume becomes passive and thus a part of the ambient flow, a number of stop criteria are invoked:

1. If the jet reaches the water surface.
2. If the jet reaches the bottom.
3. If the jet momentum is smaller than or close to the ambient flow induced momentum.
4. If the jet dies out in the stagnant conditions.
5. If the jet experiences buoyancy reversal twice.
6. If the trajectory of the jet exceeds a maximum travel distance as specified by the user.
7. If the jet exhibits strong curvature, such as going into strong opposing ambient flow.
8. If the jet reaches a domain boundary (open or close).
9. If the jet reaches dried cells.

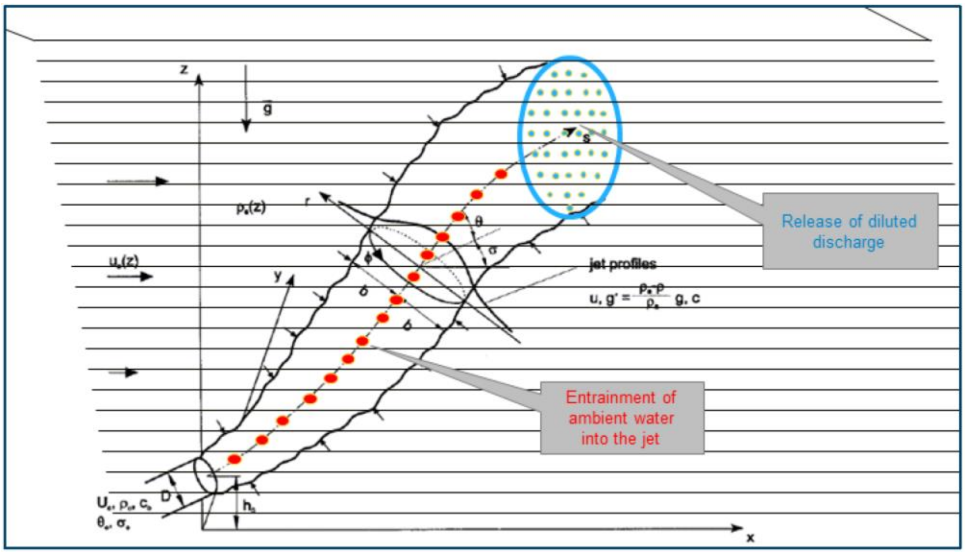

Figure 2-1: Dynamic coupling of near-field and far-field models: entrainment sinks along the plume trajectory and distributed sources at the release location.

2.3 Water quality model

2.3.1 General description

The MIKE 3 ECO Lab Model was used to simulate the far-field dispersion of a conservative tracer and faecal indicator bacteria (E.coli and enterococci). The application of the model is described in the User Manual (DHI, 2020c) while full details of the physical processes being simulated and the numerical solution techniques are described in the Scientific Documentation (DHI, 2020d).

The model simulates the transport and fate of constituents in three dimensions based on advection-dispersion and non-conservative processes. The model can be used to describe chemical, biological, ecological processes and interactions between state variables and also the physical process of sedimentation of components can be described. The hydrodynamics (water levels, currents, temperature, salinity, vertical, dispersion, horizontal dispersion and release location at the end of the near-field) are obtained via an online coupling to the MIKE 3 Flow Flexible Mesh Model and the same three-dimensional grid is used.

An ECO Lab template is used to describe the non-conservative processes relevant for each specific constituent. Since the conservative tracer undergoes advection and dispersion only without any non-conservative processes, no template is required for the conservative tracer. Faecal indicator bacteria (E.coli and enterococci) require an ECO Lab template to simulate die-off, as described below.

2.3.2 Bacteria die-off

In addition to physical dilution, the concentration of faecal indicator bacteria (E.coli and enterococci) reduces due to die-off. The die-off was implemented in the ECO Lab model as described below.

2.3.2.1 ECO Lab model equations

First order decay:

Bacterial decay can be described by the first order decay function for a duration t:

$$C(t) = C_0 e^{-k \cdot t} \quad (1)$$

where

- C = bacteria concentration [CFU.100ml^{-1}]
- C_0 = initial bacteria concentration ($t = 0$) [CFU.100ml^{-1}]
- t = time [hours]
- k = linear decay rate [hours^{-1}]

The decay rate is often expressed as T_{90}: the time needed for the 90% of the bacterial concentration to decay. Therefore, if $t = T_{90}$, $\frac{C}{C_0} = 0.1$:

$$T_{90} = \frac{ln(0.1)}{k} \quad (2)$$

where

- T_{90} = time needed for the 90% of the bacterial concentration to decay [hours]

E.coli decay model:

Erichsen, et al. (2006) adopted an E.coli decay model from Jensen (1990). The model describes the decay contributions from dark and light conditions:

$$k_{coli} = k_m + K_l \cdot I_l \quad (3)$$

where

- k_{coli} = E.coli decay rate [days^{-1}]
- k_m = decay coefficient for dark conditions [days^{-1}], see equation 4
- K_l = decay coefficient for light conditions [m^2.W^{-1}.days^{-1}] , see equation 5
- I_l = Solar irradiance [W.m^{-2}], see equation 6

The dark decay term is expressed as a function of water temperature:

$$k_m = a_T \cdot T - k_{m0} \quad (4)$$

where

- T = water temperature [°C]
- a_T = temperature dependency constant for dark reaction [h^{-1}.°C^{-1}]
- k_{m0} = initial coliform decay rate for dark reaction [h^{-1}]

The light decay coefficient is expressed as a function of water temperature, and salinity:

$$K_l = S_m \cdot \frac{b_T \cdot T + K_{l0}}{a \cdot S_m - (a-1) \cdot S} \quad (5)$$

where

- S = water salinity [PSU]
- S_m = reference salinity [PSU]
- a = correction for salinity [-]
- b_T = temperature dependency constant for light reaction [$m^2.W^{-1}.h^{-1}.°C^{-1}$]
- K_{l0} = initial coliform decay rate for light reaction [$m^2.W^{-1}.h^{-1}$]

In a water body, light attenuation can be described as a function of depth using the Lambert-Beer law:

$$I_l = I_0 \cdot e^{-E_{ta} \cdot z} \quad (6)$$

where

- I_l = solar irradiance at depth z below surface [$W.m^{-2}$]
- I_0 = surface solar irradiance [$W.m^{-2}$]
- z = depth below surface [m]
- E_{ta} = light attenuation coefficient [m^{-1}]

Enterococci decay model:

The enterococci decay rate is expressed relative to the E.coli decay rate:

$$k_{ent} = k_{coli} \cdot r \quad (7)$$

where

- r = decay rate ratio of E.coli to enterococci [-]
- k_{ent} = enterococci decay rate [$days^{-1}$]

Literature indicates that enterococci decay slower than E.coli: based on 16 samples from 6 studies – e.g. Sinton, et al. (1994) – the median value for r was 0.42 (T_{90} equivalent ratio of 2.39), which has been adopted for this study. It is noted that r ranged from 0.21 to 2.5, indicating the uncertainty level for this value.

2.3.2.2 Validation of die-off model

The ECO Lab model described above was calibrated against measurements to confirm the required constants for this study. The constants are:

- S_m = 34.5 PSU
- a = 1.54
- a_T = 2.425x10^{-3} $h^{-1}.°C^{-1}$
- k_{m0} = 4.167x10^{-3} h^{-1}
- b_T = 6.25x10^{-5} $m^2.W^{-1}.h^{-1}.°C^{-1}$
- K_{l0} = 3.13x10^{-4} $m^2.W^{-1}.h^{-1}$

The measurements were obtained from Bellair, et al. (1977) and included 162 measurement samples of hourly decay rates (T_{90}) of E.coli on the seawater surface at Balmoral Bay near Sydney, Australia. The ECO Lab model assumed a constant water temperature and salinity representative of the measured conditions. Time-varying solar radiation was obtained from the European Centre for Medium-Range Weather Forecasts (EMCWF) ERA5 global atmospheric model (ECMWF, 2020). Figure 2-2 presents the a comparison of modelled and measured E.coli decay at Balmoral Bay. Also shown are measurements of T_{90} in sewage at Durban from Livingstone et al. (1990).

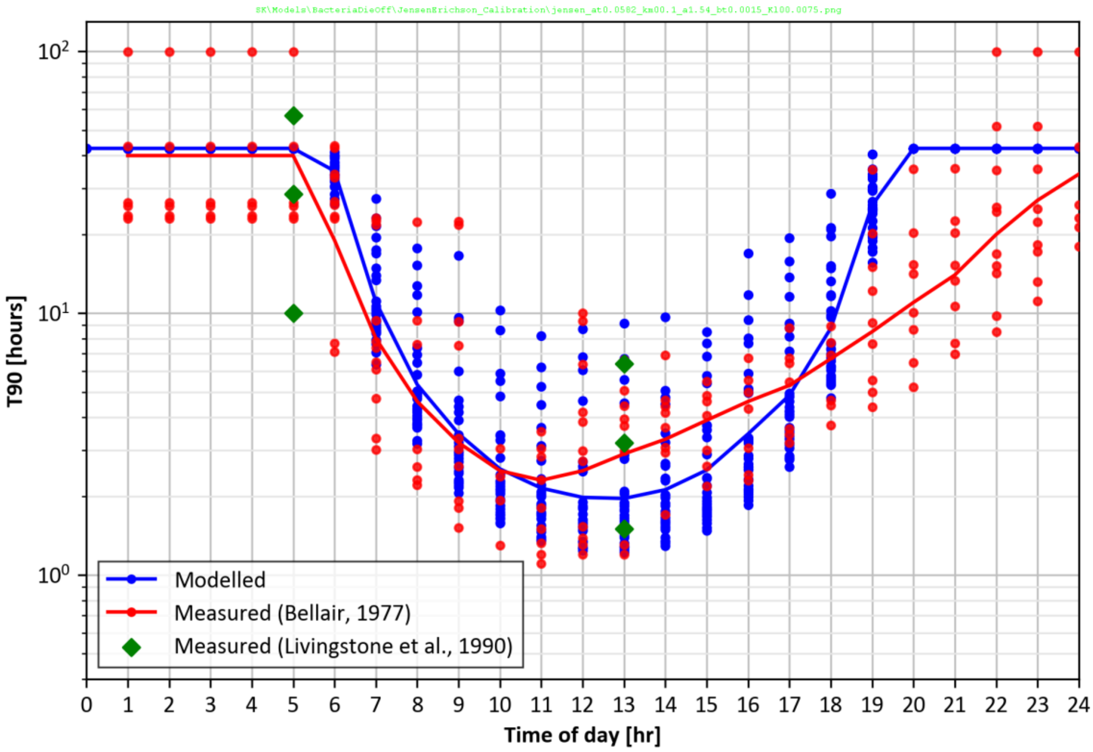

Figure 2-2: Measured and ECO Lab model comparison of E.coli decay at Balmoral Bay. The geometric mean is shown with a solid line. Also shown are measurements at Durban from Livingstone et al. (1990).

The comparison shows that the model is able to reproduce the measurements with satisfactory accuracy. Note the scatter from the model is directly proportional to the solar radiation intensity, whereas the measurements in addition include some variability in the seawater temperature, salinity and statistical randomness.

2.3.3 Model inputs

For the present Cape Town outfall study, a time and space varying surface solar irradiance I_0 was obtained from ECMWF. A constant light attenuation coefficient E_{ta}= 0.6 was applied, based on the annual average of Secchi disk measurements in Table Bay provided by Lwandle. Time and space-varying seawater temperature and salinity were obtained from the coupled hydrodynamic model.

2.4 Suspended sediment model

2.4.1 General description

The MIKE 3 Mud Transport Flexible Mesh Model was used to model the concentrations of discharged Total Suspended Solids (TSS) in the water column and where these are deposited on the seabed. This is a proxy for the fate of pollutants that adsorb to solid particles less than 63 µm, e.g. heavy metals.

The application of the model is described in the User Manual (DHI, 2020e) while full details of the physical processes being simulated and the numerical solution techniques are described in the Scientific Documentation (DHI, 2020f). The hydrodynamics (water levels, currents, temperature, salinity, vertical, dispersion, horizontal dispersion and release location at the end of the near-field) are obtained via an online coupling to the MIKE 3 Flow Flexible Mesh Model and the same three-dimensional grid is used.

The following processes are included in the simulations:

- 3D advection-dispersion of suspended sediment by currents;
- Settling of sediment through water column and deposition onto the seabed, dependent on the critical shear stress for deposition;
- Resuspension of sediment from the seabed, dependent on the critical shear stress for resuspension and the erosion coefficient;
- Bed shear stress due to combined currents and wave orbital velocities, as obtained through direct coupling with the hydrodynamic and spectral wave models.

2.4.2 Model settings

The input parameters used to model the TSS has been obtained from a previous study in Table Bay by PRDW (2017). The study calibrated a suspended sediment model to measured TSS concentrations in the water column and locations of fine sediment depo-centres. The modelled sediment comprises fine cohesive organic and inorganic particles with diameters less than 63 µm. The input parameters are listed in Table 2-1

Table 2-1: Input parameters used in the modelling of TSS.

Parameter	Unit	Value
Settling velocity of suspended sediment	m/s	$5x10^{-5}$
Critical shear stress for resuspension	N/m^2	0.2
Critical shear stress for deposition	N/m^2	0.1
Resuspension rate	$kgDW/m^2/s$	$1x10^{-4}$
Bulk density of dry sediment	kg/m^3 bulk	400

2.5 Wave model

2.5.1 General description

The MIKE 21 Spectral Waves (SW) Flexible Mesh model was used for simulating wave transformation to the nearshore. The application of the model is described in the User Manual (DHI, 2020g), while full details of the physical processes being simulated and the numerical solution techniques are described in the Scientific Documentation (DHI, 2020h). The model simulates the growth, decay and transformation of wind-generated waves and swells in offshore and coastal areas using unstructured meshes. The model used the same mesh as the hydrodynamic model. The model is fully spectral and can be run in either quasi-stationary or instationary mode, depending on the size of the model domain.

The model included the following physical phenomena:

- Dissipation due to bottom friction;
- Dissipation due to depth-induced wave breaking;
- Nonlinear energy transfer amongst the different wave components (quadruplet-wave interactions);
- Refraction and shoaling due to depth variations; and
- Generation of local wind-waves; and
- The effect of time-varying water depth due to the tide - the water depth at each time-step is computed in the hydrodynamic model including tidal and wave-setup.

2.5.2 Model settings

Bottom friction was modelled using a constant Nikuradse roughness of k_N = 0.5 m. The modelled water level from the hydrodynamic model was coupled to the wave model. The model was run in the fully spectral, quasi stationary formulation excluding the effect of additional wave generation within the model due to wind.

3. DISCHARGE CHARACTERISATION

3.1 Diffuser configuration

The Green Point diffuser is located in a depth of -26.0 m CD as shown in Figure 4-3. Table 3-1 presents the diffuser geometry and individual port configuration. The model assumes that the pipeline and diffusers are operating as described below and that there are no breakages, leaks or blockages.

Table 3-1: Diffuser geometry and flow distribution for Green Point.

Diffuser		Ports							
Section no.	**Inside diameter [mm] (1)**	**Port no. (2)**	**Port diameter [mm] (1)**	**Flow distribution [%] (3)**	**Discharge per port [l/s] (5)**	**Port velocity [m/s] (5)**	**Spacing [m] (1)**	**Level above seabed [mm]**	**Port configuration (1)**
1	355	1	150	5.8%	16.1	0.91	10	200 mm	Effluent is discharged horizontally through an elbow bend (illustrated below) with alternating discharge directions  (4)
		2	150	5.8%	16.2	0.92			
		3	150	6.0%	16.6	0.94			
		4	150	6.3%	17.5	0.99			
2	500	5	150	6.9%	19.1	1.08			
		6	150	7.0%	19.5	1.10			
		7	150	7.3%	20.1	1.14			
		8	150	7.6%	21.0	1.19			
3	630	9	125	5.5%	15.3	1.24			
		10	125	5.6%	15.6	1.27			
		11	125	5.7%	15.8	1.29			
		12	125	5.8%	16.2	1.32			
4	700	13	125	6.0%	16.6	1.35			
		14	125	6.1%	16.9	1.38			
		15	125	6.2%	17.2	1.40			
		16	125	6.3%	17.5	1.43			

Notes:

(1) Source: CSIR (1992).

(2) The ports are arranged from offshore (port no.1) to inshore (port no. 16).

(3) Based on diffuser hydraulics modelling undertaken by the CoCT

(4) Schematic representation of port configuration

(5) Calculated using the 50th percentile winter/spring discharge rates in Table 3-2.

3.2 Discharge rates

Measured flow rates were provided by the CoCT for input to the dispersion model. The measurements comprise average flow rates at 30-minute intervals and covers the model simulation period. This will ensure that the model results account for diurnal variations in flows.

Figure 3-1 and Figure 3-2 present time series plots of the Camps Bay effluent discharge rate for the winter/spring and summer/autumn periods respectively. A statistical summary is provided in Table 3-2.

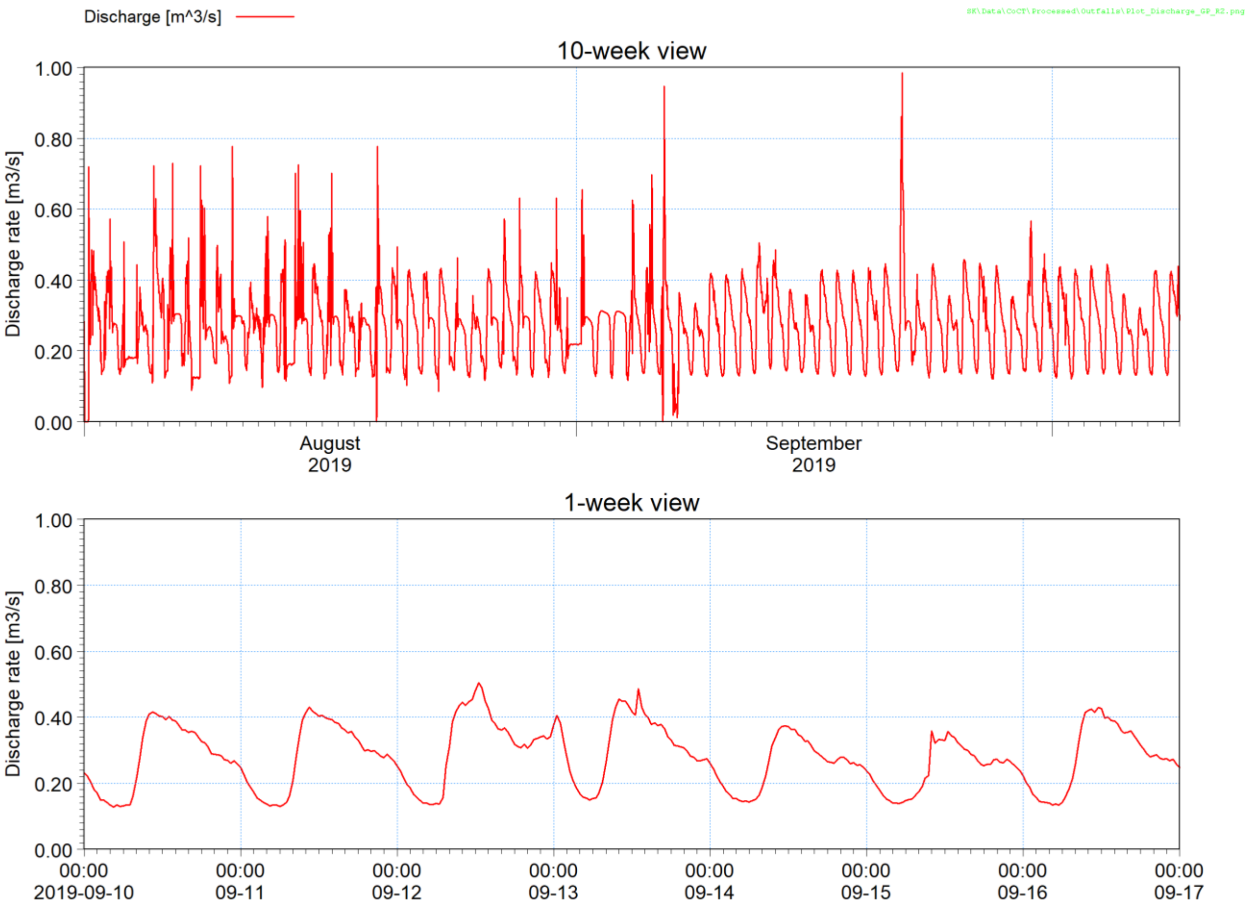

Figure 3-1: Time series of Green Point effluent discharge rate for the winter/spring period.

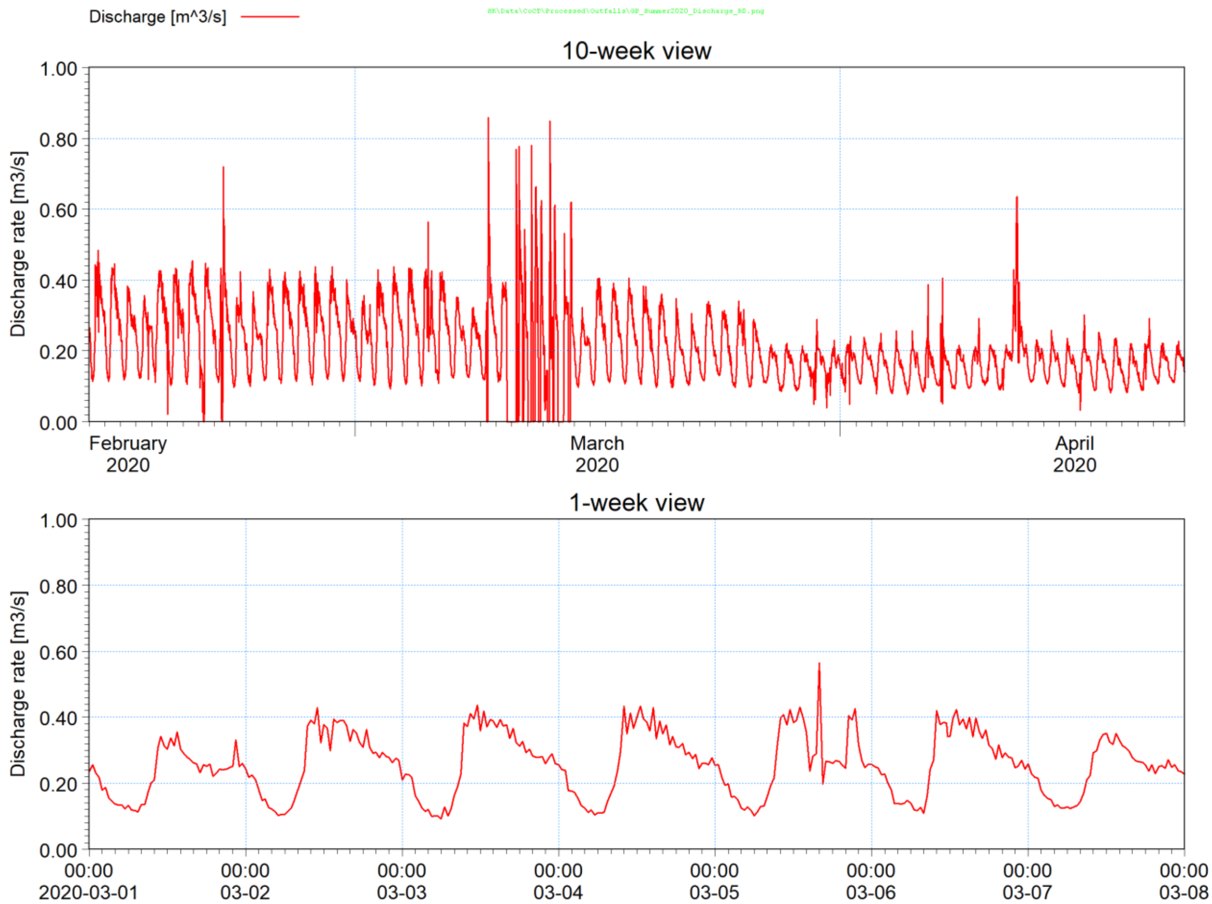

Figure 3-2: Time series of Green Point effluent discharge rate for the summer/autumn period.

Table 3-2: Green Point effluent discharge rate statistics.

Parameter	Discharge rate	
	Winter/spring	Summer/autumn
Average	23 800 m³/d	18 100 m³/d
5th percentile	0.134 m³/s	0.086 m³/s
50th percentile	0.277 m³/s	0.191 m³/s
95th percentile	0.430 m³/s	0.391 m³/s

A significant reduction in effluent discharge rates could be observed from 23 March 2020 due to a national lockdown enforced in response to the COVID-19 pandemic resulting in fewer people in the city.

3.3 Effluent concentrations

The effluent concentrations applied in the model are shown in Table 3-1

Table 3-3: Modelled effluent concentrations.

Constituent	Concentration	Comments
E.coli	1 x10^7 CFU/100 ml	Kay et al. (2008), CSIR (2017).
Enterococci	1.3 x10^6 CFU/100 ml	Kay et al. (2008)
TSS	359 mg/l	Provided by CoCT based on the average measured value in the Green Point effluent (1 August 2014 – 31 October 2019)
Tracer	100 units	All other constituents will be modelled as a conservative tracer which will have a nominal concentration of 100 units and will be used to model the achieved dilutions.

The effluent temperature was set equal to the seawater temperature at the diffuser and the effluent salinity was set to 0 psu.

3.4 Water quality guidelines

3.4.1 Required dilutions

The analysis of the constituent concentrations in the effluent, the associated water quality guidelines and the required dilutions was undertaken by the CoCT. Based on this analysis the CoCT provided PRDW with three critical constituents as listed in Table 3-4. These required dilutions will be compared to the achieved dilutions obtained from the model.

Table 3-4: Required effluent dilutions.

Constituent	Dilutions
Ammonia	106
Chemical Oxygen Demand (COD)	51
TSS	1 753

The CoCT determined the allowable mixing zone to be within a radius of 256 m from the diffuser.

3.4.2 Bacteria concentrations

The CoCT confirmed that the target values for microbiological indicators for recreational waters in the coastal marine environment should be based on the Department of Environmental Affairs guidelines (DEA, 2012), as shown in Table 3-5.

Table 3-5: Guideline concentrations for enterococci and E.coli to meet the sufficient or fair category for recreational waters in the coastal marine environment.

Constituent	90^{th} percentile concentration [CFU/100 ml]
Enterococci	≤ 185
E.coli	≤ 500

4. MODEL SETUP

4.1 Model mesh

The WG19 horizontal coordinate system was used for this study. All spatial plots include x and y axes showing the x and y coordinates in metres in the WG19 system. True north is always pointing upwards.

The model mesh comprises triangles with a resolution varying from about 3 km at the offshore boundary to 50 m in the vicinity of the diffuser. Quadrangular elements with a resolution of 25 m were used around the diffuser to resolve the effluent release into the far-field model. The vertical mesh is comprised of twelve sigma layers with equal layer thicknesses.

Figure 4-1 and Figure 4-2 and represent the three-dimensional and horizontal views of the mesh used for the outfall dispersion modelling.

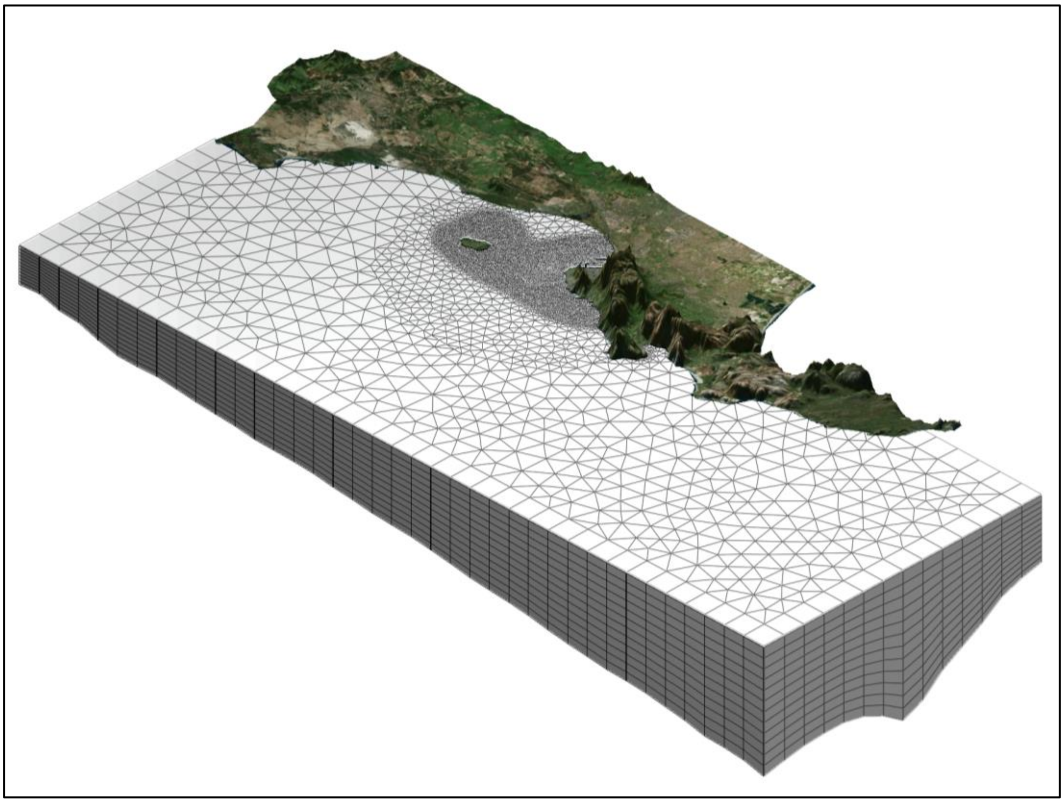

Figure 4-1: Three-dimensional representation of mesh used for the outfall dispersion modelling. Note the vertical axis is not to scale.

SK\Models\MFM\DiffuserPlot\02b_Mesh_GP_R3.png

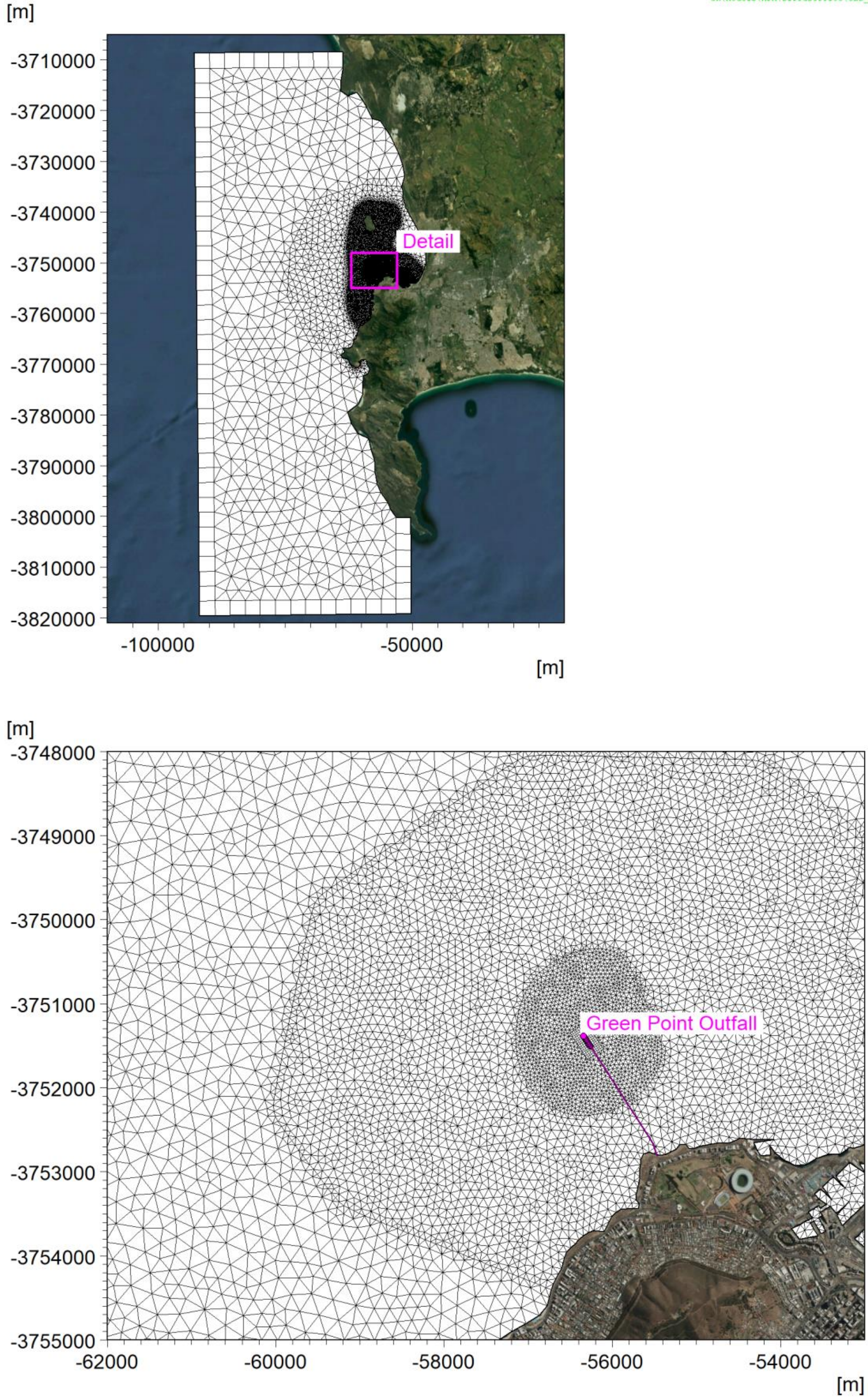

Figure 4-2: Horizontal mesh used for the outfall dispersion modelling.

4.2 Bathymetry

The vertical datum adopted in this study is Chart Datum (CD). CD is 0.825 m below Land Levelling Datum (LLD) which is also known as Mean Sea Level (MSL).

The model bathymetry has been obtained from the following sources:

- CMAP electronic hydrographic charts
- LIDAR topographic surveys landward of the high water mark

Figure 4-3 shows the model bathymetry and the locations of the ADCP and thermistor deployments used for the calibration of the model.

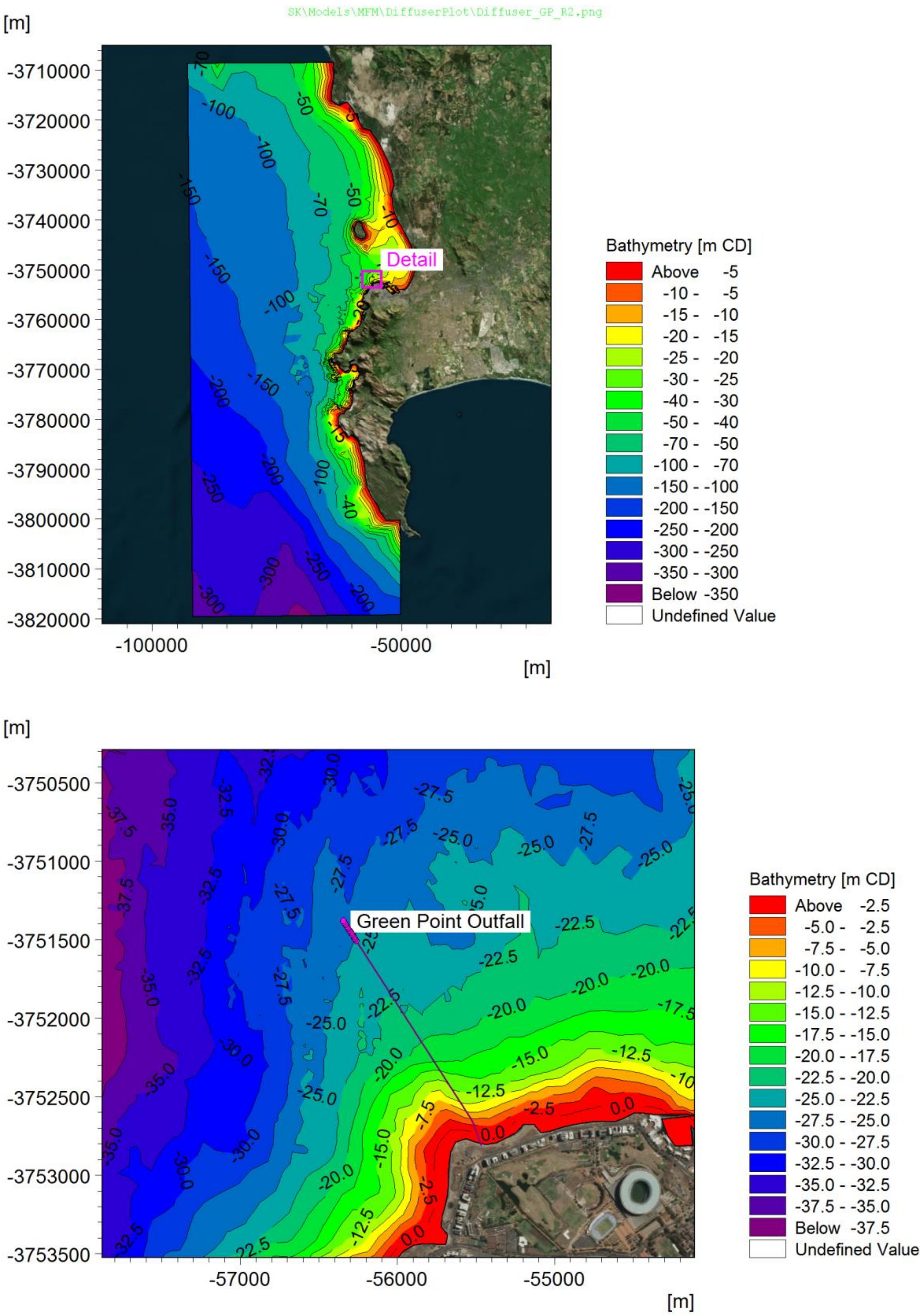

Figure 4-3: Model bathymetry.

4.3 Wind

Wind is an important forcing mechanism for currents, vertical mixing and upwelling – and thus the effluent dispersion. The wind fields near the outfalls are influenced by the surrounding mountains which require a high spatial resolution to resolve.

The Climate System Analysis Group at the University of Cape Town has kindly provided wind data from the Weather Research and Forecasting (WRF) model with a spatial resolution of 4 km and a temporal resolution of 1 hour.

Figure 4-4 shows two snapshots in time illustrating the high spatial variability in the 4 km resolution modelled winds around Cape Town.

Figure 4-5 to Figure 4-8 show comparisons between the modelled winds and measured winds at three locations around Cape Town (Cape Town International Airport, Cape Point and Koeberg) for the winter/spring and summer/autumn modelling periods.

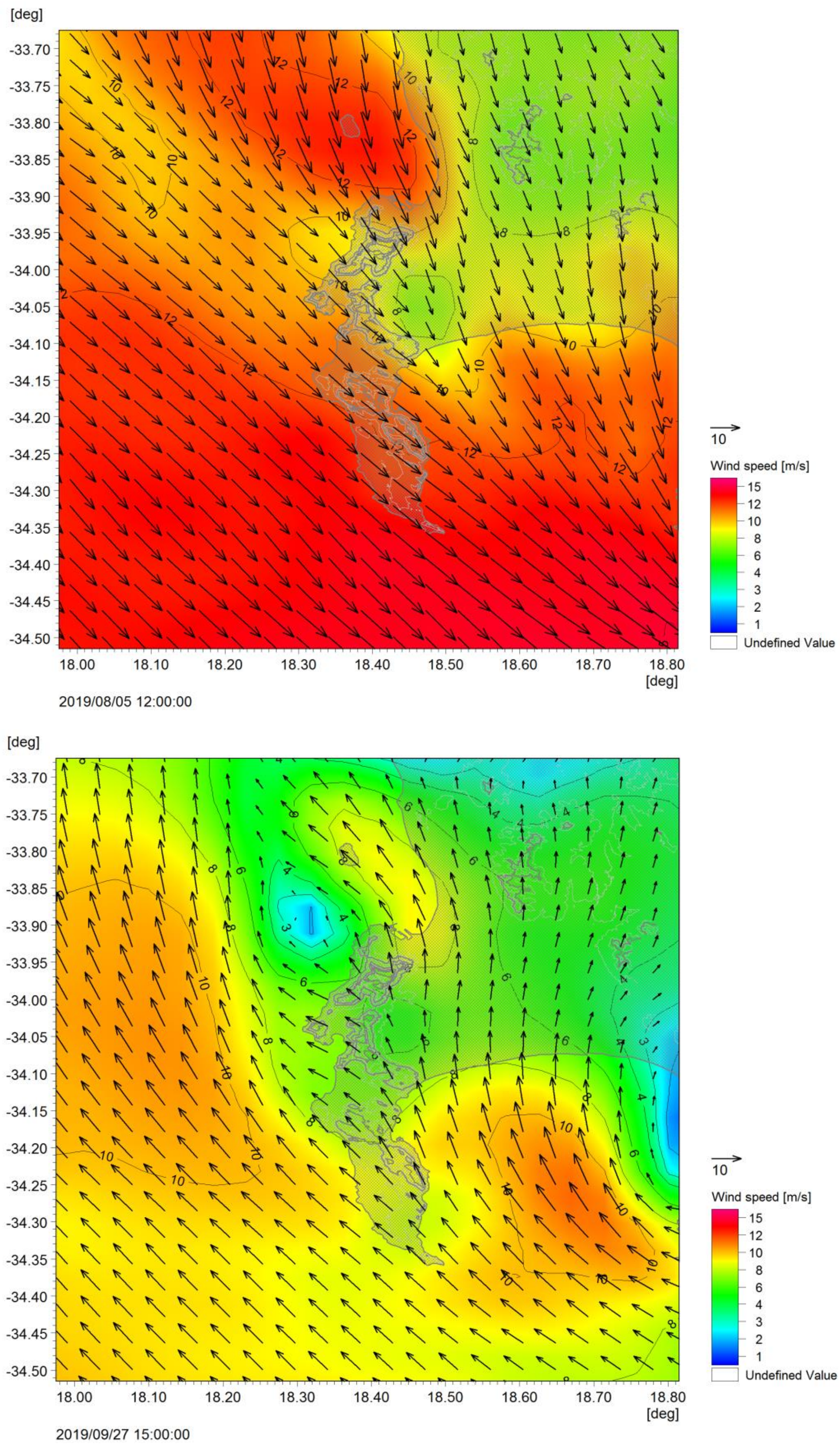

Figure 4-4: Snapshots illustrating the high spatial variability in the 4 km resolution modelled winds around Cape Town (grey lines show topography at 100 m intervals).

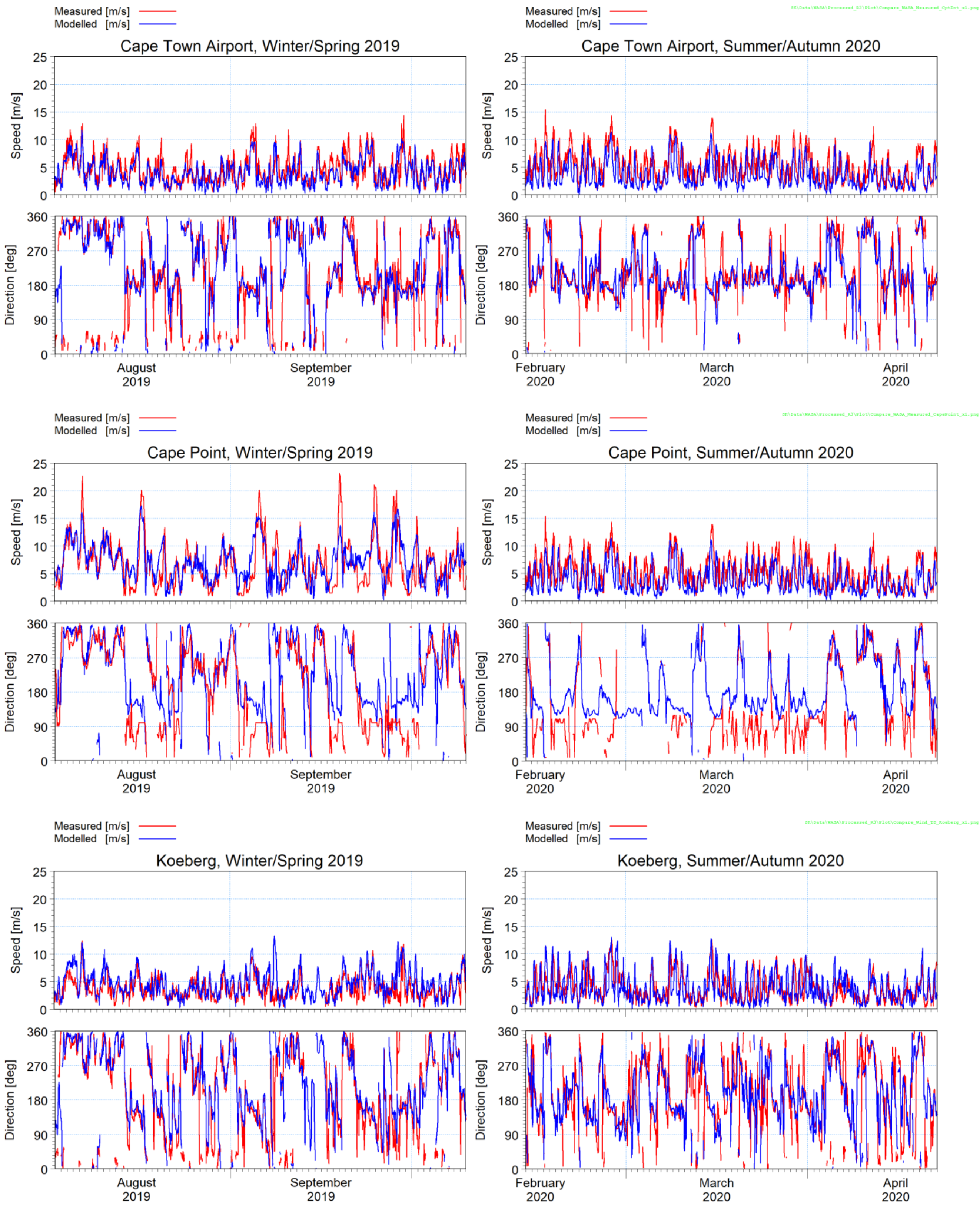

Figure 4-5: Time series of modelled compared to measured winds at Cape Town International, Cape Point and Koeberg.

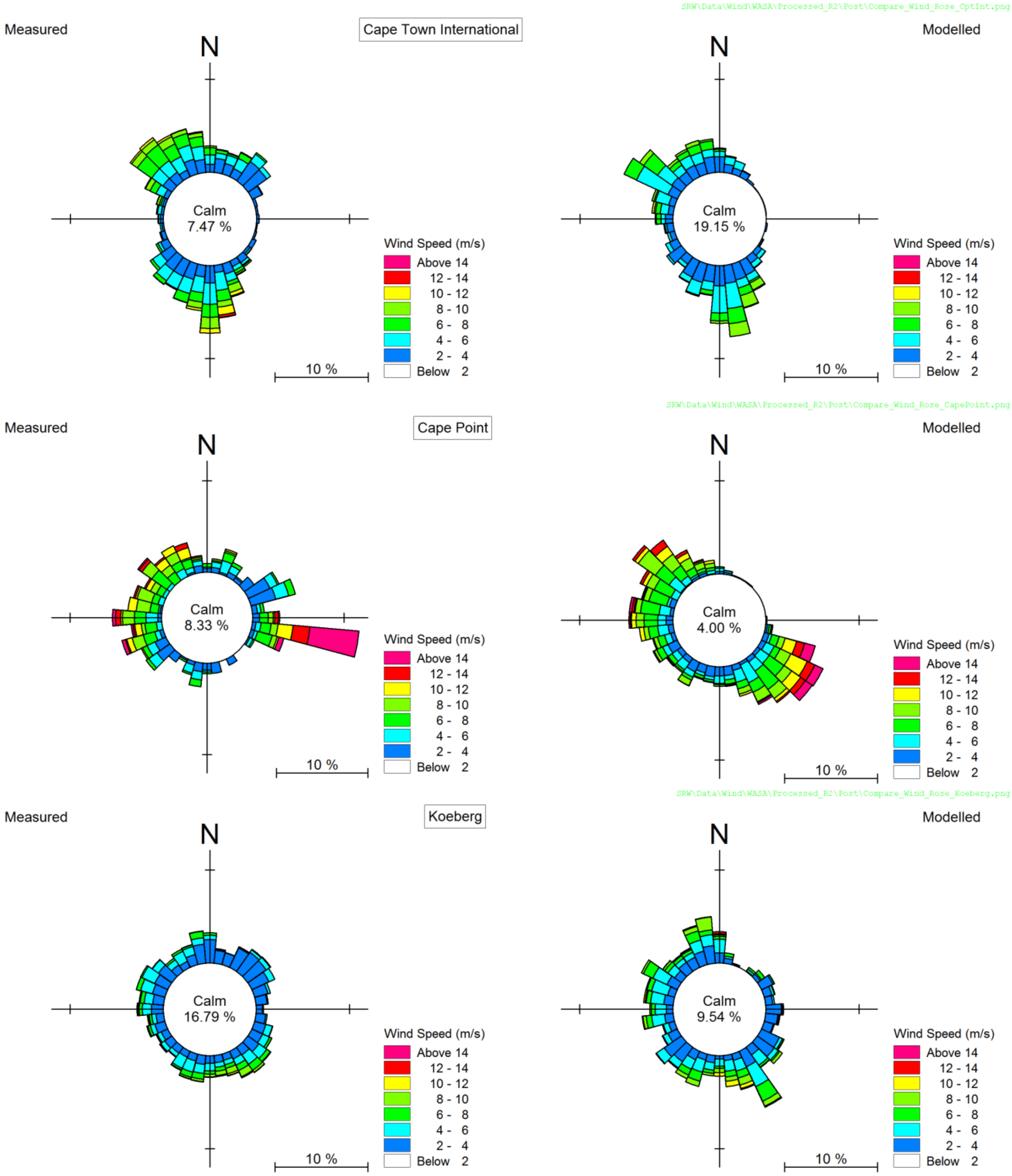

Figure 4-6: Roses of modelled compared to measured winds at Cape Town International, Cape Point and Koeberg for the winter/spring 2019 period.

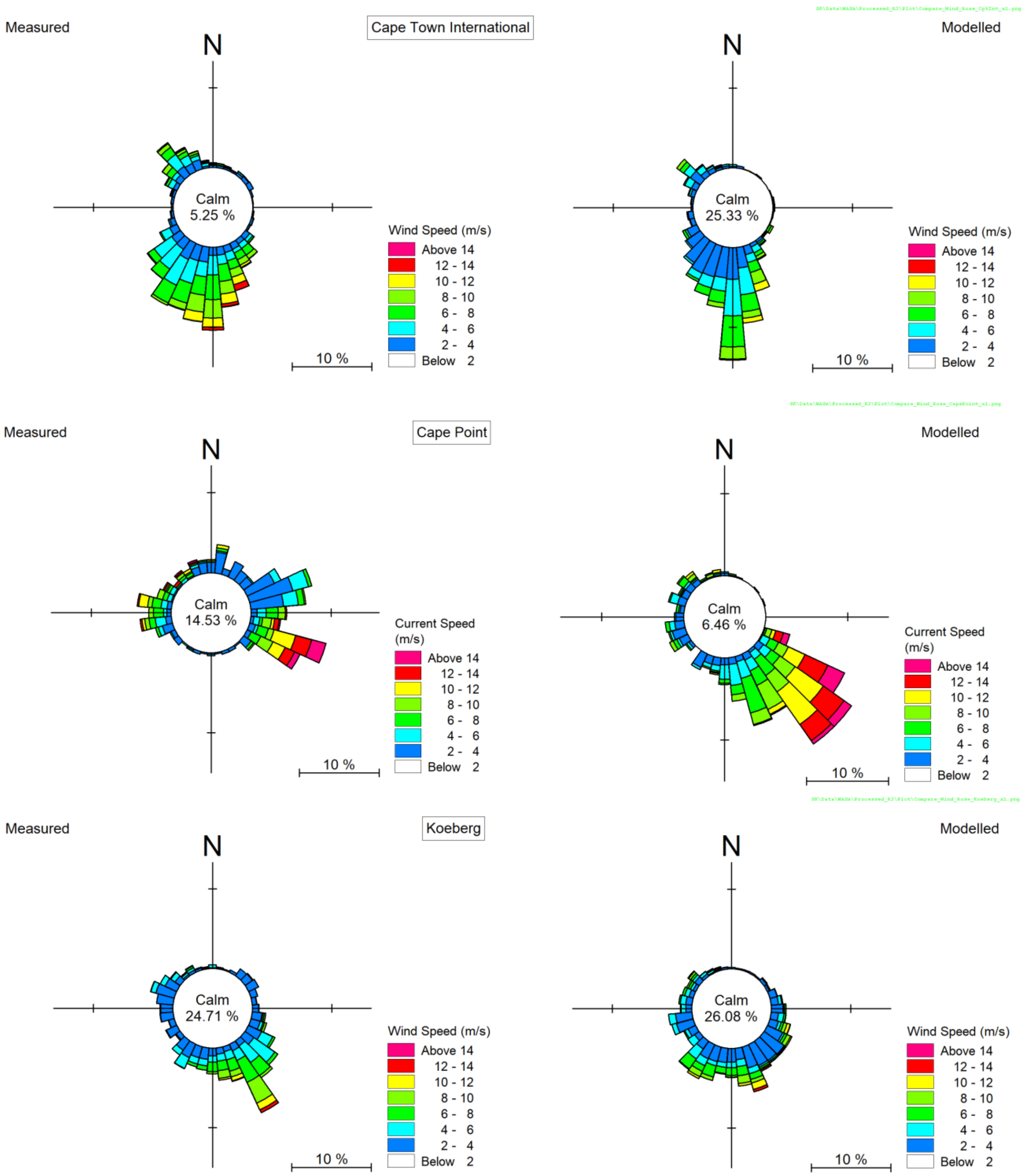

Figure 4-7: Roses of modelled compared to measured winds at Cape Town International, Cape Point and Koeberg for the summer/autumn 2020 period.

SK\Data\WASA\Processed_R3\TsPlots\Wind_Exceedance_Curves.xlsx

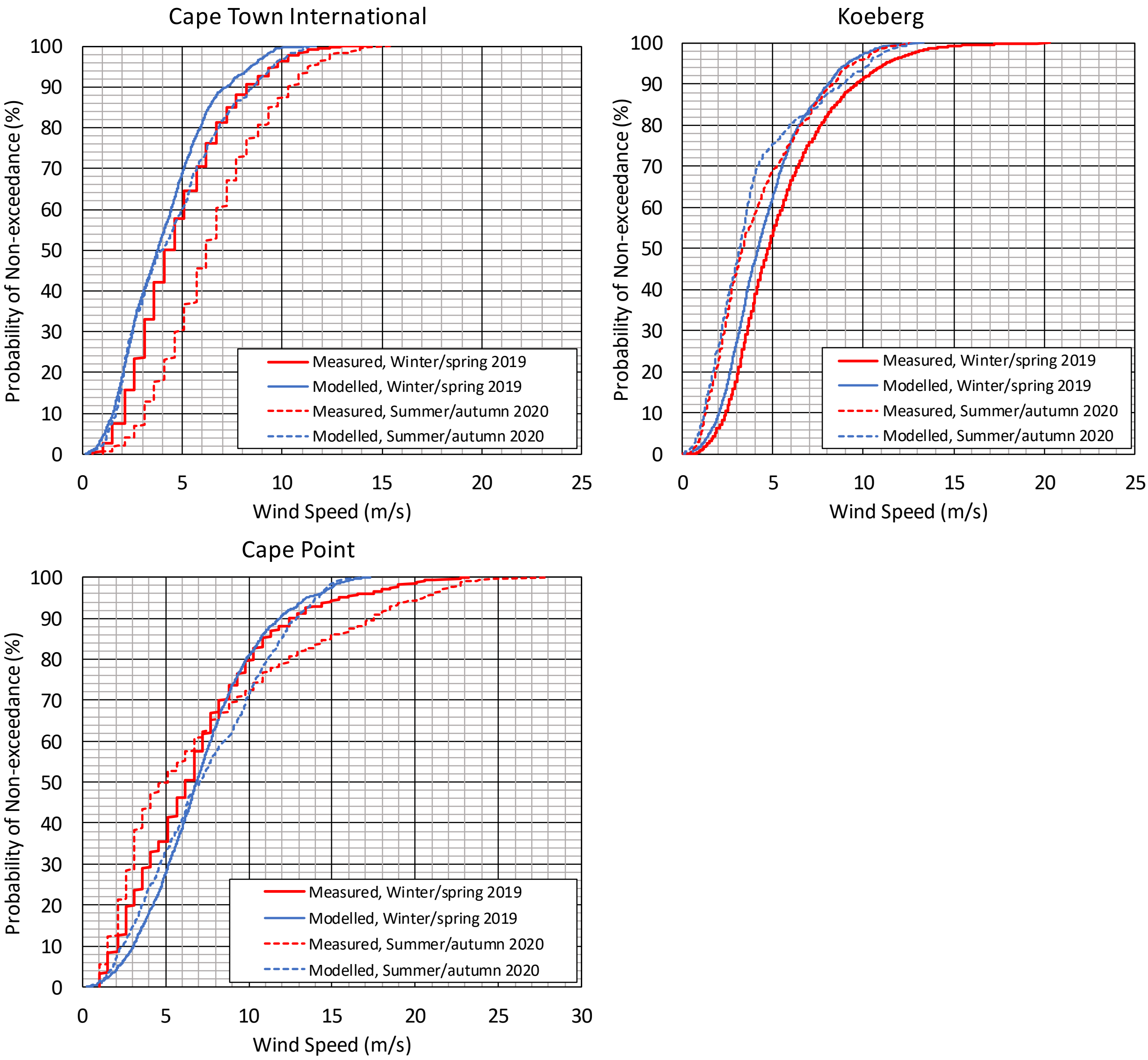

Figure 4-8: Wind speed exceedance of modelled compared to measured winds at Cape Town International, Cape Point and Koeberg.

These results indicate that the WRF modelled winds compare well to the measured winds at three different locations across Cape Town. The main discrepancies are the wind directions at Cape Point which is likely due to the steep cliffs at this location, and the modelled wind speed being approximately 1 m/s to 2 m/s lower than the measurements at Cape Town International.

4.4 Boundary conditions

The model boundary conditions are extracted from global hindcast models as described in Table 4-1:

Table 4-1: Global hindcast models used for the model boundary conditions.

Model	Parameter	Spatial resolution [˚]	Temporal resolution [hrs]
HYbrid Coordinate Ocean Model (HYCOM) global ocean circulation model (HYCOM, 2020).	Non-tidal water levels	0.08	3
	Non-tidal ocean currents		
	Seawater temperature		
	Seawater salinity		
DTU10 (Technical University of Denmark) global tidal model (DTU, 2010).	Predicted tides	0.125	Predicted from constituents.
	Predicted tidal currents	0.25	
European Centre for Medium-Range Weather Forecasts (EMCWF) ERA5 global atmospheric model (ECMWF, 2020).	Air temperature	0.25	1
	Humidity		
	Solar radiation		
National Centers for Environmental Prediction (NCEP) global wave forecast model (NCEP, 2020).	Wave spectra	0.5	3

4.5 Model settings

The vertical eddy viscosity was computed using the k-ε vertical turbulence closure scheme, while the vertical eddy dispersion was set to 0.1 times the vertical eddy viscosity. This scaling factor was applied to compensate for additional vertical mixing caused by the use of only 12 vertical layers and the associated smoothing of the vertical density gradients.

The wind friction coefficient and seabed roughness were tuned to physically realistic values which yielded the best agreement between modelled and measured currents at Green Point.

5. MODEL CALIBRATION

5.1 Winter/spring

The model was calibrated to metocean data measured by Lwandle during a 6-week period between 21 August 2019 and 3 October 2019. The measurements used for the model calibration comprise:

- ADCP measurements, including:
  - Currents measured across the depth profile in 1 m bins at 10-minute intervals.
  - Fully spectral waves, available at hourly intervals.
  - Seawater temperature at 10-minute intervals.
- Seawater temperature measured from a thermistor string, available at 5 discrete depth levels between 3 m and 14 m above the seabed. The data is only available for the first week of measurements.

The ADCP (X = -56 401 m, Y= -3 751 487 m) and thermistor string (X = -56 403 m, Y= -3 751 495 m) were deployed approximately 100 m southwest of the diffuser at a depth of -27.6 m CD. The locations are shown in Figure 5-1.

5.1.1 Waves

A wave refraction plot for a west-south-westerly wave event is shown in Figure 5-1.

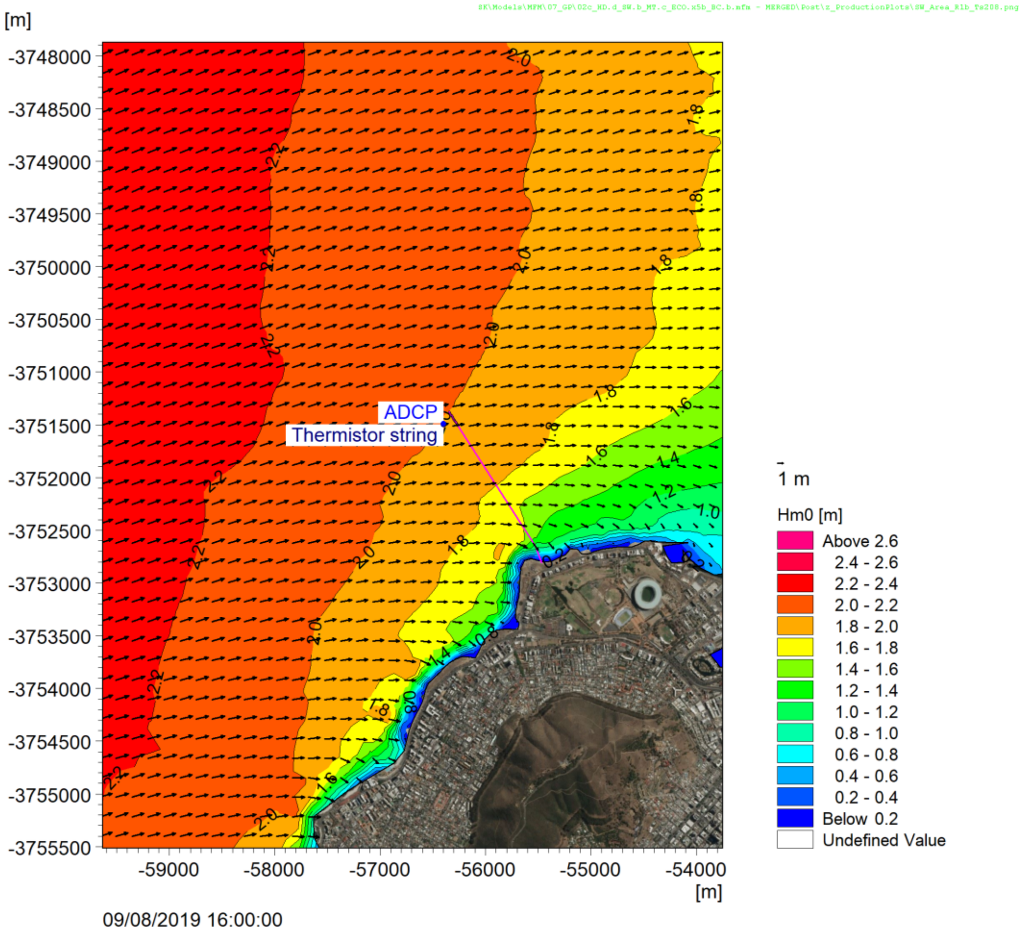

Figure 5-1: Winter/spring: Wave refraction plot for a west-south-westerly wave event. The modelled wave condition at the ADCP is H_{m0} = 2.14 m, T_P = 10.2 s, D_{MP} = 259˚.

Figure 5-2 presents a time series comparison of measured and modelled wave parameters at the ADCP. Measured and modelled wave roses are shown in Figure 5-3. By convention, wave direction is the direction from which the wave is coming, measured clockwise from true north.

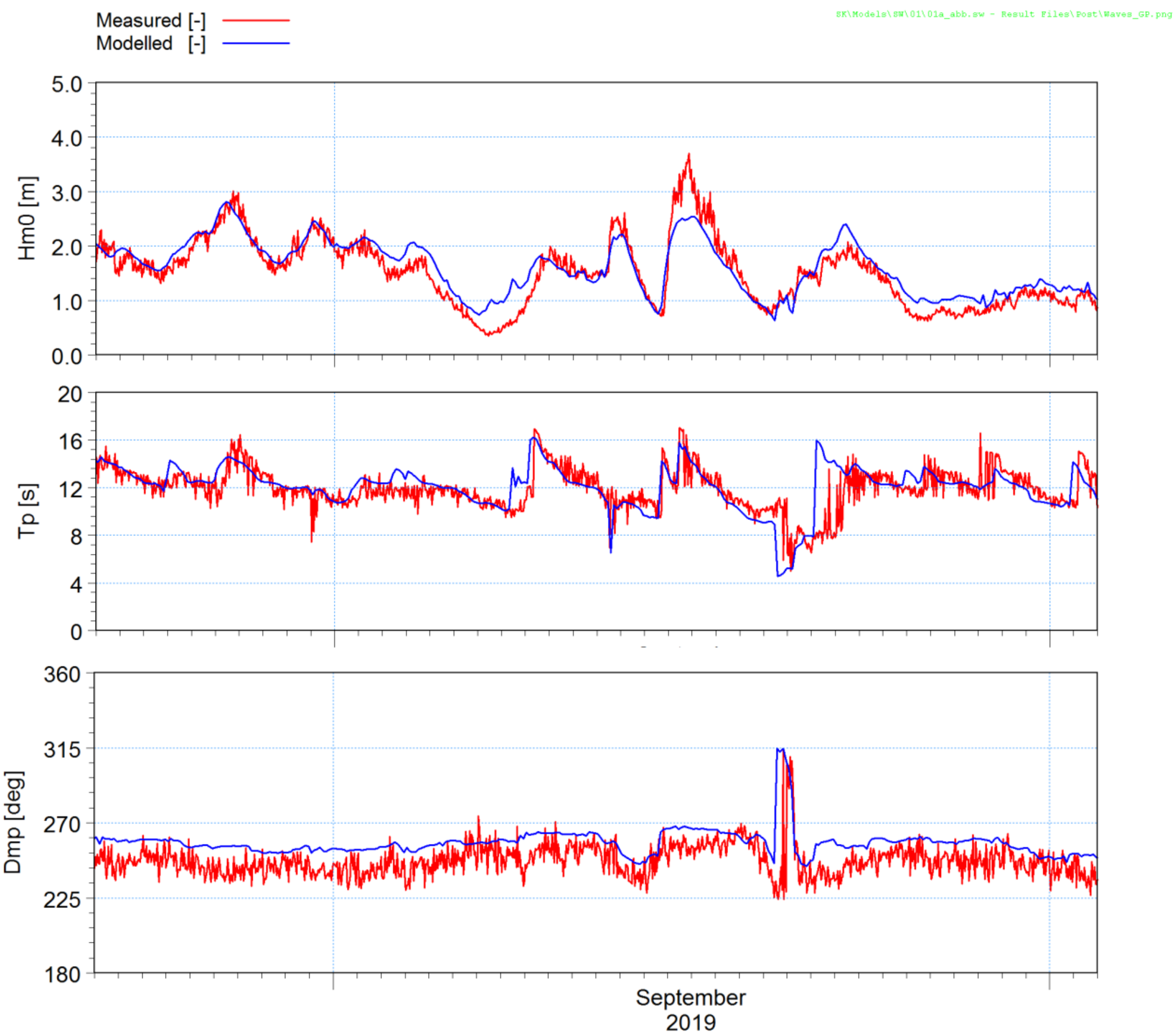

Figure 5-2: Winter/spring: Time series of measured and modelled significant wave height (H_{m0}), peak wave period (T_P) and mean wave direction at Tp (D_{MP}) at the location of the ADCP.

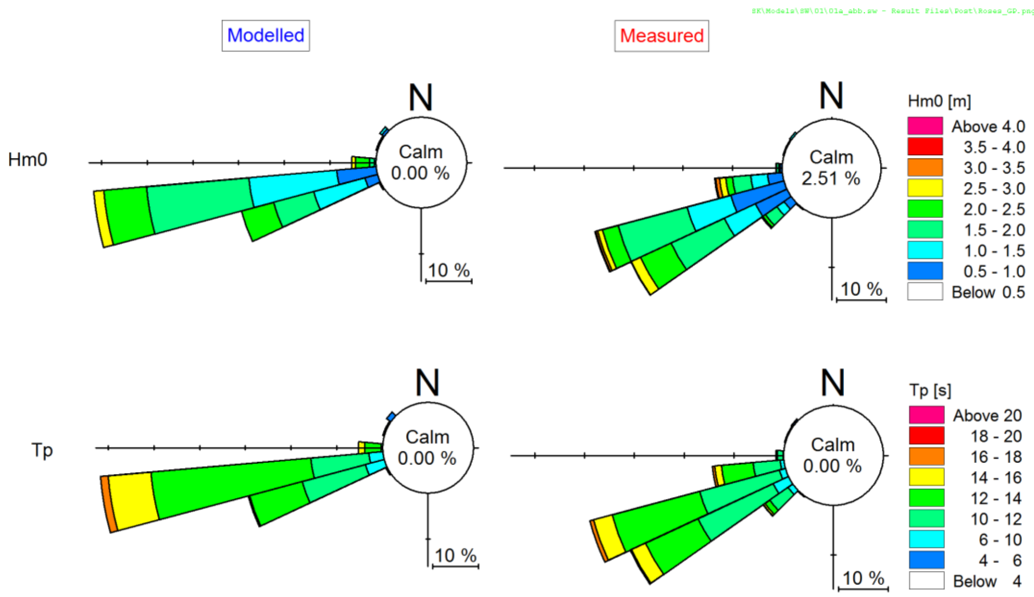

Figure 5-3: Winter/spring: Wave roses of measured and modelled H_{m0} and T_P for the 6-week deployment period at the location of the ADCP.

A good overall comparison could be observed from the time series and wave rose plots. Occasional over- or underprediction of wave heights can be observed, but there is no bias in either direction. The modelled peak wave period compared well to the measurements. The modelled mean wave direction shows a constant offset of about 10° compared to the measurements. The agreement between the ADCP measurements and the wave model outputs shows the model to be adequately calibrated for the purposes of this study

5.1.2 Water levels

The predicted tidal levels at the Port of Cape Town (X = -539 934 m, Y = -3 752 769 m) were extracted from the MIKE by DHI CMAP Electronic Charts Database (DHI, 2020i). Figure 5-4 presents a time series comparison of modelled water levels to predicted tides at the Port of Cape Town. A water level probability of non-exceedance plot is shown in Figure 5-5 for the Port of Cape Town.

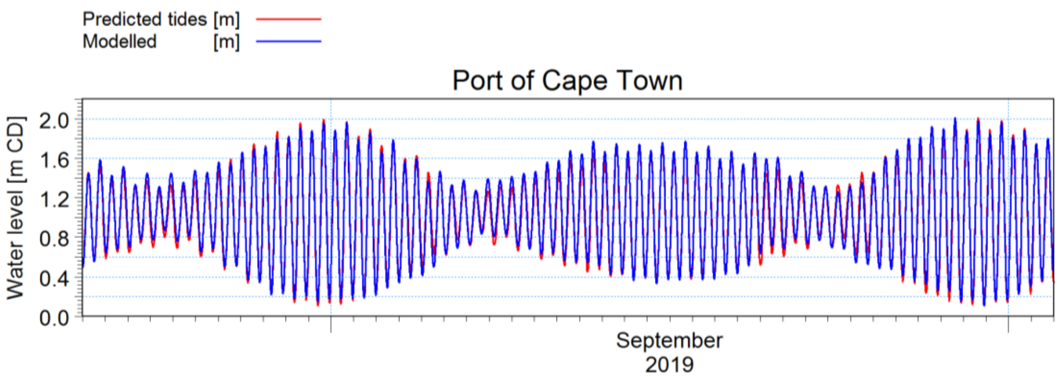

Figure 5-4: Winter/spring: Time series comparison of modelled water levels to predicted tides at the Port of Cape Town.

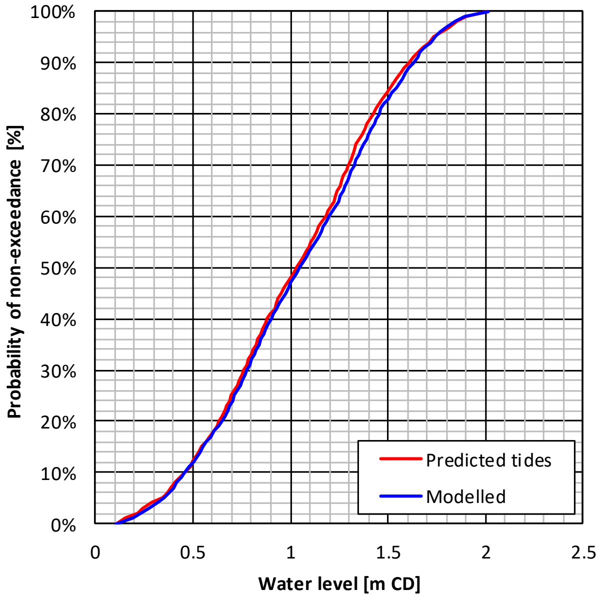

16\021d_HD-4_SW-am fm-ResultFiles\Post\[WL_Exceedance_CB.xlsx]Graphs

Probability of non-exceedance	Water level [m CD] Predicted	Water level [m CD] Modelled
5%	0.34	0.35
10%	0.45	0.46
20%	0.63	0.65
30%	0.76	0.78
50%	1.03	1.05
70%	1.30	1.33
80%	1.42	1.45
90%	1.60	1.63
95%	1.73	1.74

Figure 5-5: Winter/spring: Probability of non-exceedance for predicted tides and modelled water levels for the 6-week deployment period at the Port of Cape Town.

The comparison shows a good overall model prediction in both tidal phase and amplitude.

5.1.3 Currents

A contour plot of instantaneous currents during a west-south-westerly wave/north-westerly wind event is shown in Figure 5-6. The modelled currents were compared to the measurements near the seabed (3.8 m above the seabed) and near the surface (23.8 m above the seabed). Figure 5-7 presents a time series comparison of the modelled and measured currents at the ADCP. Non-exceedance curves of current speed for the 6-week period are shown Figure 5-8. Current rose comparisons of modelled and measured currents are presented in Figure 5-9. Note that current direction is by convention the direction towards which the current is flowing.

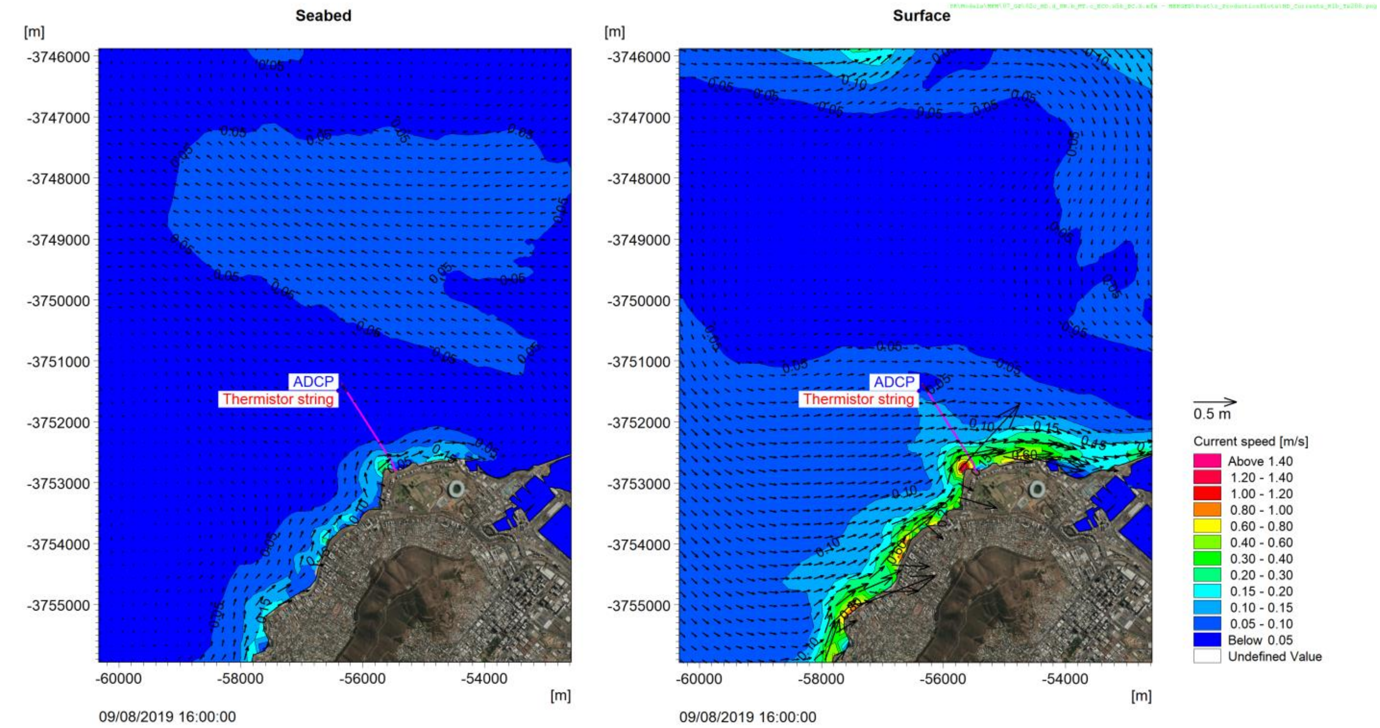

Figure 5-6: Winter/spring: Contour plot of instantaneous seabed (left) and surface (right) currents during a west-south-westerly wave/north-westerly wind event (shown in Figure 5-1).

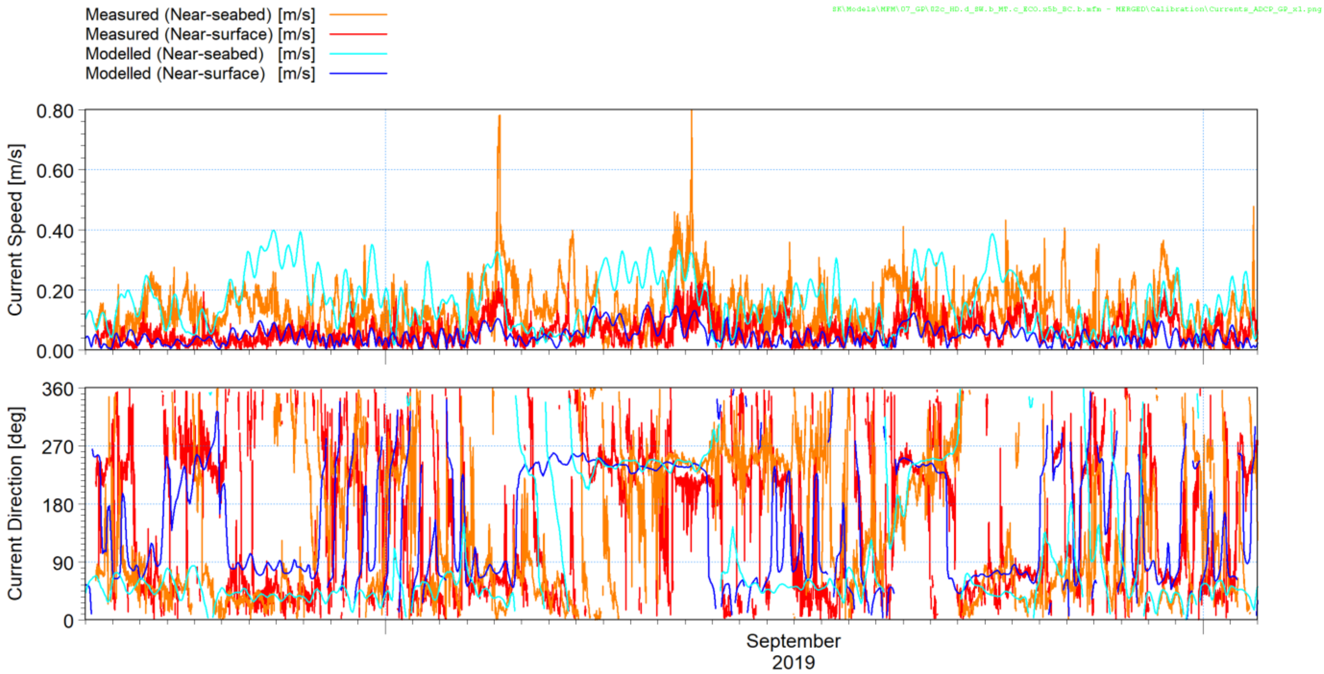

Figure 5-7: Winter/spring: Time series comparison of measured and modelled current speed and direction at the ADCP.

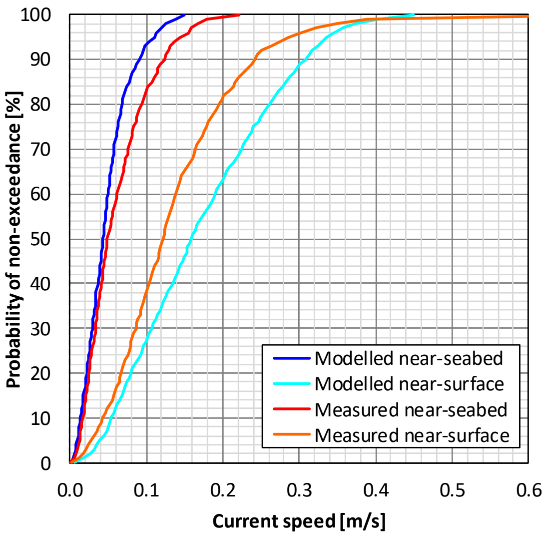

Proability of non-exceedance [%]	Current speed [m/s]			
	Near-seabed		Near-surface	
	Modelled	Measured	Modelled	Measured
10	0.01	0.02	0.05	0.04
20	0.02	0.03	0.08	0.07
30	0.03	0.03	0.11	0.09
40	0.04	0.04	0.13	0.10
50	0.04	0.05	0.16	0.12
60	0.05	0.06	0.19	0.14
70	0.06	0.08	0.22	0.16
80	0.07	0.09	0.26	0.19
90	0.09	0.12	0.31	0.24

Figure 5-8: Winter/spring: Probability of non-exceedance for measured and modelled current speed for the 6-week deployment period at the ADCP.

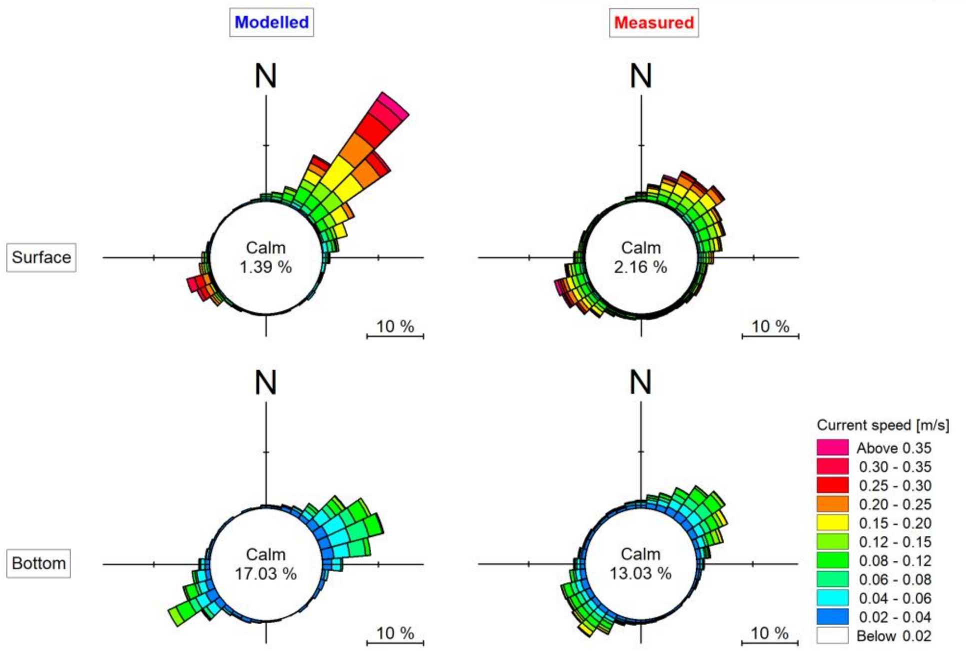

Figure 5-9: Measured and modelled current roses for the 6-week deployment period at the ADCP.

The model shows a tendency to overpredict the operational current speeds near the surface and underpredict the stronger currents near the seabed. The dominant current directions are well represented at both depths, although the model tends to underpredict the occurrence of south-westerly currents near the surface . Note that that more directional spreading is expected in the measurements due to high frequency processes such as eddies and edge waves that are not included in the model boundary conditions.

Overall the model is able to reproduce the main features of the currents and is considered to be acceptable for the purposes of this study.

5.1.4 Temperature

The modelled seawater temperatures were compared to one week of thermistor string measurements near the seabed (3.0 m above the seabed) and at mid-depth (14.0 m above the seabed) and to ADCP measurements near the seabed for the full calibration period. Figure 5-10 presents a time series comparison of the modelled and measured seawater temperatures. Non-exceedance curves of seabed and mid-depth temperatures for the 6-week period are shown Figure 5-11. Figure 5-12 presents a non-exceedance curve of stratification (seabed to mid-depth) from the modelled temperatures. Note that the thermistor string measurements were excluded from the exceedance curves due to the limited data availability.

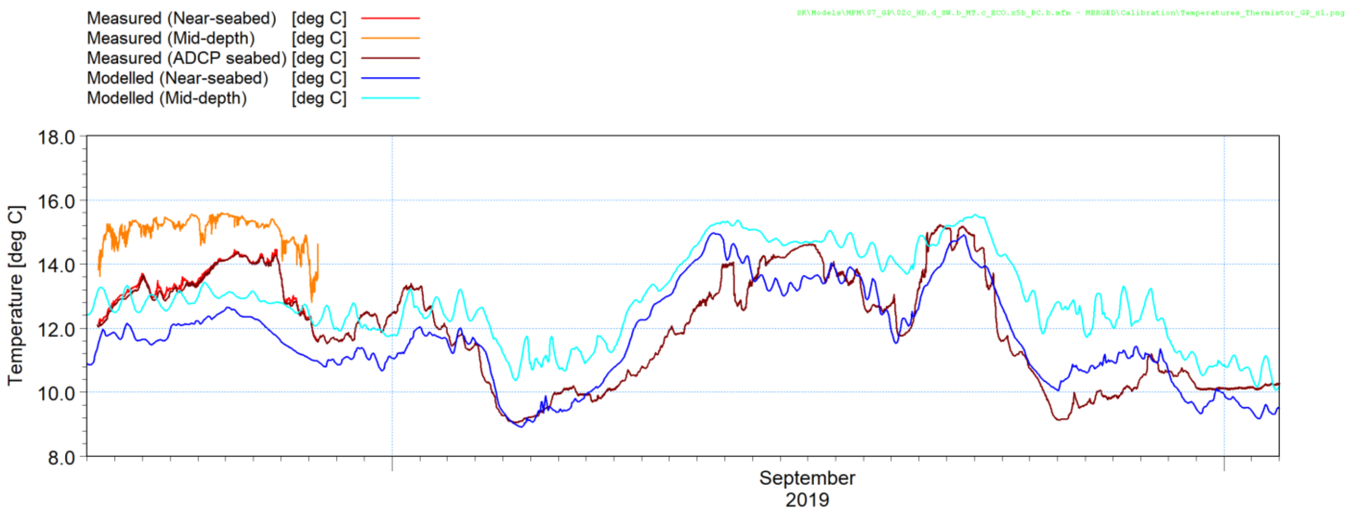

Figure 5-10: Winter/spring: Time series of measured and modelled seawater temperatures.

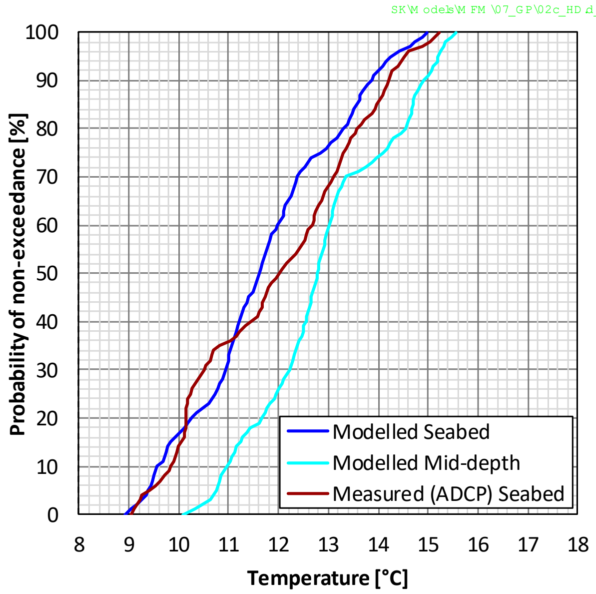

Proability of non-exceedance [%]	Temperature [°C]			
	Near-seabed		Mid-depth	
	Modelled	Measured	Modelled	Measured
10	9.6	9.9	11.0	N/A
20	10.3	10.1	11.7	N/A
30	10.9	10.5	12.2	N/A
40	11.2	11.5	12.5	N/A
50	11.6	12.0	12.8	N/A
60	12.0	12.7	13.0	N/A
70	12.4	13.1	13.4	N/A
80	13.3	13.6	14.6	N/A
90	13.9	14.2	14.9	N/A

Figure 5-11: Winter/spring: Probability of non-exceedance of measured and modelled seawater temperatures for the 6-week deployment period.

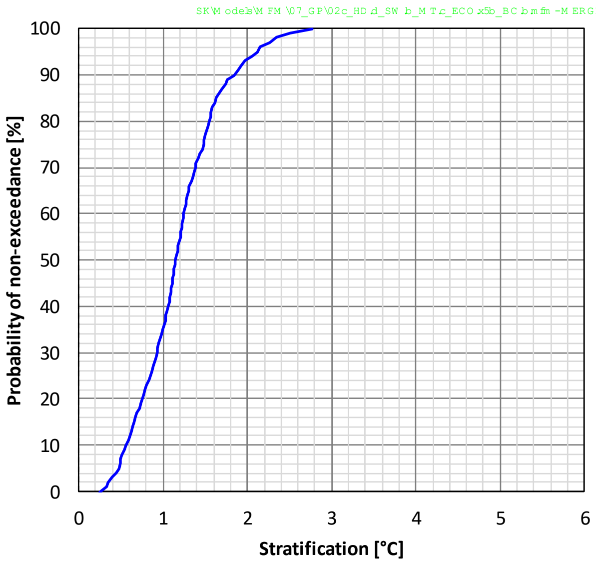

Proability of non-exceedance [%]	Modelled stratification [°C]
10	0.56
20	0.76
30	0.92
40	1.06
50	1.15
60	1.25
70	1.38
80	1.55
90	1.84

Figure 5-12: Winter/spring: Probability of non-exceedance of modelled seawater temperature stratification (near-seabed to mid-depth) for the 6-week deployment period.

The measured time series shows that the seawater temperatures are complex and vary over a range of time-scales due to upwelling, solar radiation and other dynamic processes. The model is able to predict the mean trend in seabed seawater temperatures including some of the discrete dynamic events. Periodic over- or underprediction of seabed temperatures can be observed, however the model shows a good statistical distribution of temperatures. The accuracy of the modelled stratification is inconclusive due to the limited availability of thermistor string measurements. The model is considered to be adequately calibrated for seawater temperature for the purposes of this study.

5.2 Summer/autumn

The model was calibrated to metocean data measured by Lwandle during a 10-week period between 13 February 2020 and 23 April 2020. The measurements used for the model calibration comprise:

- ADCP measurements, including:
  - Currents measured across the depth profile in 1 m bins at 10-minute intervals.
  - Fully spectral waves, available at hourly intervals.
- Seawater temperature measured from a thermistor string, available at 5 discrete depth levels from 3 m above the seabed to the surface.

The ADCP (X = -56 401 m, Y= -3 751 482 m) and thermistor string (X = -56 409 m, Y= -3 751 488 m) were deployed approximately 100 m southwest of the diffuser at a depth of -27.6 m CD. The locations are shown in Figure 5-13.

5.2.1 Waves

A wave refraction plot for a west-south-westerly wave event is shown in Figure 5-13.

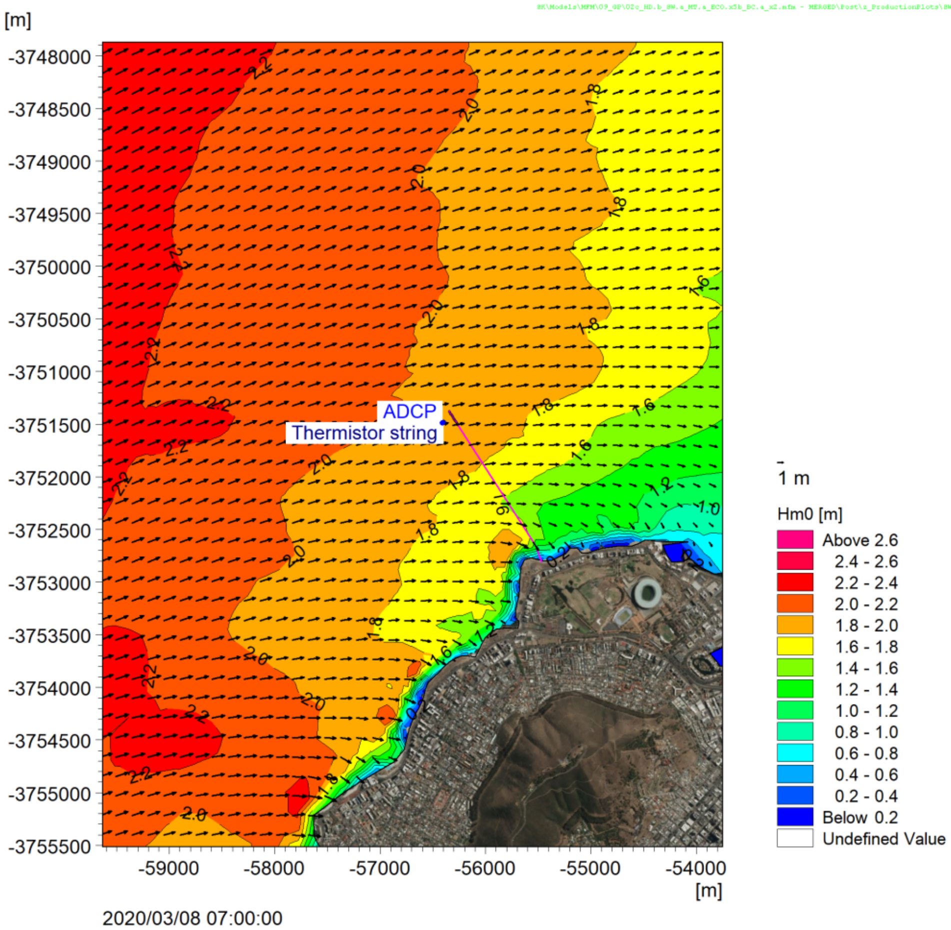

Figure 5-13: Summer/autumn: Wave refraction plot for a west-south-westerly wave event. The modelled wave condition at the ADCP is H_{m0} = 1.94 m, T_P = 15.1 s, D_{MP} = 259˚.

Figure 5-14 presents a time series comparison of measured and modelled wave parameters at the ADCP. Measured and modelled wave roses are shown in Figure 5-15.

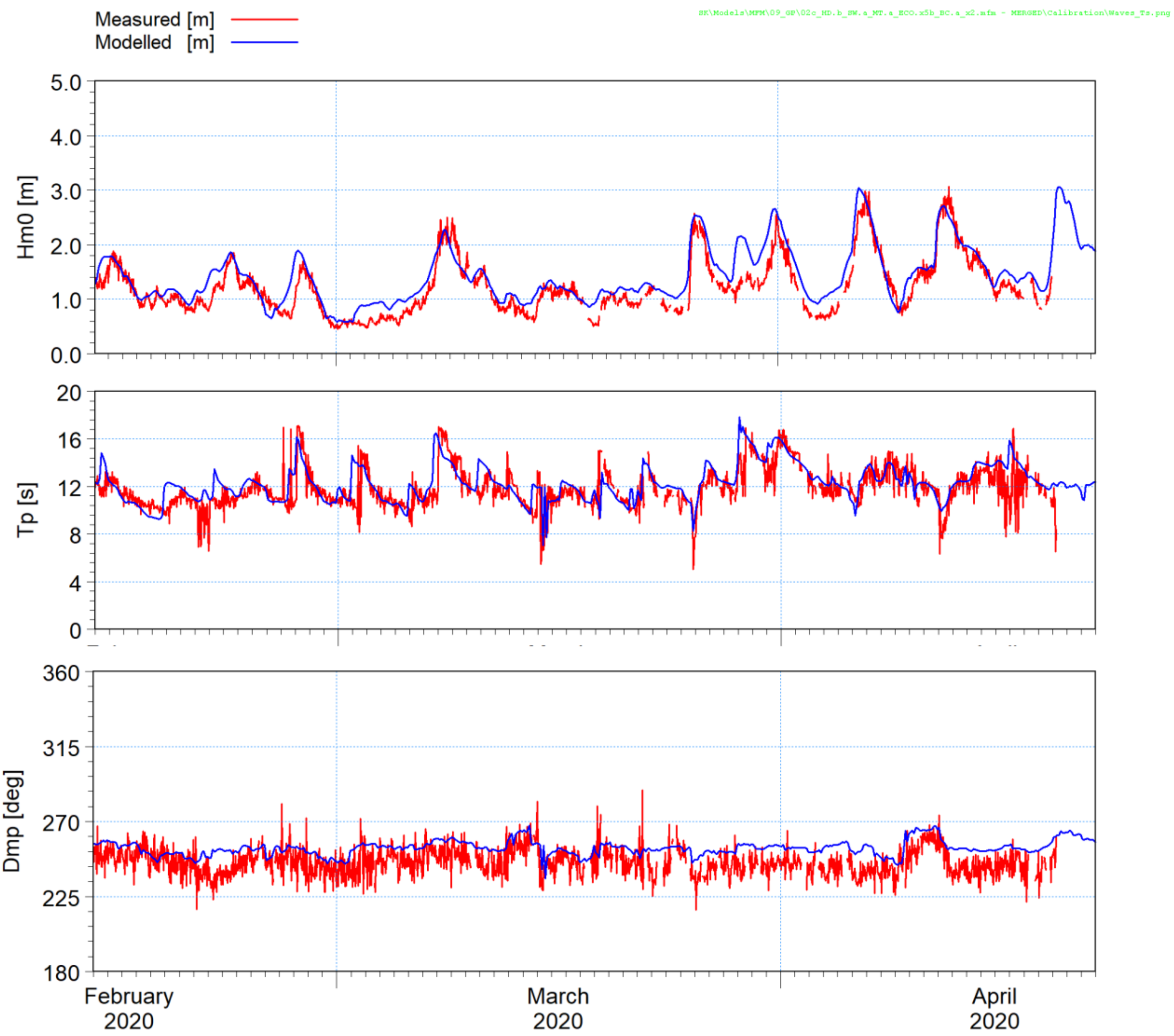

Figure 5-14: Summer/autumn: Time series of measured and modelled significant wave height (H_{m0}), peak wave period (T_P) and mean wave direction at Tp (D_{MP}) at the location of the ADCP.

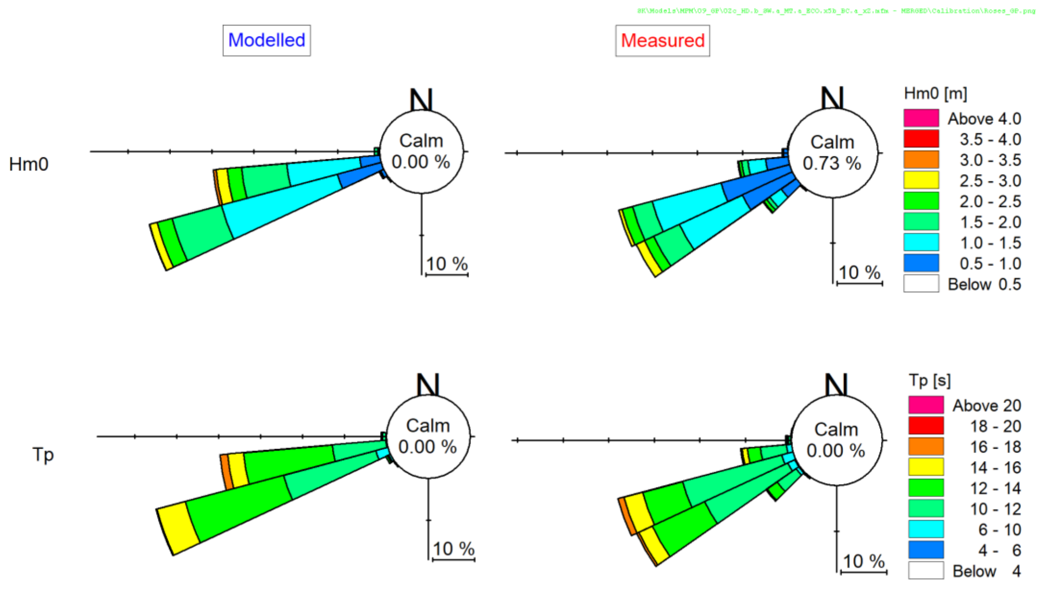

Figure 5-15: Summer/autumn: Wave roses of measured and modelled H_{m0} and T_P for the 10-week deployment period at the location of the ADCP.

The significant wave height is occasionally over- or underpredicted by the model, but there is no systematic bias. There is a good correlation between modelled and measured peak wave period and wave directions, but the latter shows a constant offset of about 10°. Overall the model shows sufficient for the purposes of this study.

5.2.2 Water levels

The predicted tidal levels at the Port of Cape Town (X = -539 934 m, Y = -3 752 769 m) were extracted from the MIKE by DHI CMAP Electronic Charts Database (DHI, 2020i). Figure 5-16 presents a time series comparison of modelled water levels to predicted tides at the Port of Cape Town. A water level probability of non-exceedance plot is shown in Figure 5-17 for the Port of Cape Town.

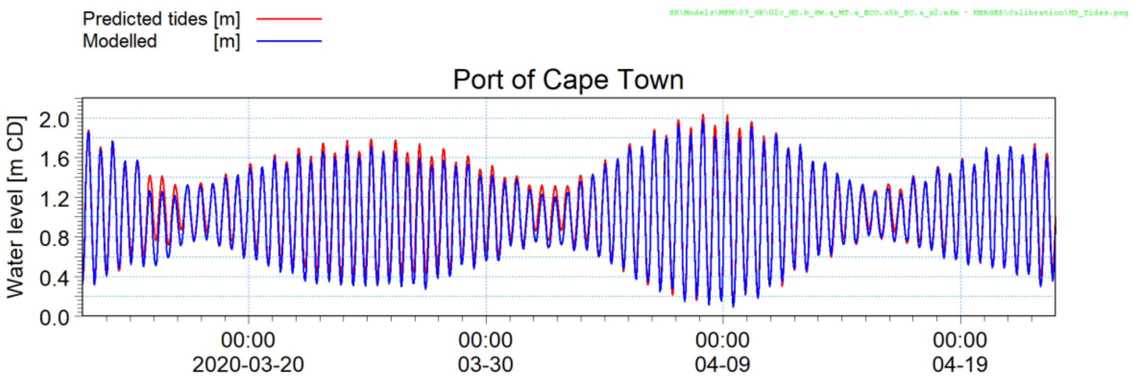

Figure 5-16: Summer/autumn: Time series comparison of modelled water levels to predicted tides at the Port of Cape Town.

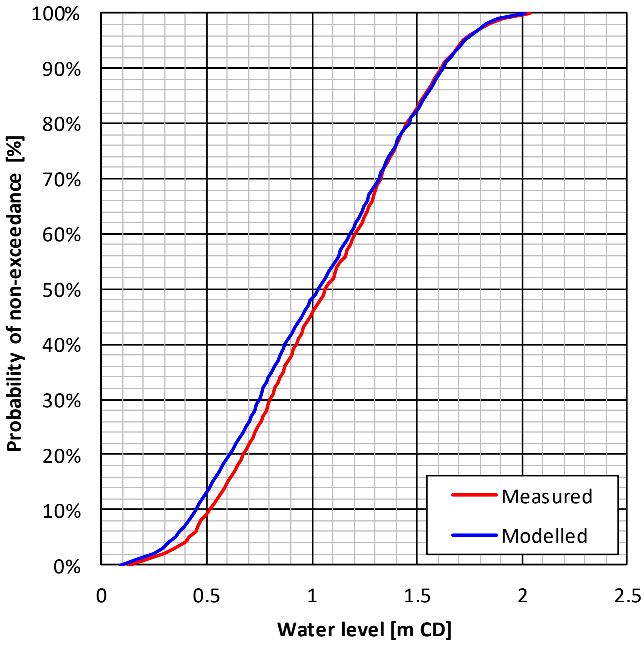

) x5b_BC a_x2 m fm -MERGED\Calibration\[CompareTs_HD_Tides.xlsx]Graphs

Probability of non-exceedance	Water level [m CD]	
	Measured	Modelled
5%	0.42	0.35
10%	0.51	0.45
20%	0.67	0.61
30%	0.80	0.75
50%	1.07	1.03
70%	1.32	1.32
80%	1.45	1.46
90%	1.62	1.62
95%	1.72	1.73

Figure 5-17: Summer/autumn: Probability of non-exceedance for predicted tides and modelled water levels for the 10-week period at the Port of Cape Town.

The model shows a good overall model prediction in both tidal phase and amplitude. The slight setdown observed during the first half of the calibration period is likely due to wind effects which are included in the model but not in the predicted tide.

5.2.3 Currents

A contour plot of instantaneous currents during a west-south-westerly wave/southerly wind event is shown in Figure 5-18. The modelled currents were compared to the measurements near the seabed (5.0 m above the seabed) and near the surface (25 m above the seabed). Figure 5-19 presents a time series comparison of the modelled and measured currents at the ADCP. Non-exceedance curves of current speed for the 10-week period are shown Figure 5-20. Current rose comparisons of modelled and measured currents are presented in Figure 5-21.

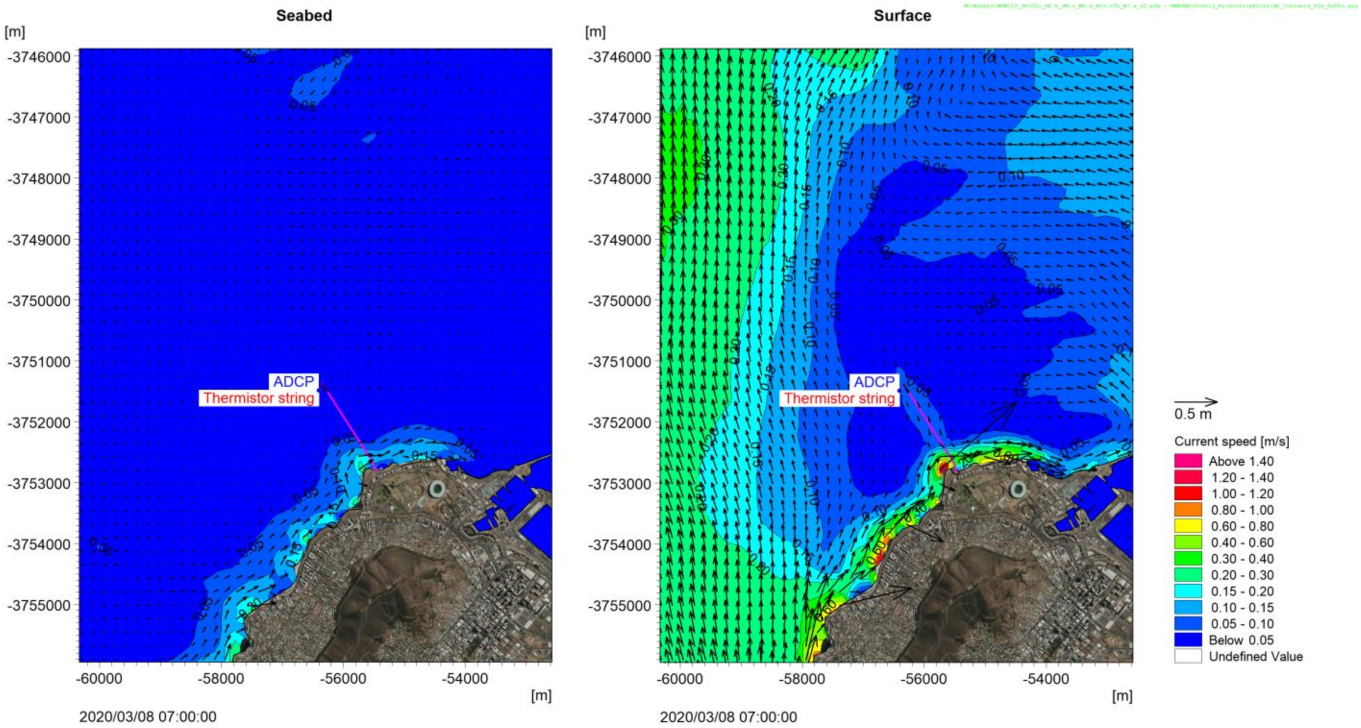

Figure 5-18: Summer/autumn: Contour plot of instantaneous seabed (left) and surface (right) currents during a west-south-westerly wave/southerly wind event (shown in Figure 5-13).

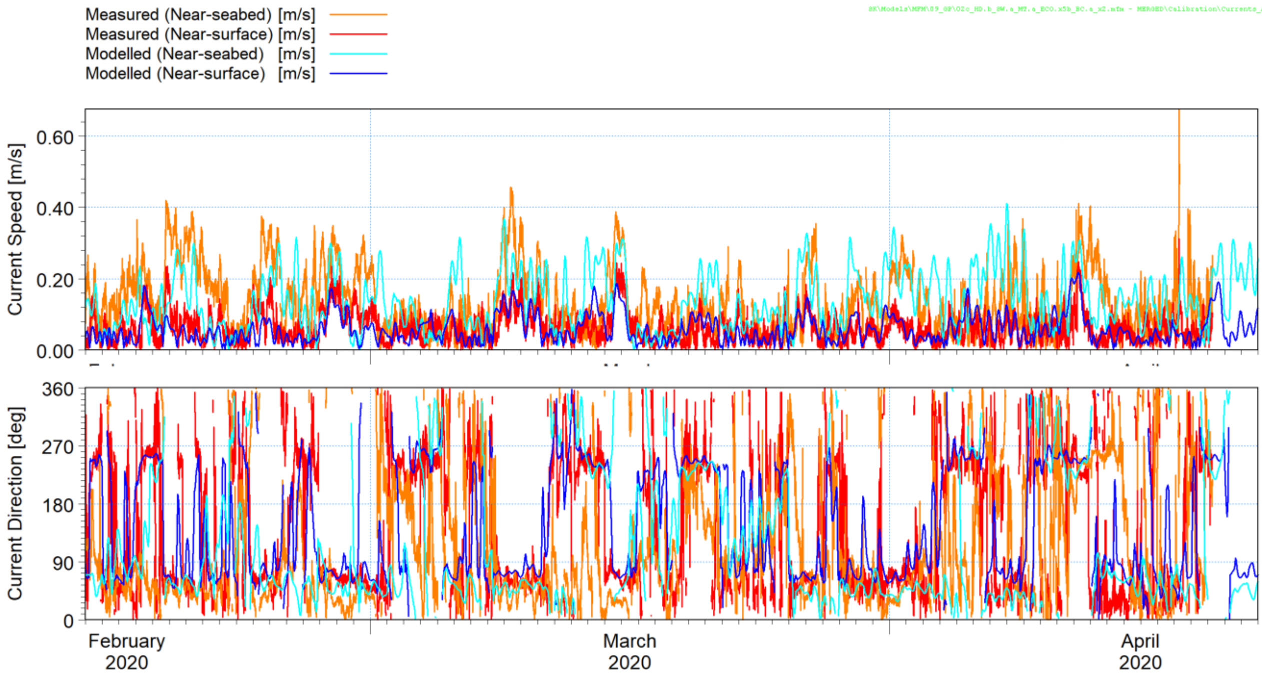

Figure 5-19: Summer/autumn: Time series comparison of measured and modelled current speed and direction at the ADCP.

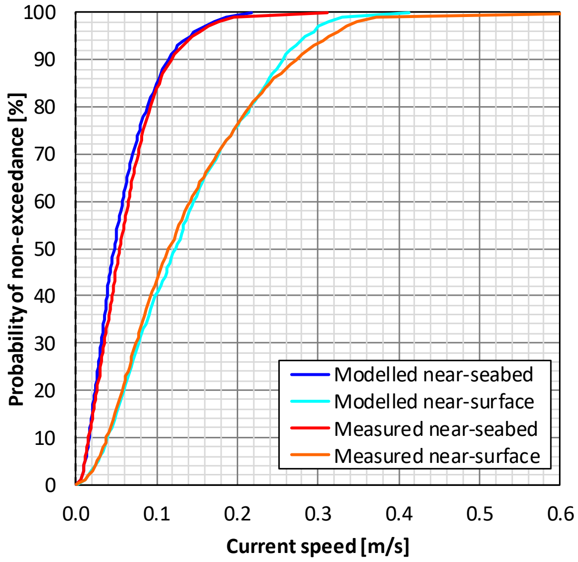

Proability of non-exceedance [%]	Current speed [m/s]			
	Near-seabed		Near-surface	
	Modelled	Measured	Modelled	Measured
10	0.02	0.02	0.04	0.04
20	0.02	0.03	0.06	0.06
30	0.03	0.04	0.08	0.07
40	0.04	0.05	0.10	0.09
50	0.05	0.05	0.12	0.12
60	0.06	0.07	0.15	0.14
70	0.07	0.08	0.18	0.18
80	0.09	0.09	0.22	0.22
90	0.11	0.12	0.26	0.27

Figure 5-20: Summer/autumn: Probability of non-exceedance for measured and modelled current speed for the 10-week deployment period at the ADCP.

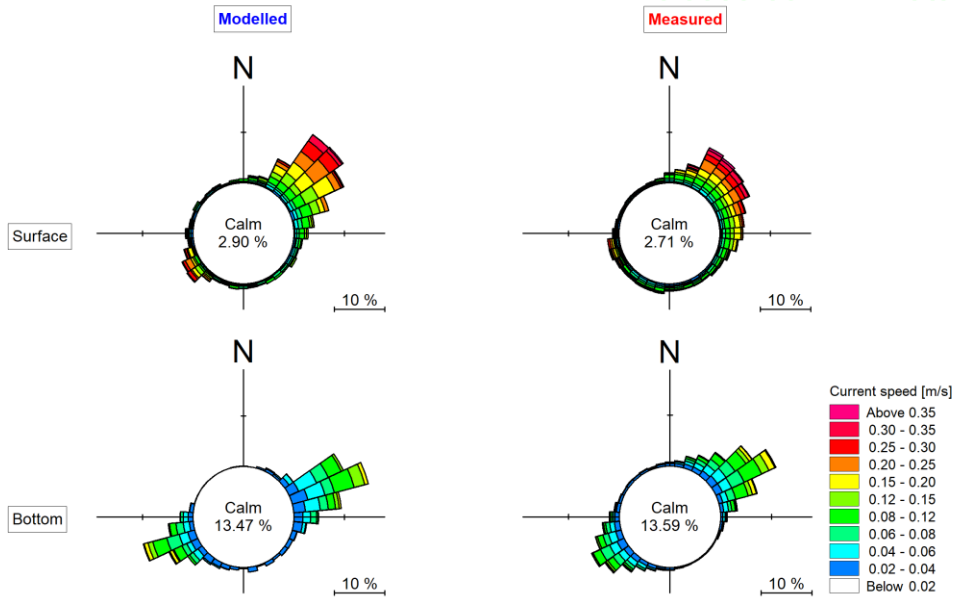

Figure 5-21: Summer/autumn: Measured and modelled current roses for the 10-week deployment period at the ADCP.

The model shows a good correlation with the measured operational current speeds while underpredicting some of the stronger near-surface currents. The dominant current directions are well represented at both depths.

The model is able to reproduce the main features of the currents and is considered to be acceptable for the purposes of this study.

5.2.4 Temperature

The modelled seawater temperatures were compared to measurements near the seabed (1.9 m above the seabed), mid-depth (11.6 m above the seabed) and at the surface (0.5 m to 1 m below the surface). Figure 5-22 presents a time series comparison of the modelled and measured seawater temperatures. Non-exceedance curves of seabed, mid-depth and surface temperatures for the 10-week period are shown Figure 5-23. Figure 5-24 presents a non-exceedance curve of stratification (near-seabed to mid-depth and near-seabed to surface) from the measured and modelled temperatures.

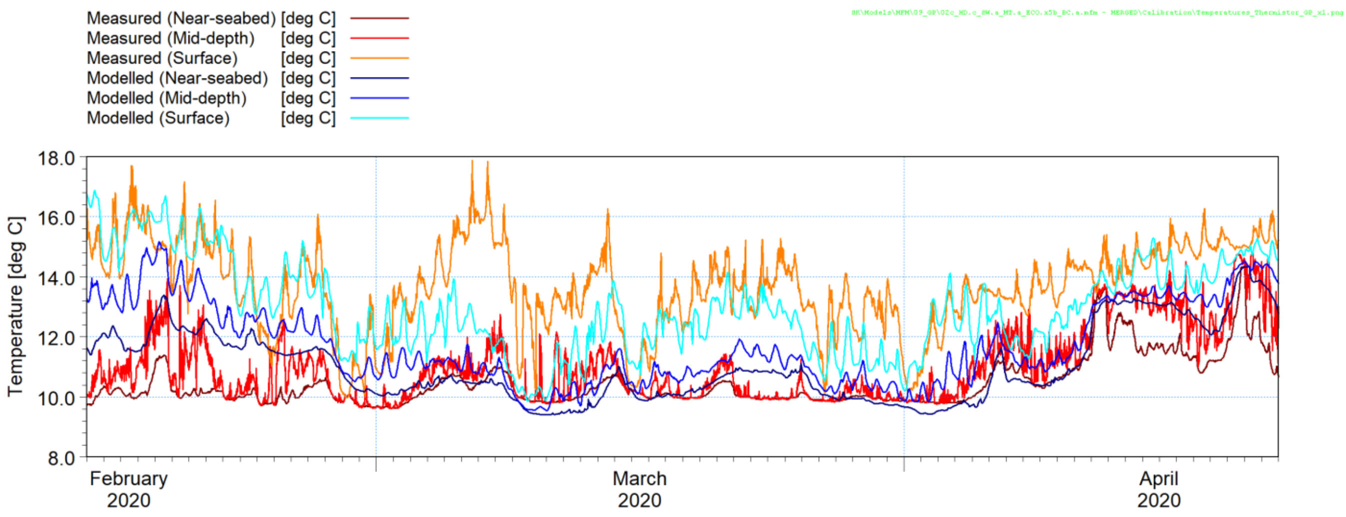

Figure 5-22: Summer/autumn: Time series of measured and modelled seawater temperatures.

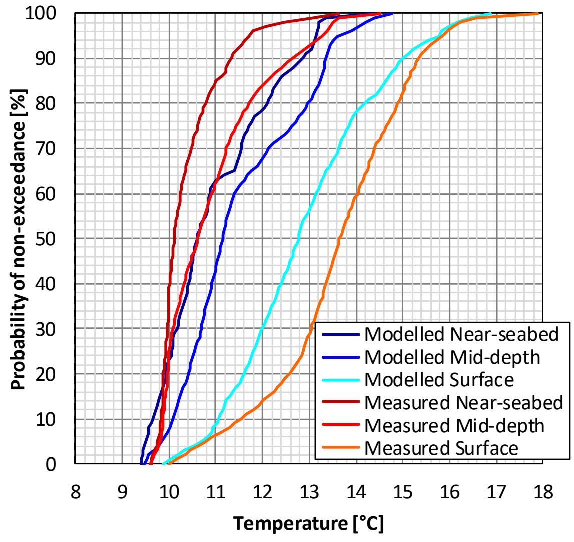

Probability of non-exceedance [%]	Temperature [°C] Near-seabed Modelled	Near-seabed Measured	Mid-depth Modelled	Mid-depth Measured	Surface Modelled	Surface Measured
10	9.7	9.8	10.1	9.9	11.1	11.5
20	9.9	9.9	10.4	10.0	11.6	12.6
30	10.2	10.0	10.7	10.1	12.0	13.0
40	10.4	10.0	10.9	10.3	12.4	13.4
50	10.6	10.1	11.1	10.6	12.8	13.6
60	10.9	10.2	11.4	10.9	13.2	14.1
70	11.5	10.5	12.1	11.2	13.6	14.4
80	12.1	10.8	13.0	11.7	14.2	14.9
90	12.9	11.3	13.4	12.7	15.0	15.3

Figure 5-23: Summer/autumn: Probability of non-exceedance of measured and modelled seawater temperatures for the 10-week deployment period.

SK\Models\MFM\09_GP\02c_HD.c_SW a_MTa_ECO.x5b_BC.am.fm - MERGED\Calibration\[Summary_Exceedance_Plots_R0.xlsx]Stratification

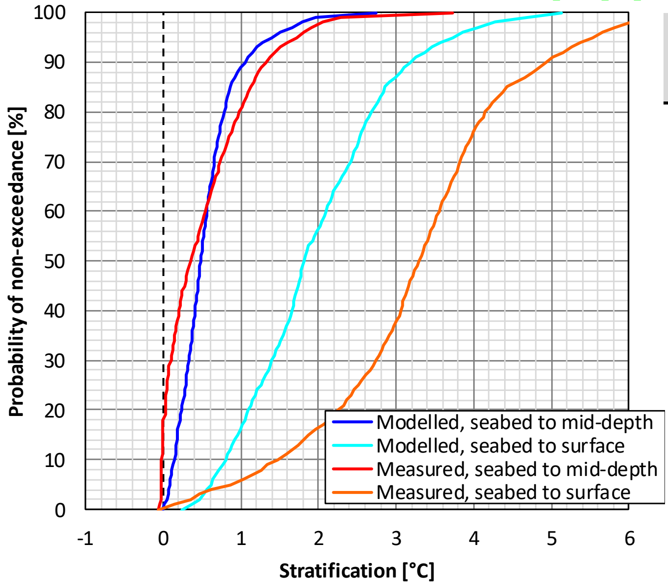

Proability of non-exceedance [%]	Stratification [°C] Seabed to mid-depth		Seabed to surface	
	Modelled	Measured	Modelled	Measured
10	0.14	-0.02	0.81	1.47
20	0.24	0.02	1.10	2.25
30	0.33	0.10	1.40	2.75
40	0.41	0.20	1.65	3.06
50	0.48	0.34	1.80	3.30
60	0.56	0.54	2.09	3.56
70	0.66	0.73	2.42	3.82
80	0.78	0.98	2.68	4.15
90	1.05	1.32	3.17	4.93

Figure 5-24: Summer/autumn: Probability of non-exceedance of measured and modelled seawater temperature stratification (near-seabed to mid-depth and near-seabed to surface) for the 10-week deployment period.

The measured time series shows that the seawater temperatures are complex and vary over a range of time-scales due to upwelling, solar radiation and other dynamic processes. The model is able to predict the mean trend in seabed seawater temperatures including some of the discrete dynamic events. The model shows the sub-surface temperatures tend to be overpredicted while the surface temperatures tend to be underpredicted. Note that the surface temperature was measured between 0.5 m and 1 m below the surface, whereas the surface temperature of the model is averaged over 2.3 m due to the vertical mesh resolution. The modelled near-seabed to mid-depth stratification varies between over- and under-prediction but shows a fair comparison to the measurements, while the seabed to surface stratification is underpredicted by the model. Since the near-field mixing is more sensitive to temperature gradients closer to the diffuser, i.e. lower in the water column, the model is considered to be adequately calibrated for seawater temperature for the purposes of this study.

6. MODEL RESULTS

6.1 Winter/spring

The outfall dispersion model was run for a 10-week period between 1 August 2019 and 9 October 2019 to represent environmental conditions for winter and spring.

The model outputs are the concentrations of E.coli, enterococci, TSS and a conservative tracer in each horizontal and vertical element of the computational mesh at 1-hour intervals throughout the simulation period.

6.1.1 Plume dynamics

Figure 6-1 and Figure 6-2 present examples of the current vectors and E.coli plume at a moment in time for a southerly and north-westerly wind condition. These results show the complex 3D dynamic behaviour of the plume.

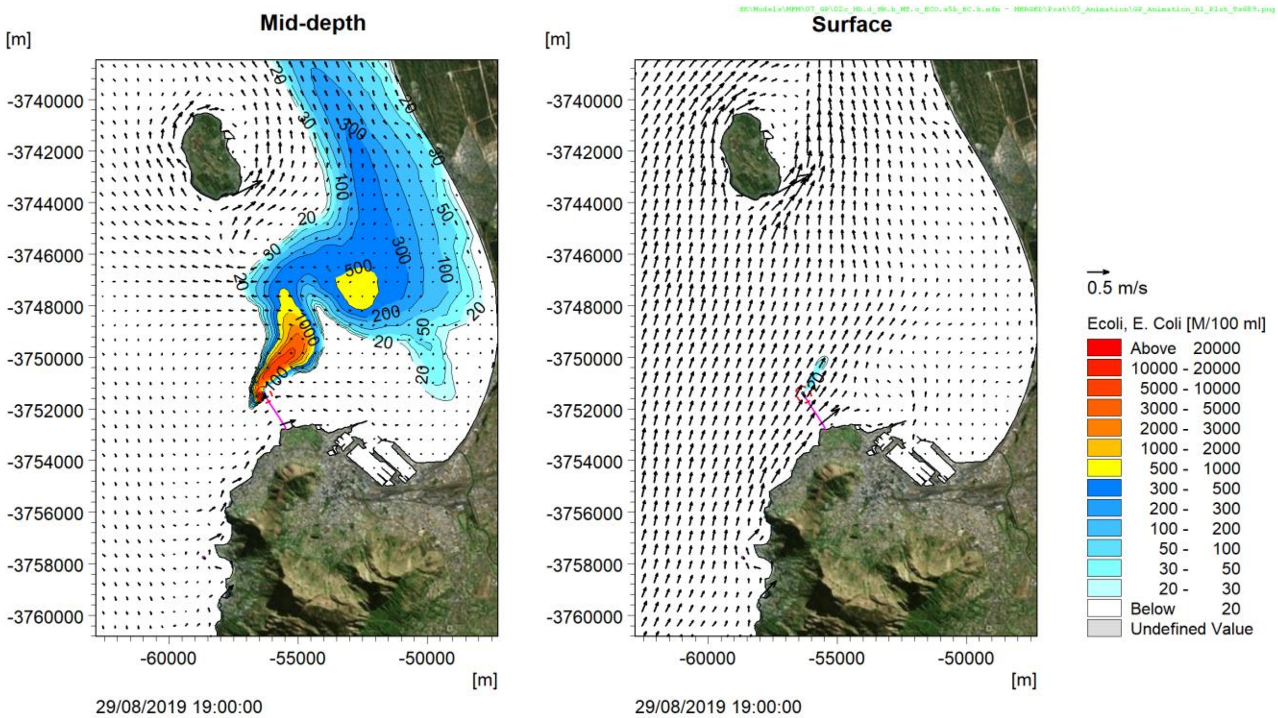

Figure 6-1: Winter/spring: Current vectors and E.coli plume at a moment in time during a southerly wind condition.

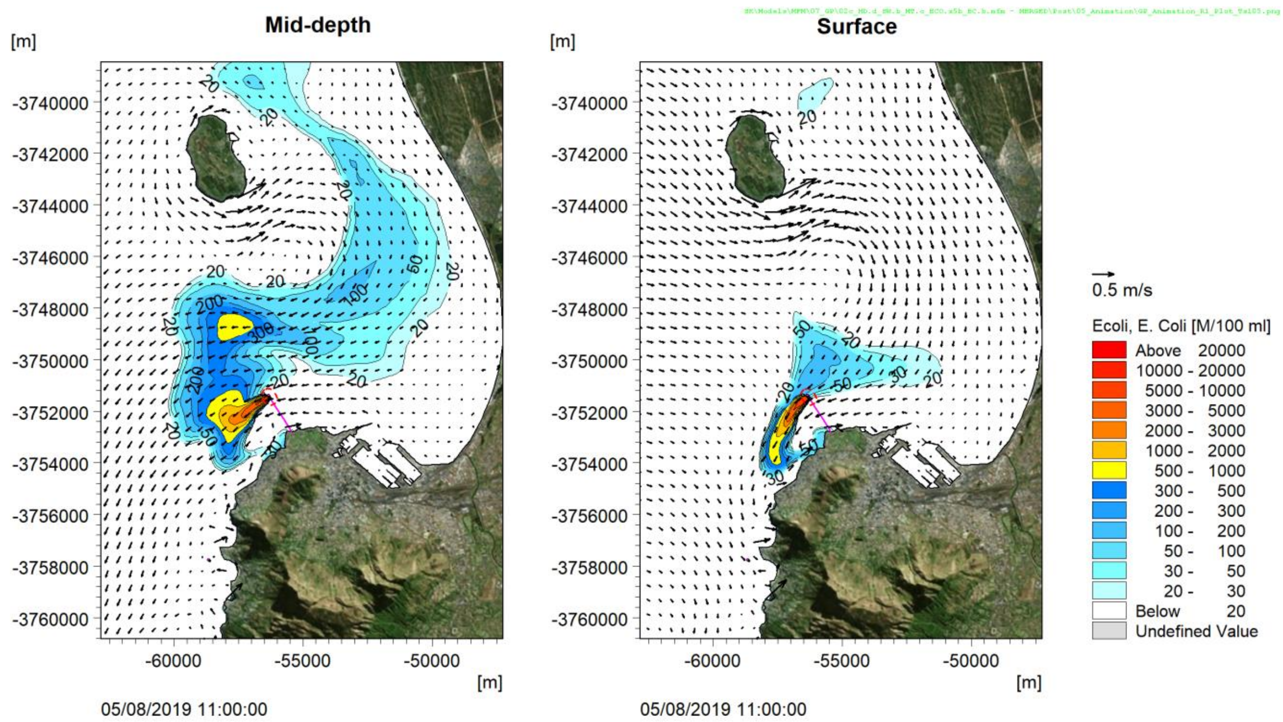

Figure 6-2: Winter/spring: Current vectors and E.coli plume at a moment in time during a north-westerly wind condition.

6.1.2 Dilutions

The concentrations from the conservative tracer were processed to number of dilutions using the equation:

$$Number\ of\ dilutions = \frac{Effluent\ concentration}{Dispersed\ concentration}$$

The modelled outputs were further processed to extract the 5th percentile number of dilutions in each horizontal and vertical element of the computational mesh. The 5th percentile number of dilutions will be exceeded 95% of the time and are thus close to the expected minimum number of dilutions (i.e. close to the worst case).

Figure 6-3, Figure 6-4 and Figure 6-5 present the 5th percentile dilutions at the seabed, mid-depth and surface. Mid-depth is the depth below the surface equal to 60% of the local water depth, which was selected as the worst dilutions at Green Point occurred at this depth. Figure 6-6 shows a cross section of the 5th percentile number of dilutions extracted along the longest axis of the plume (marked by the dashed green line on the contour plots). Dilutions less than 2 000 are shown in orange as this is close to the dilution required for TSS of 1 753 as discussed in Section 3.4.1. Dilutions greater than 2 000 are shown in shades of blue. Although these exceed the required dilutions for the identified critical constituents, they provide information on the far-field behaviour of the plume.

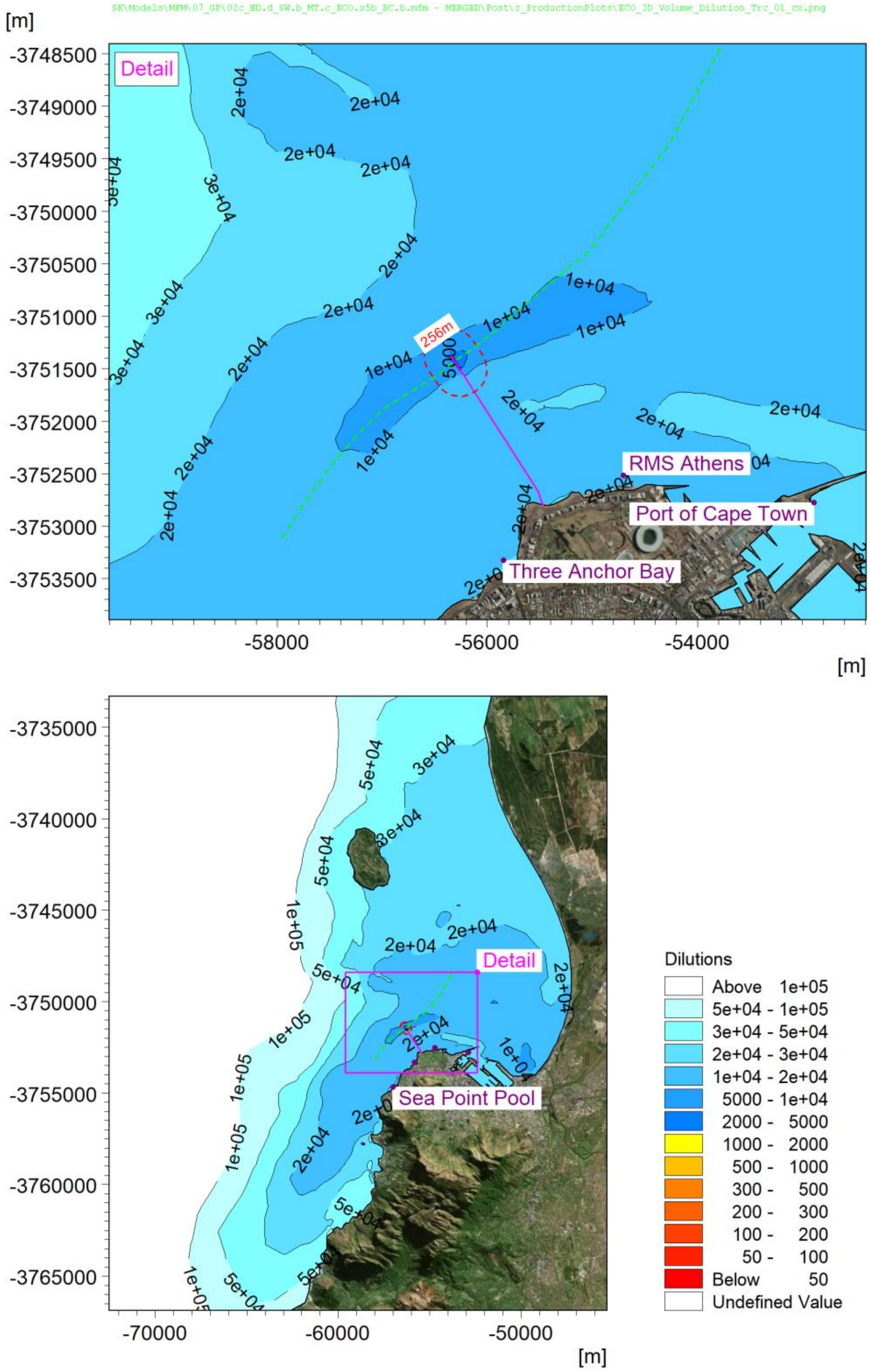

Figure 6-3: Winter/spring: Number of dilutions at the seabed, 5th percentile.

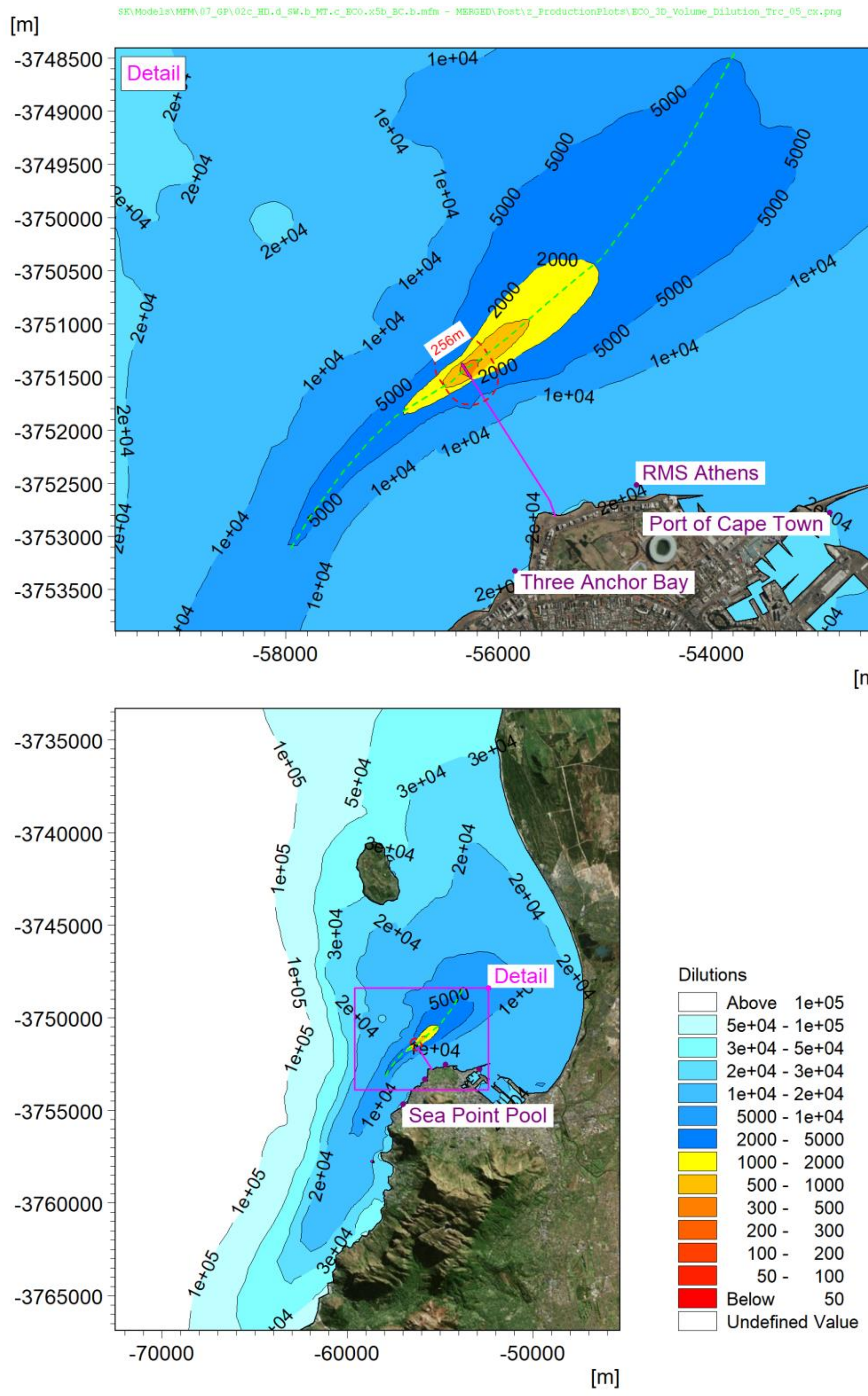

Figure 6-4: Winter/spring: Number of dilutions at mid-depth, 5th percentile.

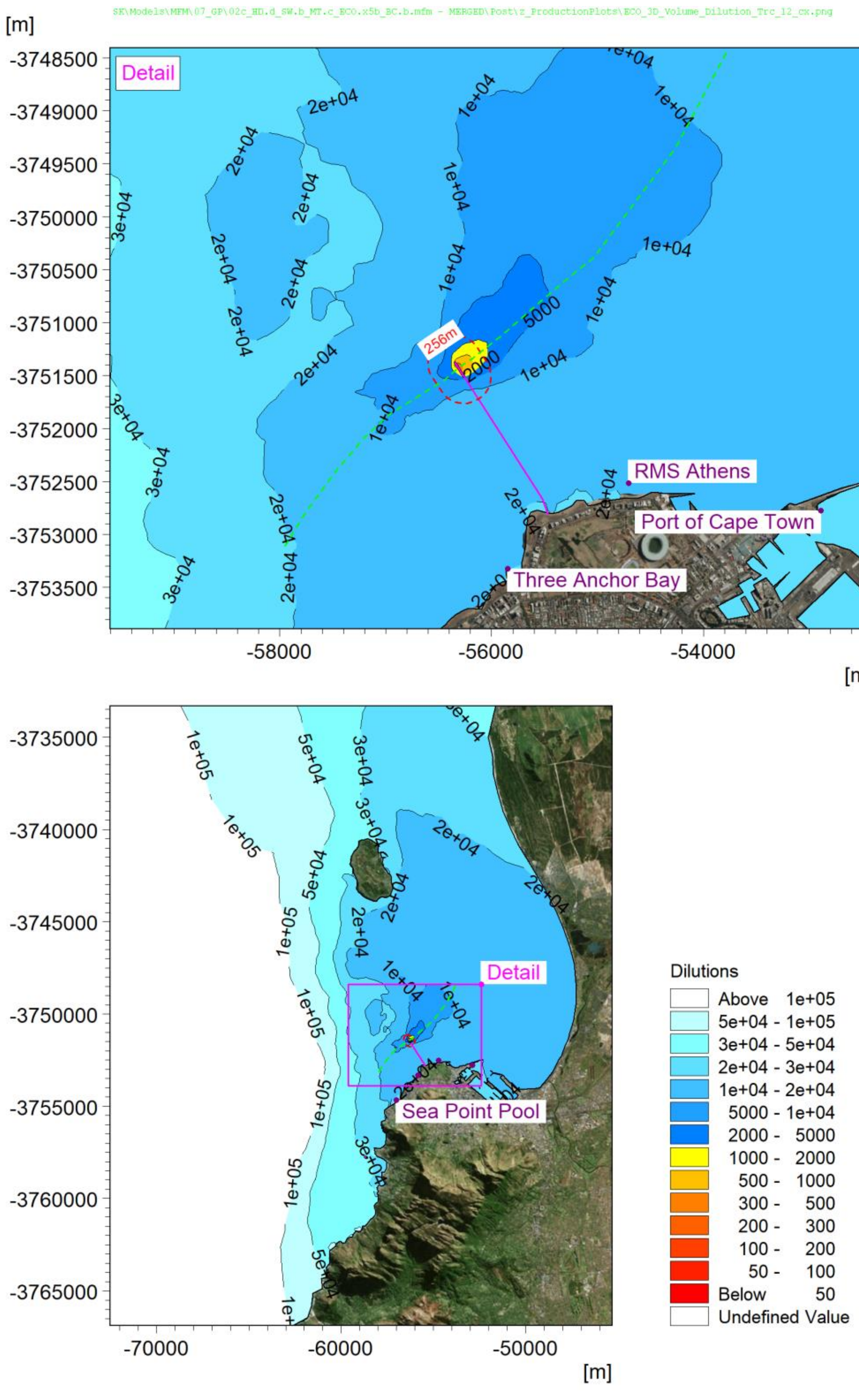

Figure 6-5: Winter/spring: Number of dilutions at the surface, 5th percentile.

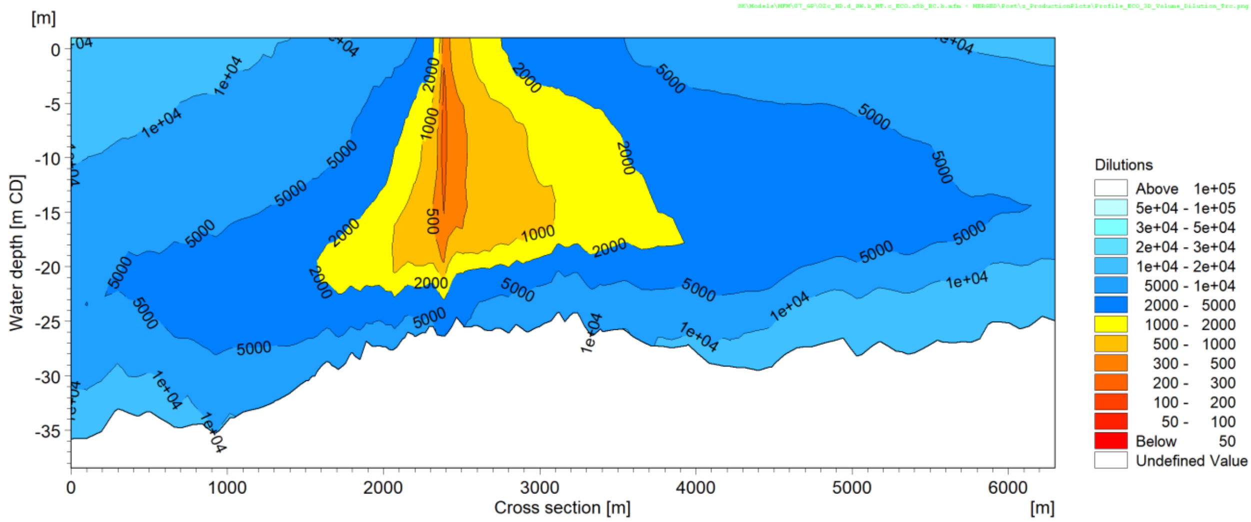

Figure 6-6: Winter/spring: Cross-section of 5th percentile number of dilutions.

The minimum dilutions achieved at the edge of the mixing zone was extracted from the 5th percentile dilutions and is presented Table 6-1.

Table 6-1: Winter/spring: Minimum number of dilutions achieved at the edge of the mixing zone.

Parameter	Value
Minimum number of dilutions achieved at any depth along the edge of the allowable mixing zone (radius = 256 m), 5th percentile	528

The distance from the diffuser to achieve the required dilutions for the three critical constituents (Table 3-4) are presented in Table 6-2.

Table 6-2: Winter/spring: Distance to achieve dilutions, 5th percentile.

Constituent	Dilutions required	Distance
Ammonia	106	< 25 m
COD	51	< 25 m
TSS	1 753	1 400

The spreading of the mixing zone is dominated by the longshore currents. South-west of the diffuser the currents are characterised by a narrower stream following the coastline. North-east of the diffuser the currents exhibit more two-dimensional features (i.e. variability in flow directions and horizontal eddies as the plume is advected towards Table Bay) which increases the mixing and spreading of the plume.

The effluent plume rises due to its buoyancy and usually becomes passive at mid-depth due to mixing with the ambient currents or trapping by stratification. Periodic surfacing of the plume happens during periods of high effluent flows or stagnant hydrodynamic conditions.

The minimum number of dilutions achieved in the allowable mixing zone is 528. The constituent requiring the highest dilutions is TSS, which achieved the 1 753 required dilutions 1 400 m from the diffuser. Ammonia and COD achieved the required dilutions in within 25 m. Note that distances smaller than 25 m could not be measured in the model, due to the mesh resolution.

6.1.3 Bacteria

In addition to dilutions by hydrodynamic processes the bacterial concentrations are further reduced due to bacterial die-off (as described in Section 2.3.2). Figure 6-7 presents the surface and seabed T_{90} values for E.coli and enterococci, extracted in the middle of the Green Point diffuser at a depth of -26.0 m CD. Recall from Section 2.3.2.1 the median T_{90} ratio of enterococci to E.coli is 2.39.

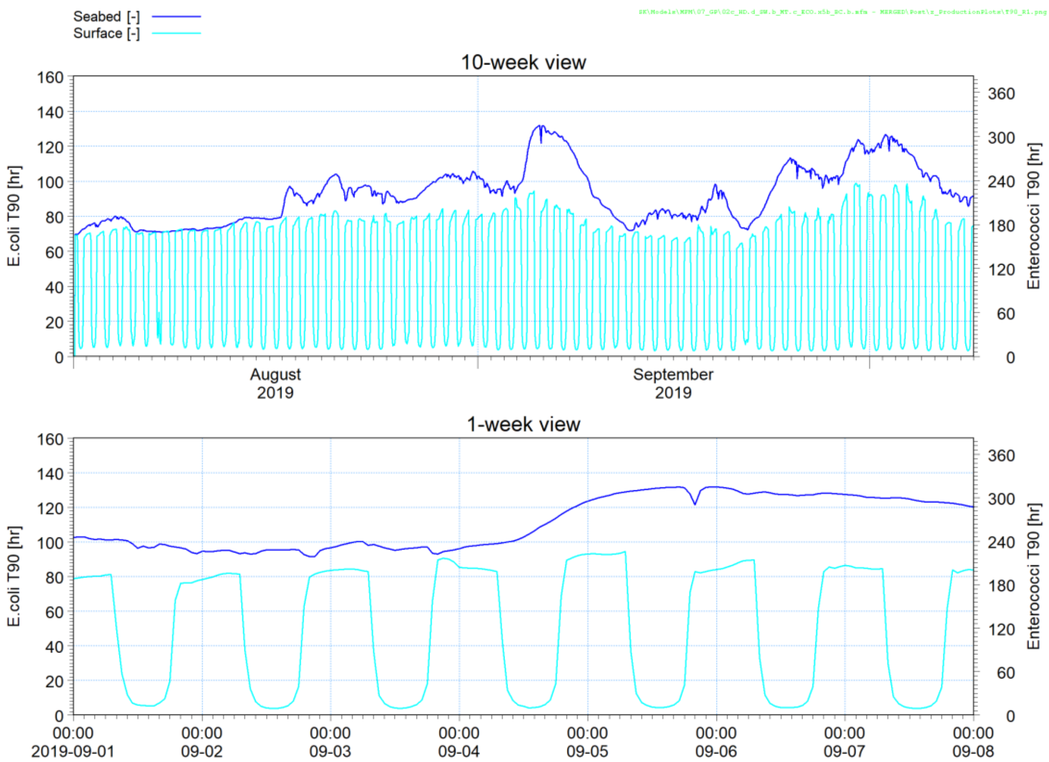

Figure 6-7: Winter/spring: Surface and seabed T_{90} values for E.coli and enterococci.

A significant diurnal variation in die-off rates due to the solar radiation can be observed at the surface, while the seabed remains mostly unaffected due to light attenuation. In the absence of light, the seawater temperature dominates the die-off processes and the stratification determines the gradient between the surface and seabed T_{90} values.

Based on the DEA guidelines (Table 3-5), the model outputs of bacterial concentrations were further processed to extract the 90th percentile concentration at each horizontal and vertical element of the computational mesh for the full simulation period. The 90th percentiles were only sampled during daylight hours (between 07:00 to 18:00) to emulate the recommended microbiological sampling regime in the guidelines.

6.1.3.1 E.coli

Figure 6-8, Figure 6-9 and Figure 6-10 present the 90th percentile E.coli concentrations at the seabed, mid-depth and surface. Concentrations greater than 500 CFU/100 ml are shown in orange as this is the guideline for E.coli as discussed in Section 3.4.2. Concentrations less than 500 CFU/100 ml are shown in shades of blue. Although these are less than the guideline, they provide information on the far-field behaviour of the plume. A time series of highest E.coli concentrations at any depth at four key locations (Port of Cape Town, RMS

Athens wreck (Thermopylae surf spot), Three Anchor Bay and Sea Point Pool) is shown in Figure 6-11. The locations are shown in the contour plots.

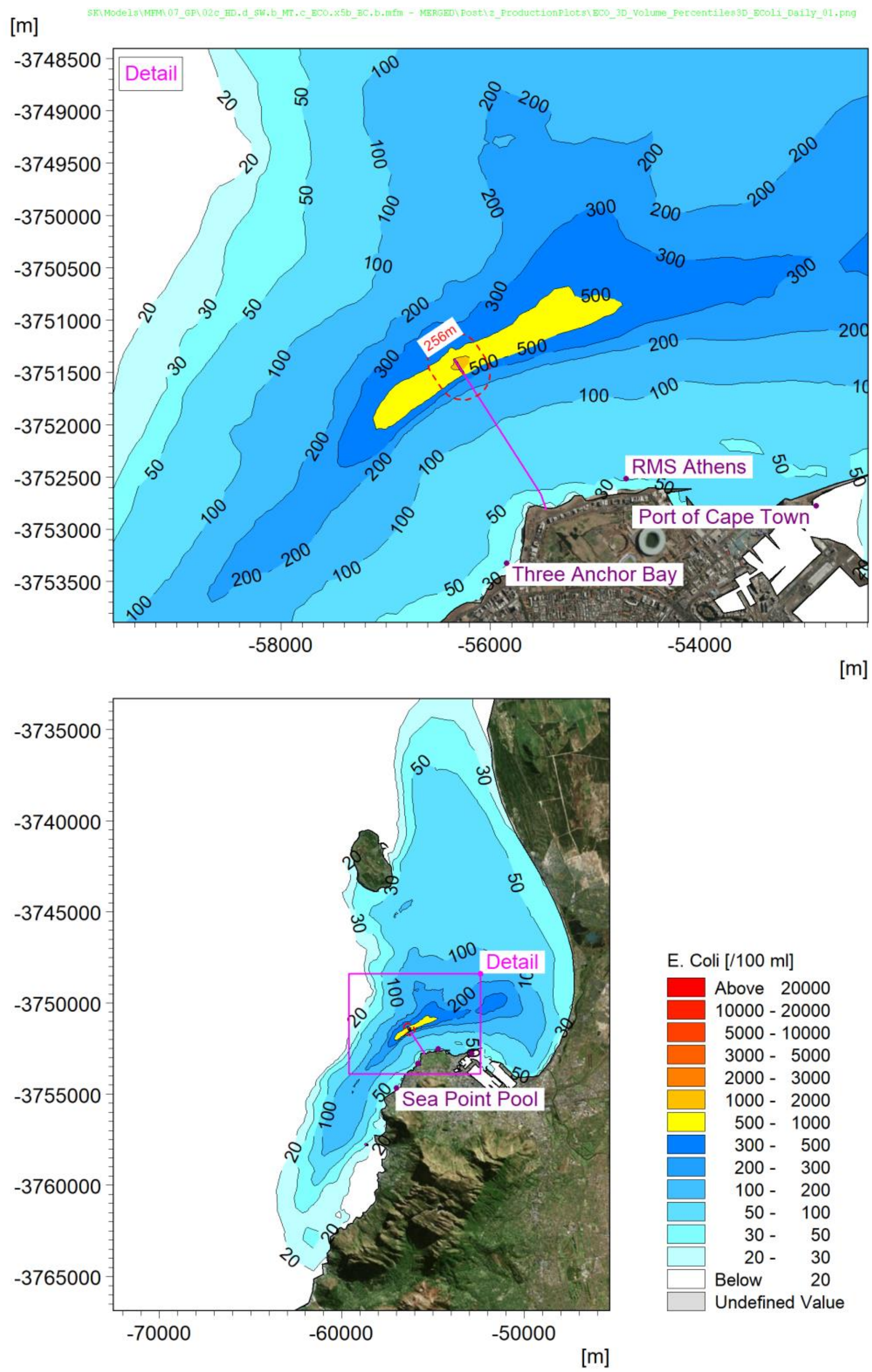

Figure 6-8: Winter/spring: E.coli concentration at the seabed, 90th percentile for daylight hours (07:00 – 18:00).

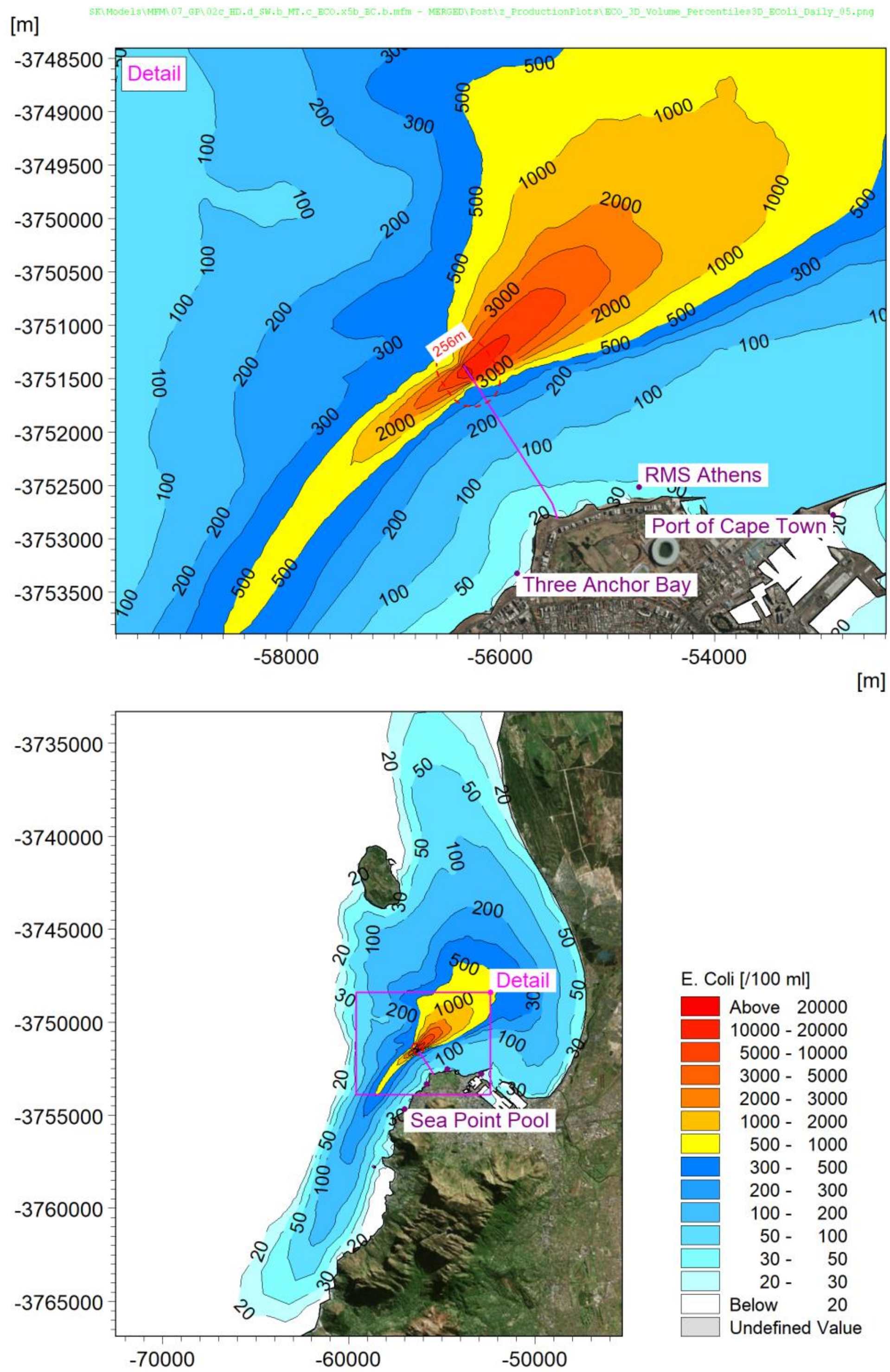

Figure 6-9: Winter/spring: E.coli concentration at mid-depth, 90th percentile for daylight hours (07:00 – 18:00).

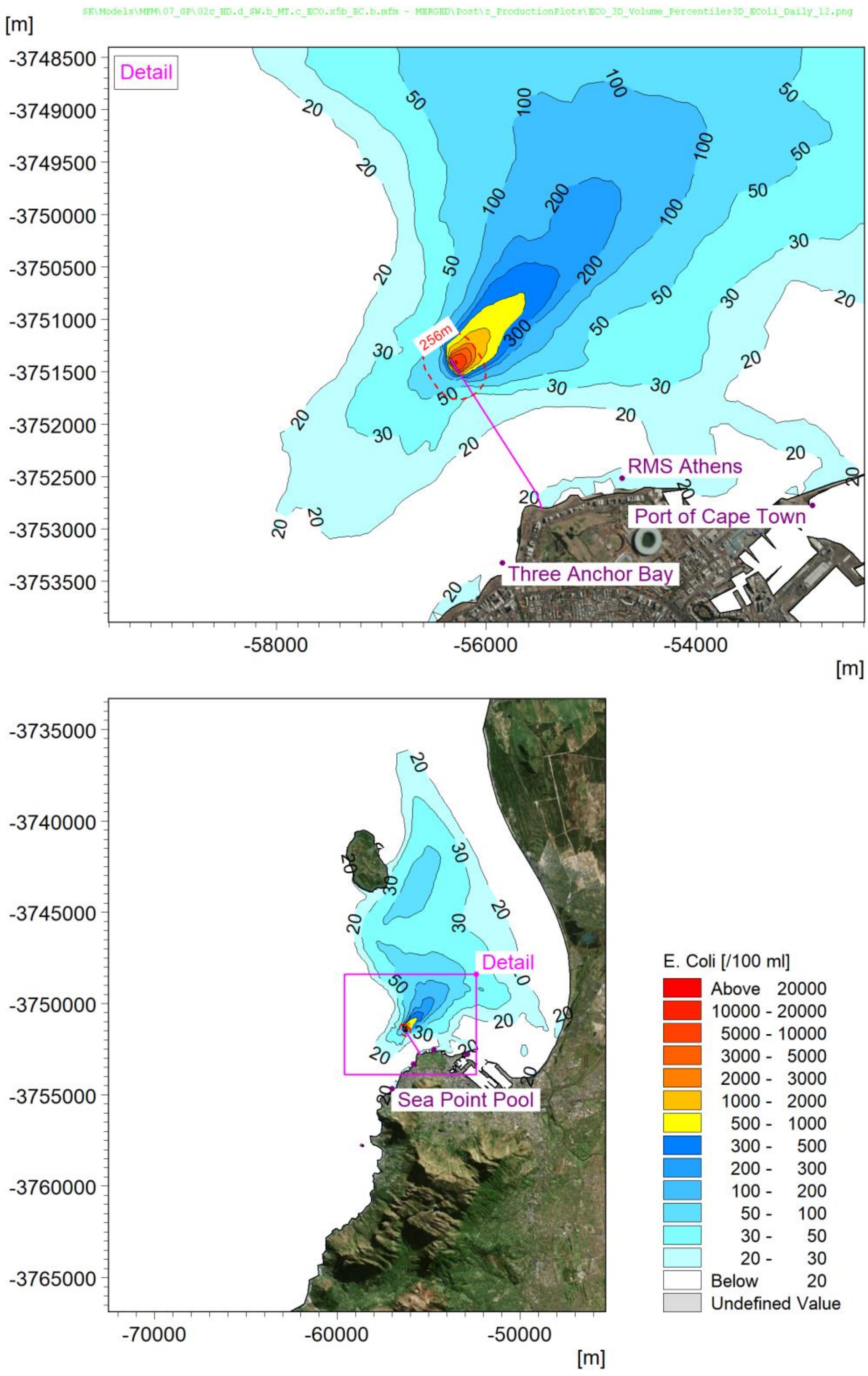

Figure 6-10: Winter/spring: E.coli concentration at the surface, 90th percentile for daylight hours (07:00 – 18:00).

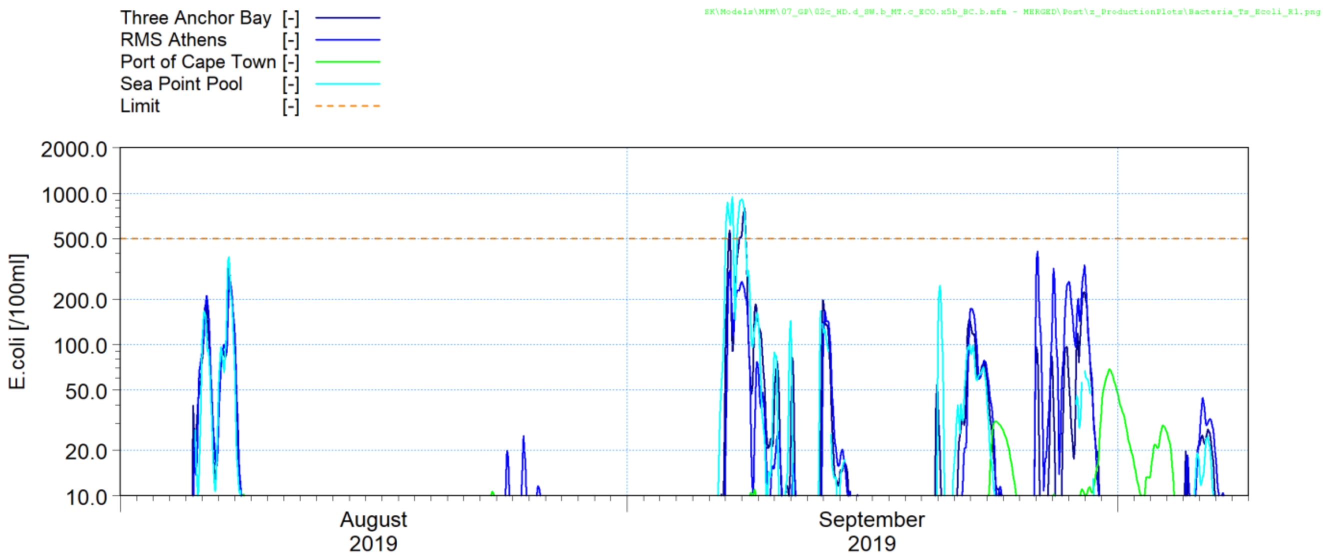

Figure 6-11: Winter/spring: Time series of highest E.coli concentration at any depth at four key locations. The water quality guideline (500 CFU/100 ml 90th percentile in daylight) is also shown in orange.

A mixing zone distance of 6 300 m was required to meet the 90th percentile water quality guideline of 500 CFU/100 ml. The contour plots show that the 90th percentile E.coli concentrations were the highest at mid-depth and concentrations above the 500 CFU/100 ml guideline did not intersect with the shoreline. The E.coli concentrations at the key locations only exceeded 500 CFU/100 ml on two occasions in the 10-week winter/spring period. Since the duration of this event was less than 10% of the daylight time these locations met the water quality guidelines.

6.1.3.2 Enterococci

Figure 6-12, Figure 6-13 and Figure 6-14 present the 90th percentile enterococci concentrations at the seabed, mid-depth and surface. Concentrations greater than 185 CFU/100 ml are shown in orange as this is the guideline for enterococci as discussed in Section 3.4.2. Concentrations less than 185 CFU/100 ml are shown in shades of blue. Although these are less than the guideline, they provide information on the far-field behaviour of the plume. A time series of enterococci concentrations at four key locations is shown in Figure 6-15.

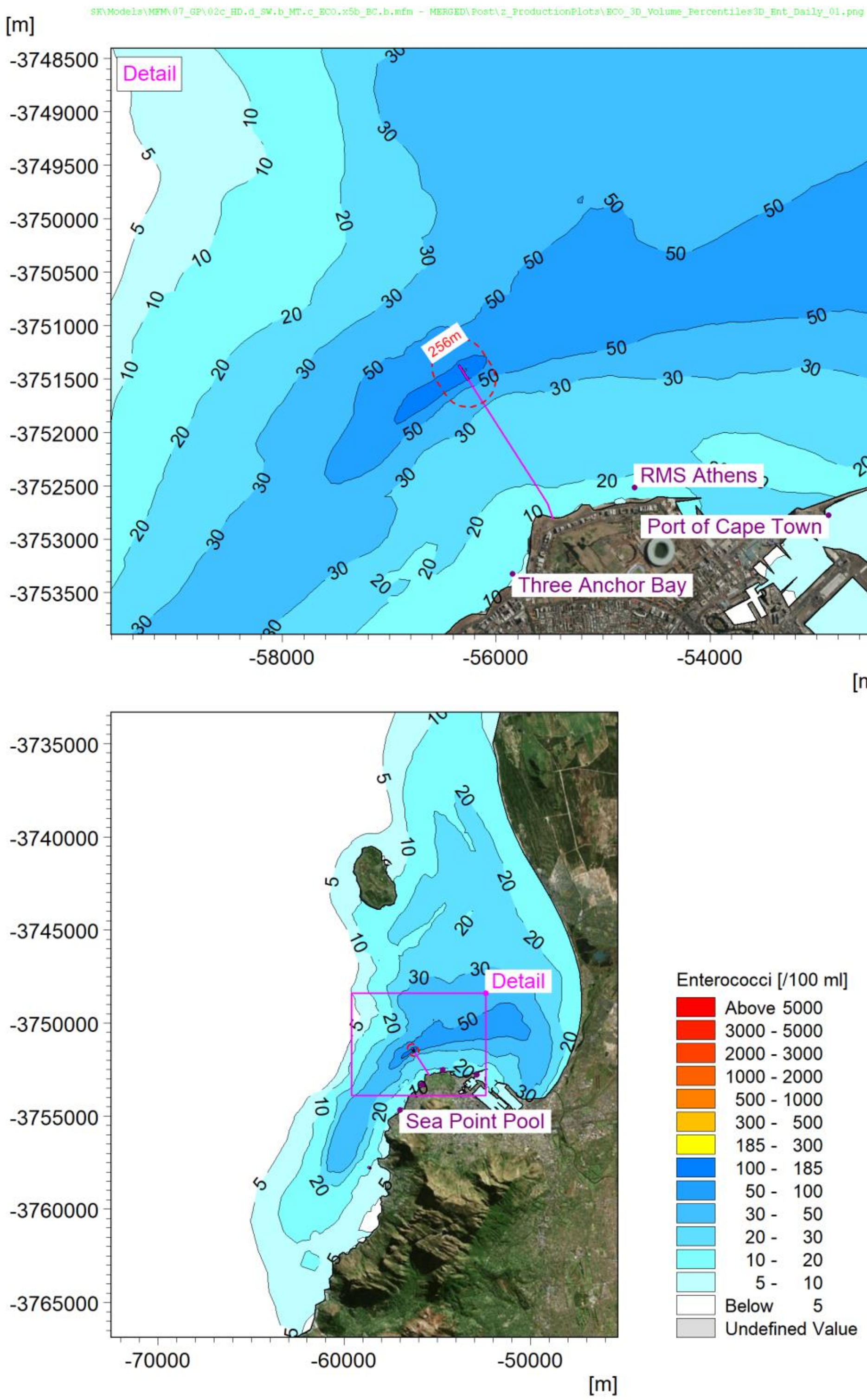

Figure 6-12: Winter/spring: Enterococci concentration at the seabed, 90th percentile for daylight hours (07:00 – 18:00).

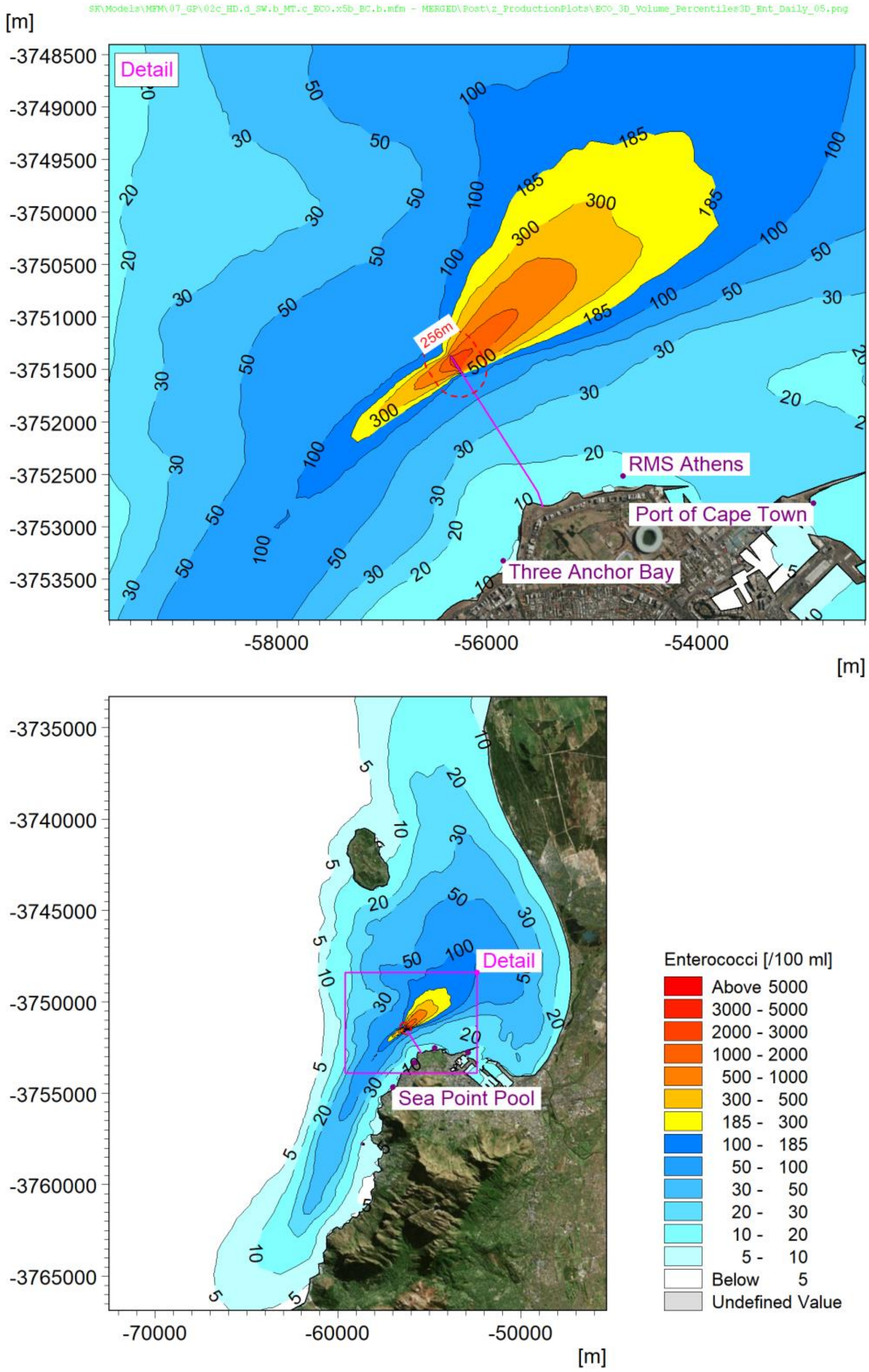

Figure 6-13: Winter/spring: Enterococci concentration at mid-depth, 90th percentile for daylight hours (07:00 – 18:00).

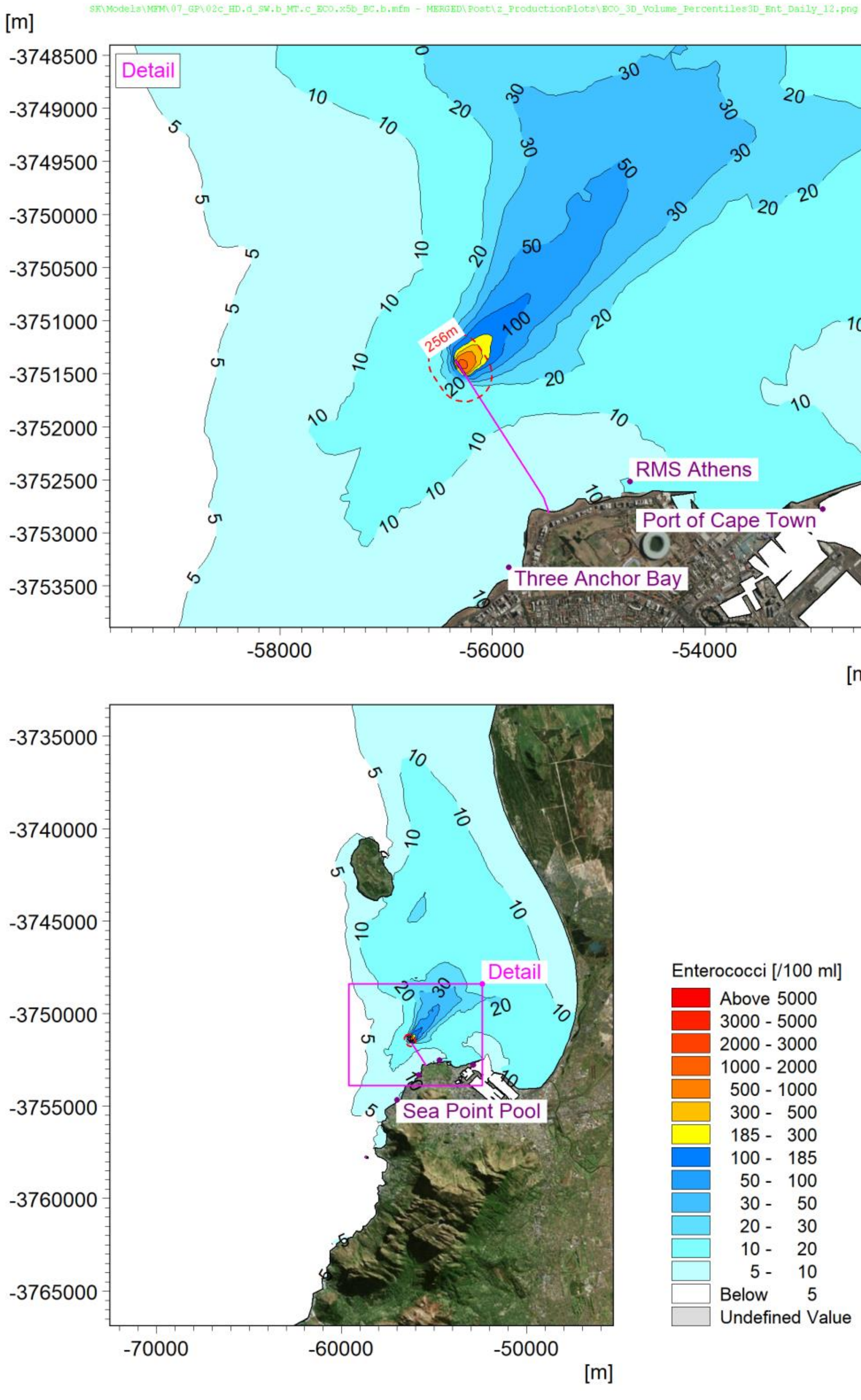

Figure 6-14; Winter/spring: Enterococci concentration at the surface, 90th percentile for daylight hours (07:00 – 18:00).

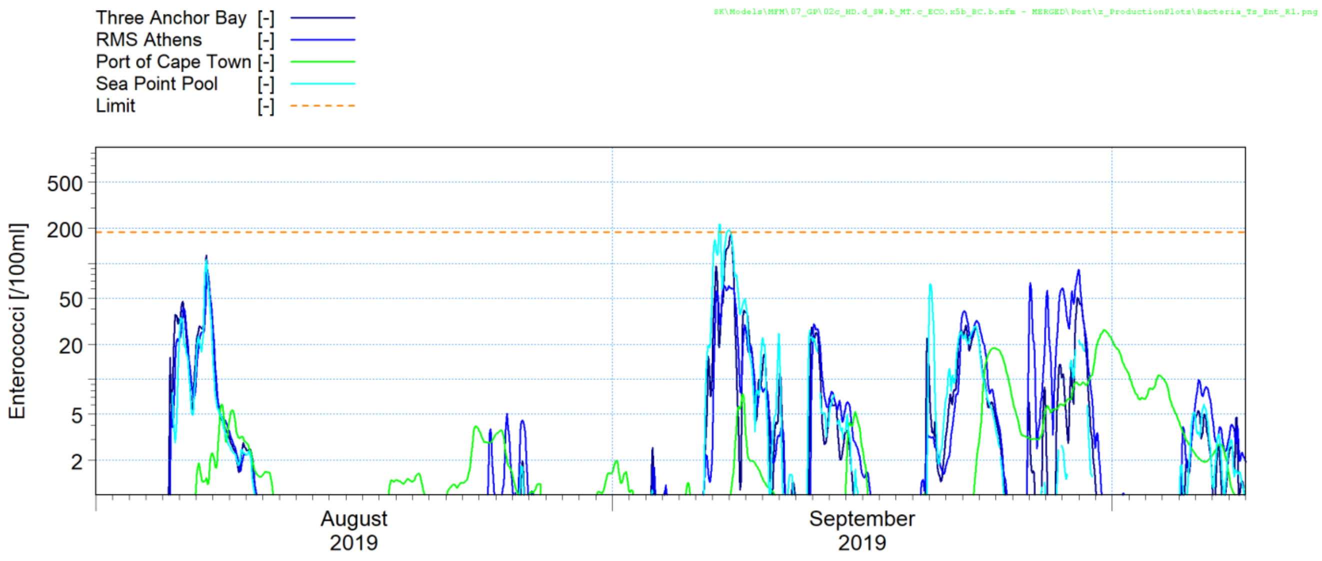

Figure 6-15: Winter/spring: Time series of highest enterococci concentration at any depth at four key locations. The water quality guideline (185 CFU/100 ml 90th percentile in daylight) is also shown in orange.

A mixing zone distance of 3 200 m was required to meet the 90th percentile water quality guideline of 185 CFU/100 ml. The contour plots show that the 90th percentile enterococci concentrations were the highest at mid-depth and concentrations above the 185 CFU/100 ml guideline did not intersect with the shoreline. The enterococci concentrations at the key locations only exceeded 185 CFU/100 ml on two occasions in the 10-week winter/spring period

6.1.3.3 Discussion

Based on the applicable water quality guidelines (discussed in Section 3.4.2), E.coli requires a greater mixing zone distance to meet the guidelines compared to enterococci.

The bacteria plumes have the highest concentrations at mid depth (the depth below the surface equal to 60% of the local water depth) where the plume usually becomes trapped. Solar radiation further reduces concentrations closer to the surface (illustrated in Figure 6-7).

During typical conditions the plume will be advected alongshore. Onshore movement can occur during certain north-westerly wind conditions (e.g. current direction reversal causing the plume to approach the coastline in the process) or during local upwelling events associated with south-westerly winds.

6.1.4 Total suspended solids

The concentrations of TSS were modelled in the water column and specifically where these were deposited on the seabed. This is a proxy for the fate of pollutants that adsorb to solid particles, e.g. heavy metals.

Figure 6-16 presents the bed mass of TSS at the end of the 10-week simulation. The deposited mass in the main depo-centres (demarcated in red) are summarised in Table 6-3. The table also includes the total mass of TSS that were advected outside of the model domain through the boundaries and TSS in suspension at the end of the run.

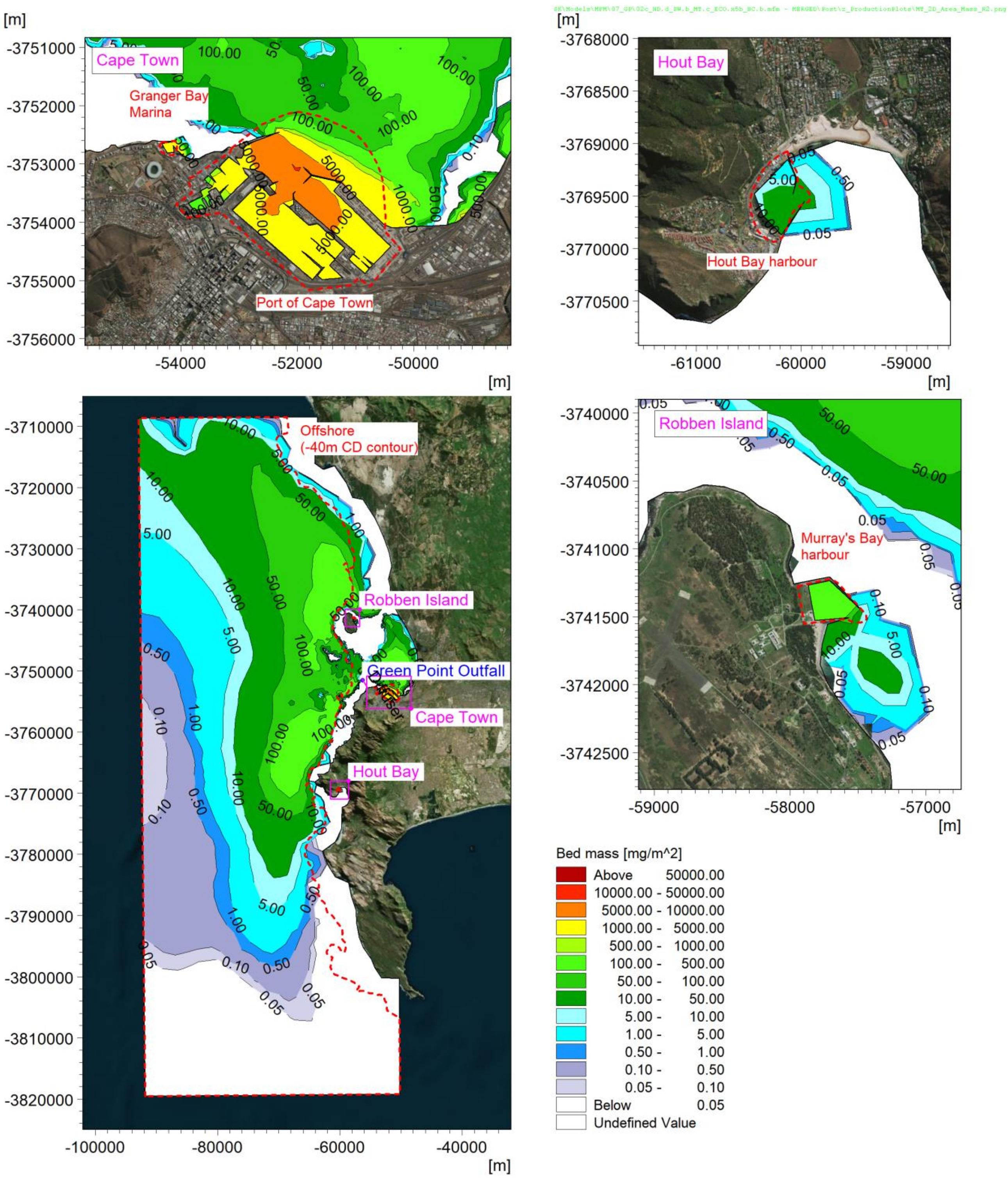

Figure 6-16: Winter/spring: Bed mass of TSS distribution at the end of the 10-week winter/spring period.

Table 6-3: Winter/spring: Integrated mass at the end of the 10-week simulation period.

Area	Mass [kg]	% released
Port of Cape Town	17 200	3.0%
Murray's Bay Harbour	24	< 0.1%
Granger Bay	69	< 0.1%
Hout Bay	1.9	< 0.1%
Offshore (-40 m CD contour)	74 500	12.8%
Out of domain	324 000	55.9%
Suspended	164 000	28.2%
Total mass released	**589 000**	**100%**

The highest concentrations are observed in the sheltered depo-centres, i.e. the Port of Cape Town, Granger Bay marina, Murray's Bay harbour and Hout Bay harbour where the bed shear stress due to waves and currents are sufficiently low to allow deposition. Accumulation also occurs in exposed areas where the water depth is greater than approximately 40 m due to the wave orbital velocities not exerting sufficient stress on the seabed to resuspend the sediment particles.

The largest depo-centre is the Port of Cape Town with approximately 3.0% of the TSS released from the Green Point outfall accumulating in the port. These results can be used in the design and interpretation of sediment quality sampling studies.

6.2 Summer/autumn

The outfall dispersion model was run for a 10-week period between 13 February 2020 and 23 April 2020, coinciding with the calibration period, to represent environmental conditions for summer and autumn.

The model outputs are the concentrations of E.coli, enterococci, TSS and a conservative tracer in each horizontal and vertical element of the computational mesh at 1-hour intervals throughout the simulation period.

6.2.1 Plume dynamics

Figure 6-17 and Figure 6-18 present examples of the current vectors and E.coli plume at a moment in time for a south-easterly and north-westerly wind condition. These results show the complex 3D dynamic behaviour of the plume.

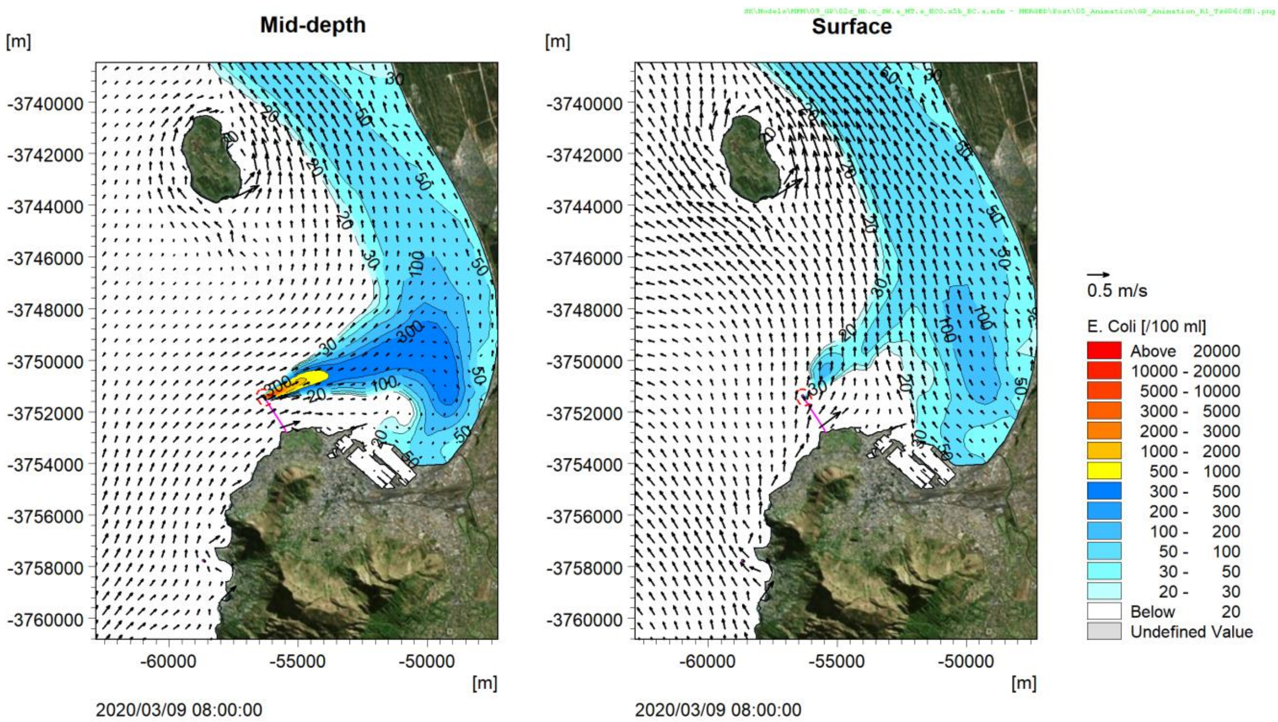

Figure 6-17: Summer/autumn: Current vectors and E.coli plume at a moment in time during a south-easterly wind condition.

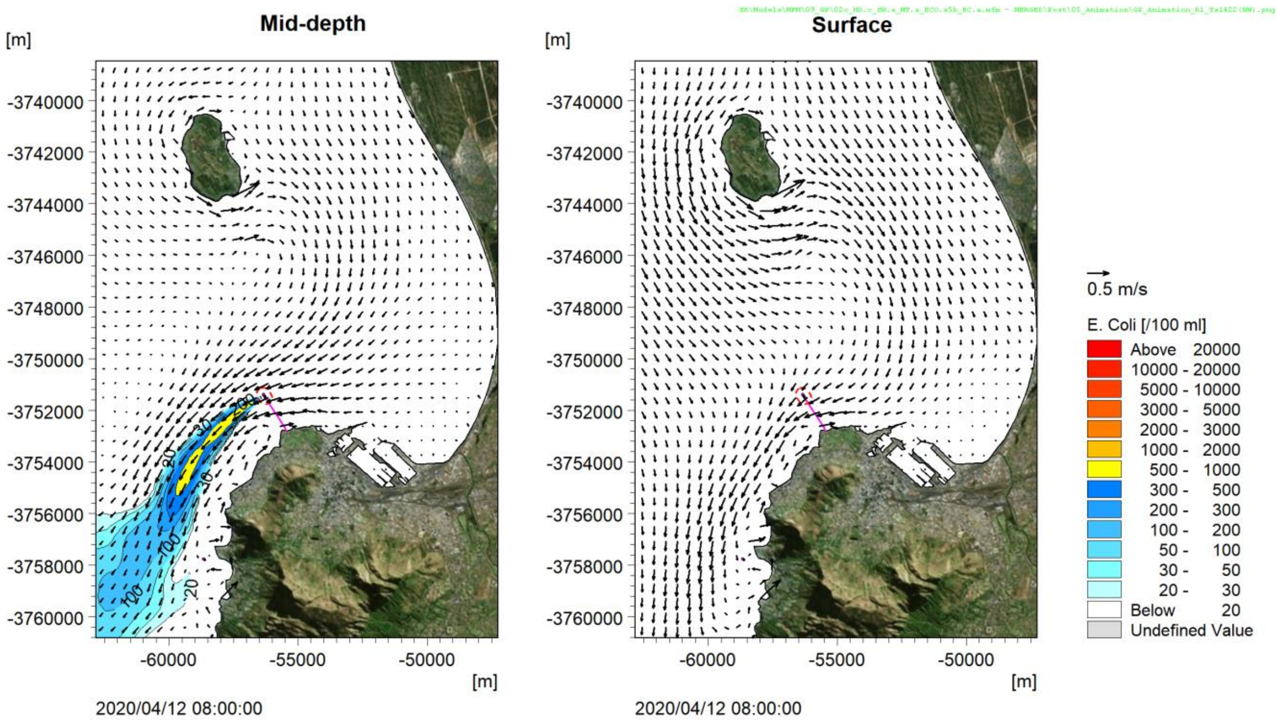

Figure 6-18: Summer/autumn: Current vectors and E.coli plume at a moment in time during a north-westerly wind condition.

6.2.2 Dilutions

The concentrations from the conservative tracer were processed to obtain the 5th percentile number of dilutions in each horizontal and vertical element of the computational mesh as discussed in Section 6.1.2.

Figure 6-19, Figure 6-20 and Figure 6-21 present the 5th percentile dilutions at the seabed, mid-depth and surface. Mid-depth is the depth below the surface equal to 55% of the local water depth, which was selected as the worst dilutions at Green Point occurred at this depth. Figure 6-19 shows a cross section of the 5th percentile number of dilutions extracted along the longest axis of the plume (marked by the dashed green line on the contour plots). Dilutions less than 2 000 are shown in orange as this is close to the dilution required for TSS of 1 753 as discussed in Section 3.4.1. Dilutions greater than 2 000 are shown in shades of blue. Although these exceed the required dilutions for the identified critical constituents, they provide information on the far-field behaviour of the plume.

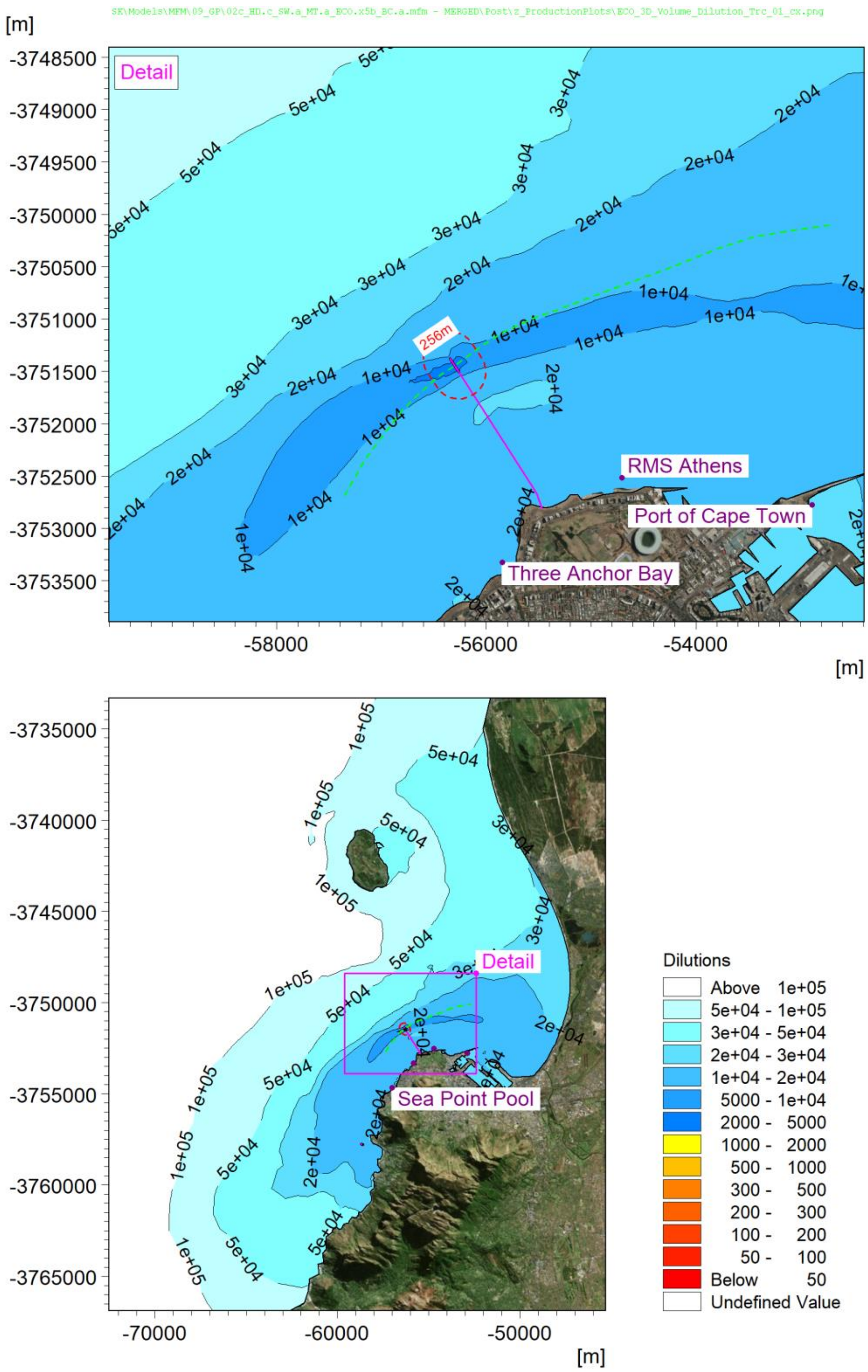

Figure 6-19: Summer/autumn: Number of dilutions at the seabed, 5th percentile.

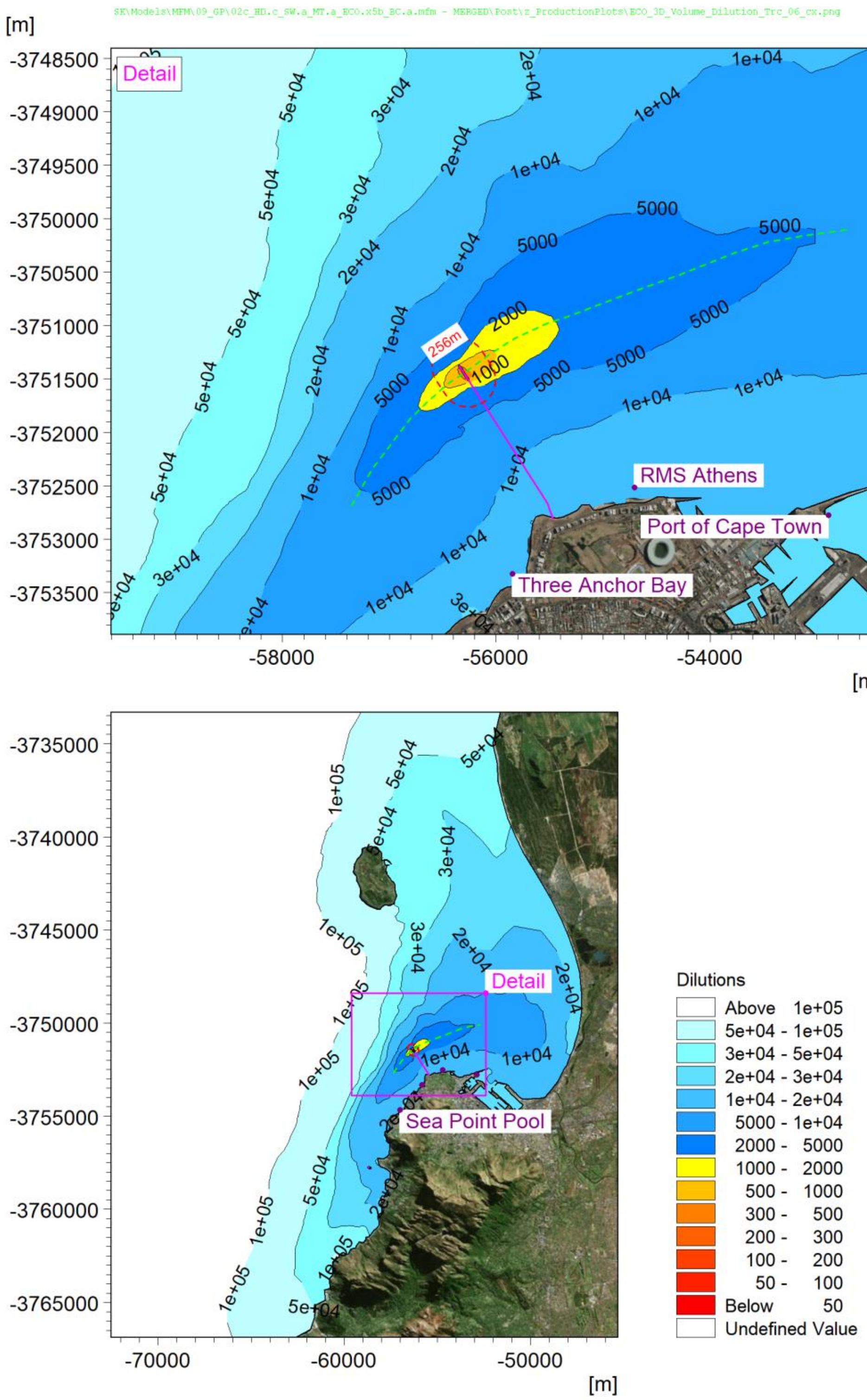

Figure 6-20: Summer/autumn: Number of dilutions at mid-depth, 5th percentile.

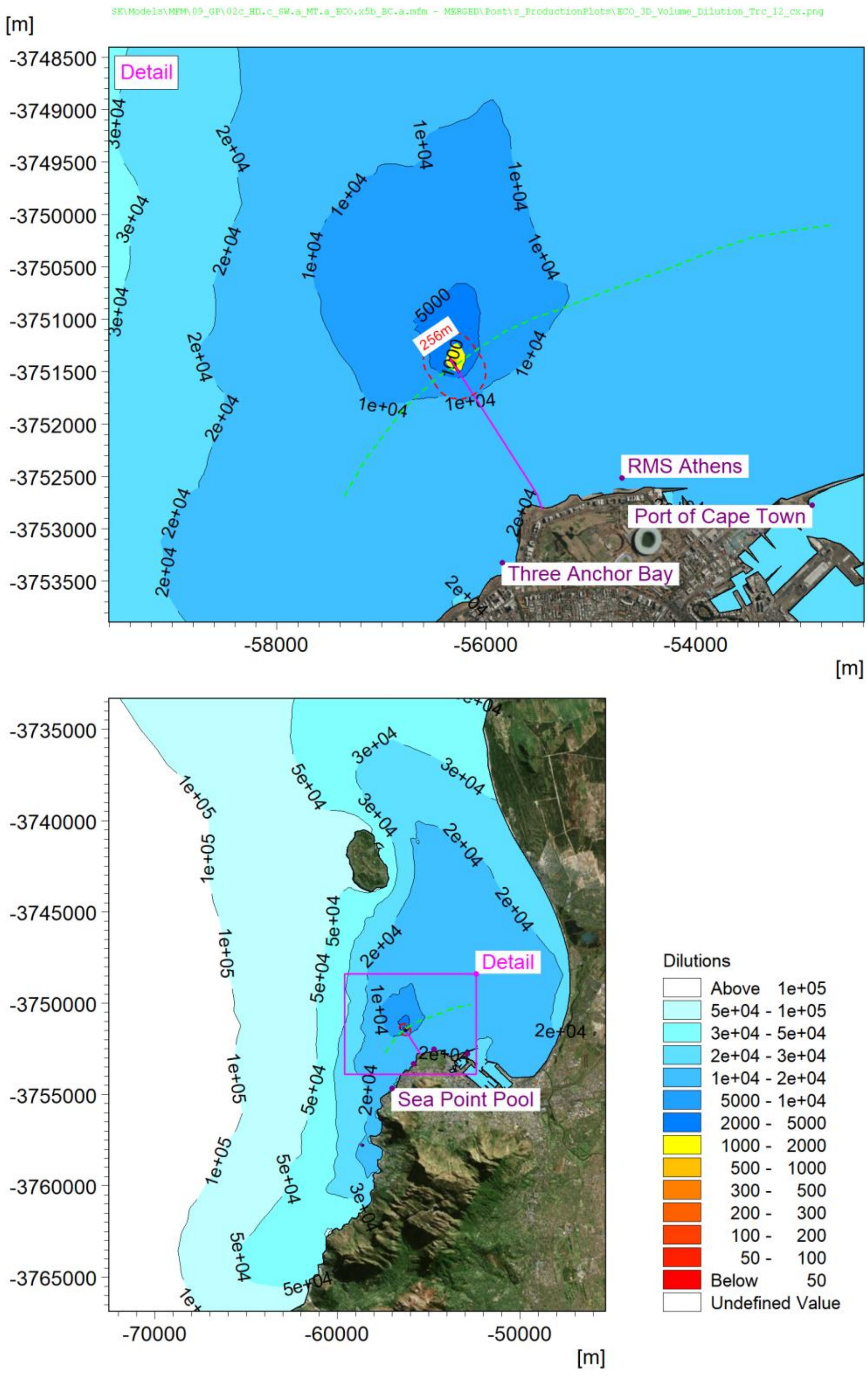

Figure 6-21: Summer/autumn: Number of dilutions at the surface, 5th percentile.

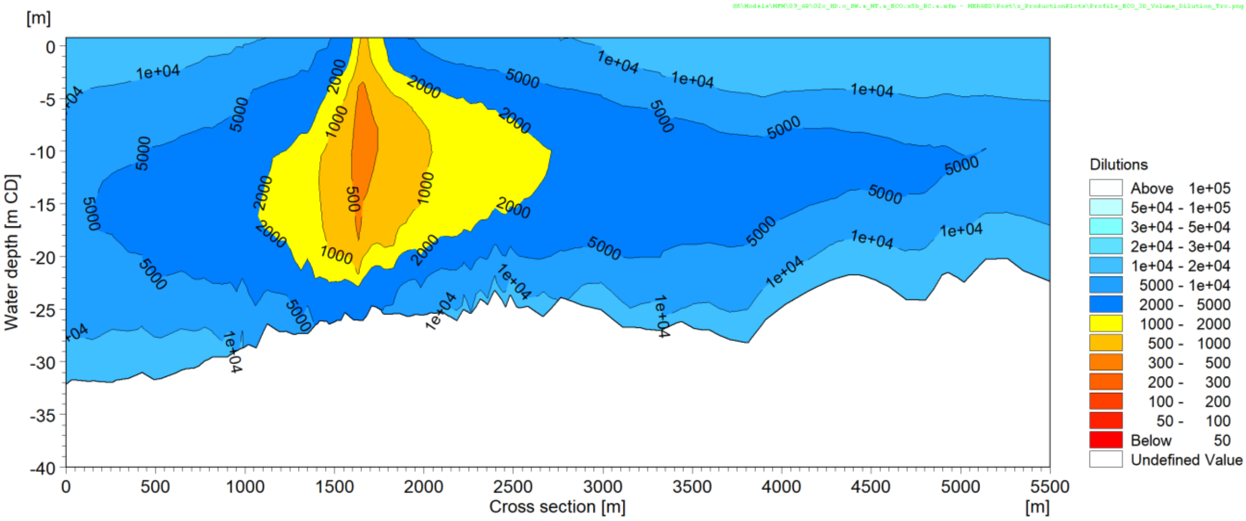

Figure 6-22: Summer/autumn: Cross-section of 5th percentile number of dilutions.

The minimum dilutions achieved at the edge of the mixing zone was extracted from the 5th percentile dilutions and is presented Table 6-4.

Table 6-4: Summer/autumn: Minimum number of dilutions achieved at the edge of the mixing zone.

Parameter	Value
Minimum number of dilutions achieved at any depth along the edge of the allowable mixing zone (radius = 256 m), 5th percentile	687

The distance from the diffuser to achieve the required dilutions for the three critical constituents (Table 3-4) are presented in Table 6-5.

Table 6-5: Summer/autumn: Distance to achieve dilutions, 5th percentile.

Constituent	Dilutions required	Distance
Ammonia	106	< 25 m
COD	51	< 25 m
TSS	1 753	940

The spreading of the mixing zone is dominated by the longshore currents. South-easterly winds, which are frequent in the summer, advect the plumes east into Table Bay and then northward with the longshore current. As observed in Section 6.1.2, the lowest dilutions are at mid-depth, due to mixing with the ambient currents or trapping by stratification. Periodic surfacing of the plume happens during periods of high effluent flows or stagnant hydrodynamic conditions

The minimum number of dilutions achieved in the allowable mixing zone is 687. The constituent requiring the highest dilutions is TSS, which achieved the 1 753 required dilutions 940 m from the diffuser. Ammonia and COD achieved the required dilutions in within 25 m. Note that distances smaller than 25 m could not be measured in the model, due to the mesh resolution.

6.2.3 Bacteria

In addition to dilutions by hydrodynamic processes the bacterial concentrations are further reduced due to bacterial die-off (as described in Section 2.3.2). Figure 6-23 presents the surface and seabed T_{90} values for

E.coli and enterococci, extracted in the middle of the Green Point diffuser at a depth of -26.0 m CD. Recall from Section 2.3.2.1 the median T_{90} ratio of enterococci to E.coli is 2.39.

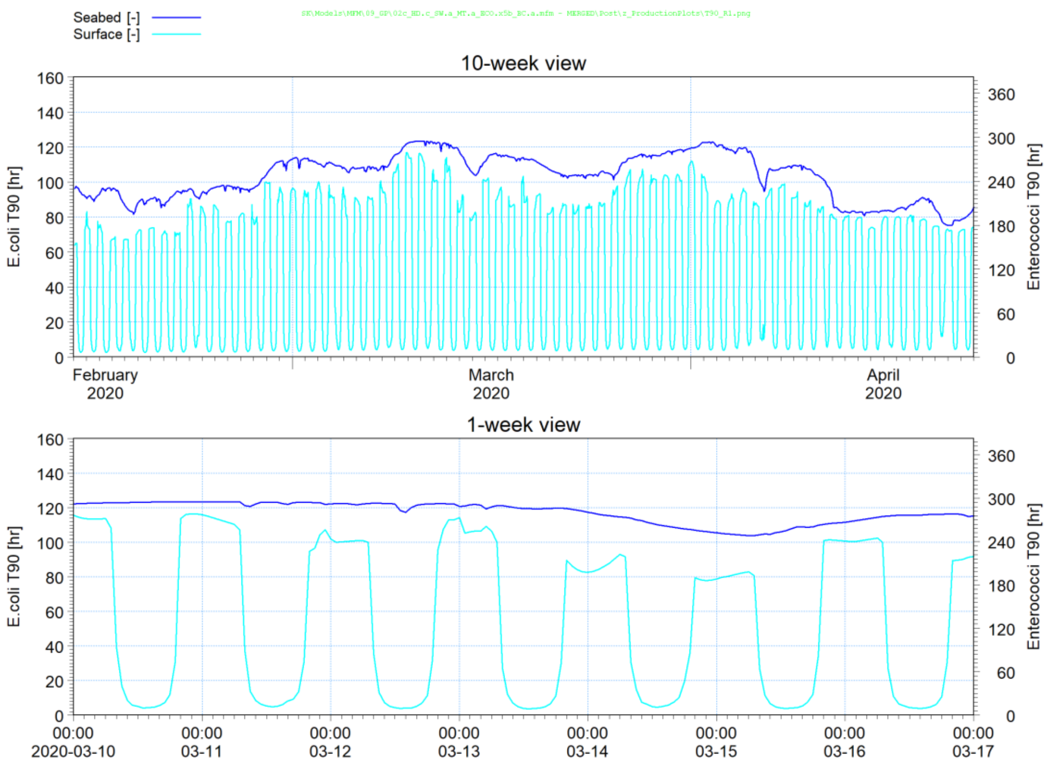

Figure 6-23: Summer/autumn: Surface and seabed T_{90} values for E.coli and enterococci.

A significant diurnal variation in die-off rates due to the solar radiation can be observed at the surface, while the seabed remains mostly unaffected due to light attenuation. In the absence of light, the seawater temperature dominates the die-off processes and the stratification determines the gradient between the surface and seabed T_{90} values.

The model outputs of bacterial concentrations were processed to extract the 90th percentile during daylight hours (between 07:00 to 18:00) to emulate the recommended microbiological sampling regime in the guidelines.

6.2.3.1 E.coli

Figure 6-24, Figure 6-25 and Figure 6-26 present the 90th percentile E.coli concentrations at the seabed, mid-depth and surface. Concentrations greater than 500 CFU/100 ml are shown in orange as this is the guideline for E.coli as discussed in Section 3.4.2. Concentrations less than 500 CFU/100 ml are shown in shades of blue. Although these are less than the guideline, they provide information on the far-field behaviour of the plume. A time series of highest E.coli concentrations at any depth at four key locations (Port of Cape Town, RMS Athens wreck (Thermopylae surf spot), Three Anchor Bay and Sea Point Pool) is shown in Figure 6-27. The locations are shown in the contour plots.

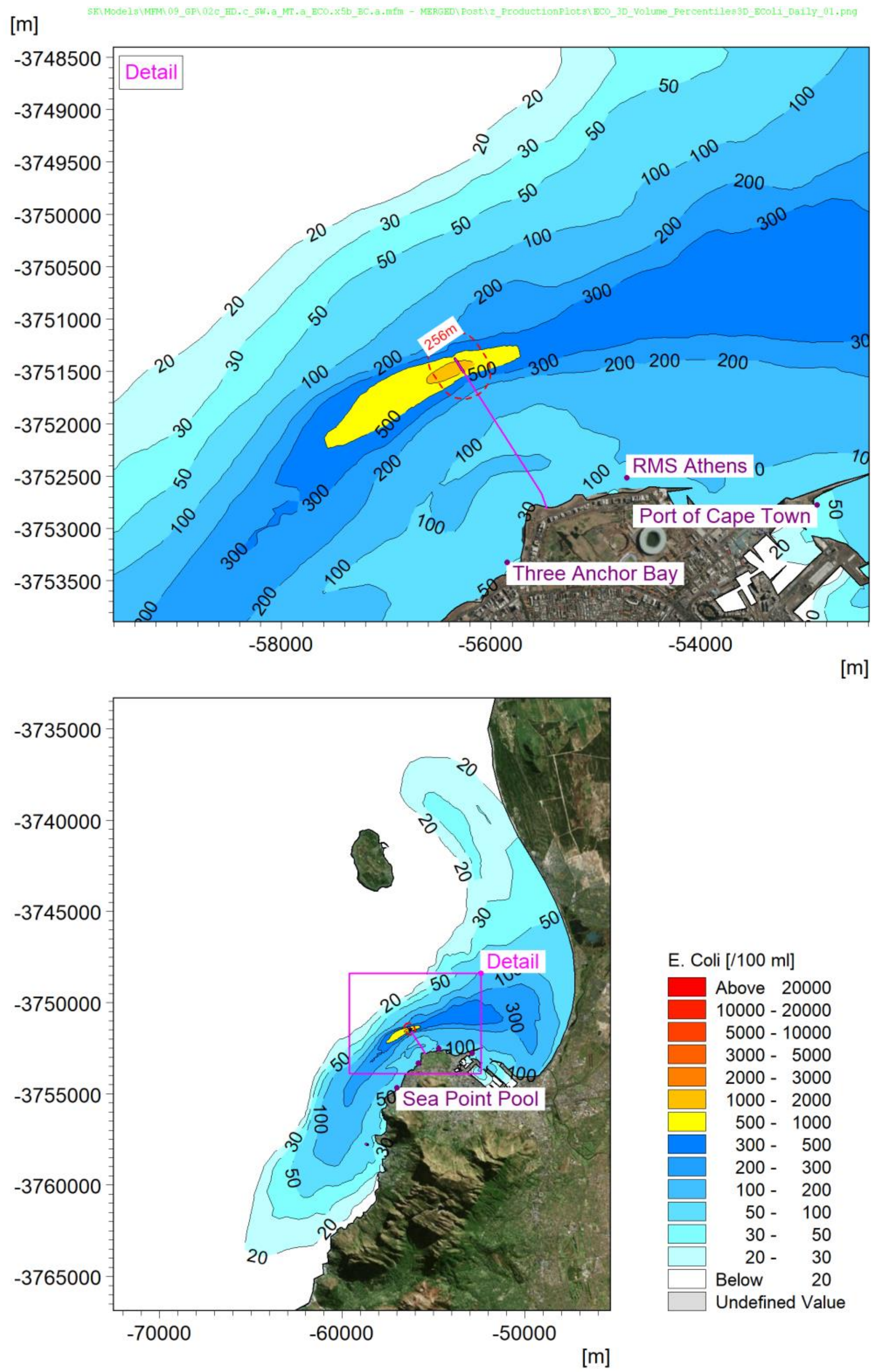

Figure 6-24: Summer/autumn: E.coli concentration at the seabed, 90th percentile for daylight hours (07:00 – 18:00).

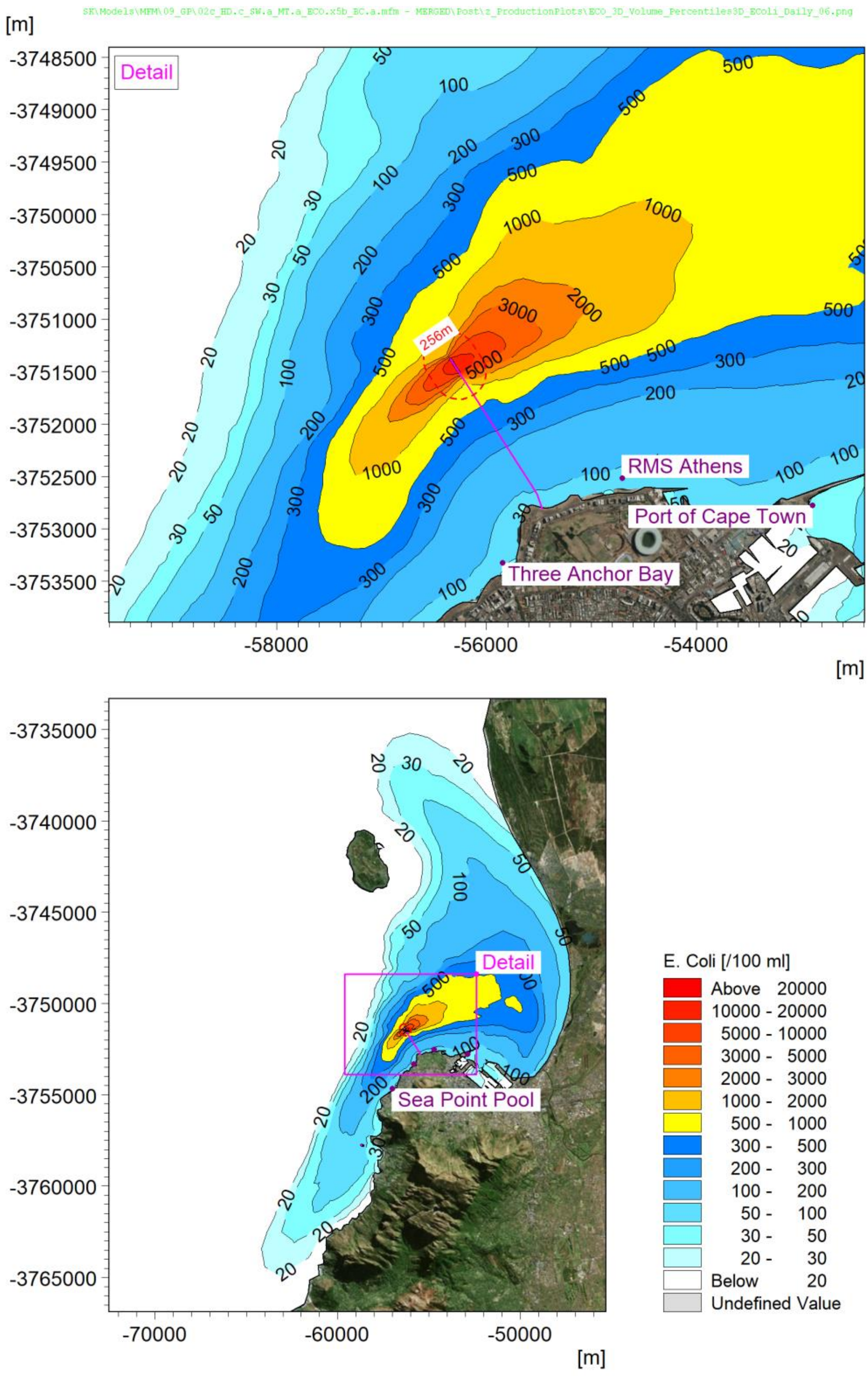

Figure 6-25: Summer/autumn: E.coli concentration at mid-depth, 90th percentile for daylight hours (07:00 – 18:00).

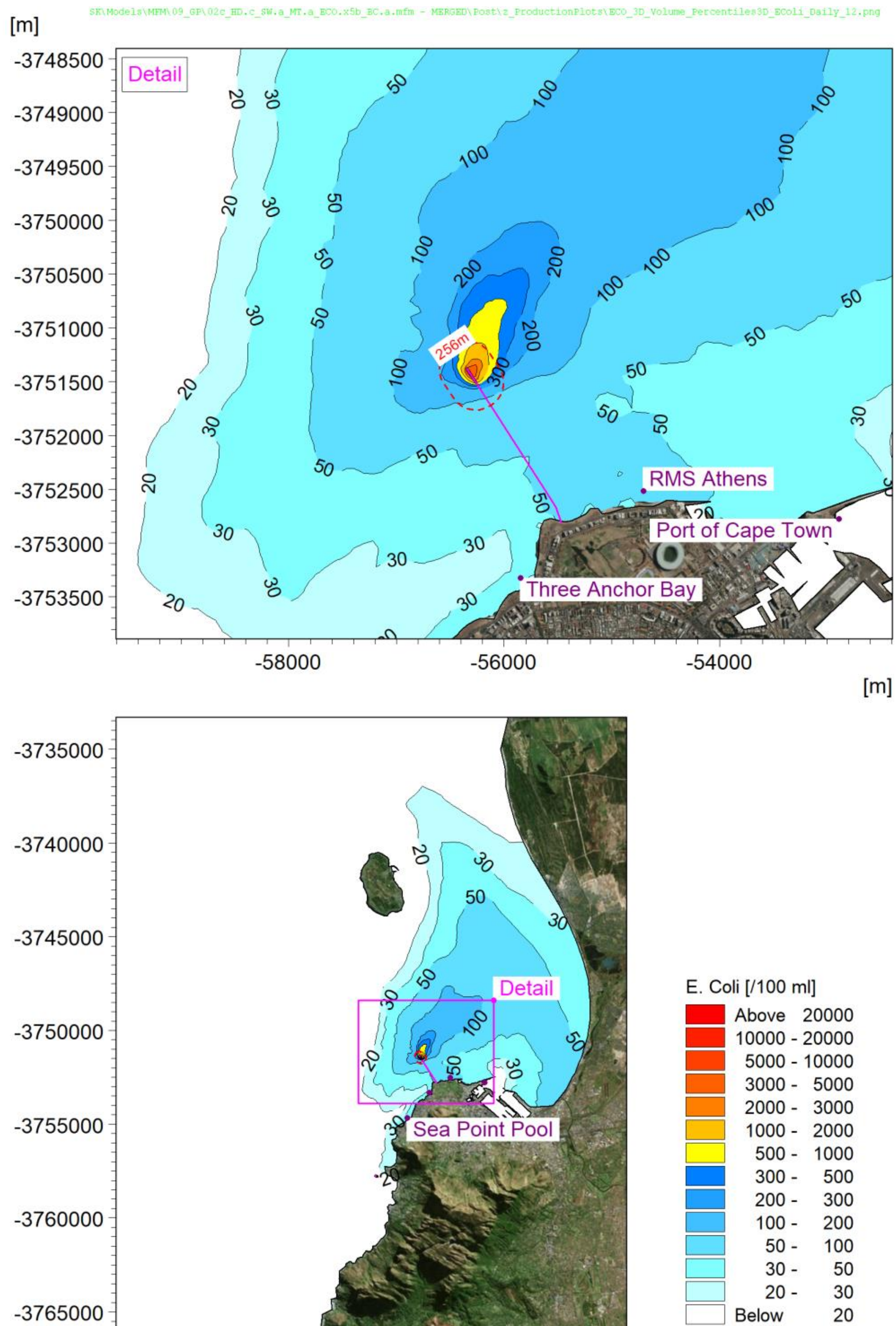

Figure 6-26: Summer/autumn: E.coli concentration at the surface, 90th percentile for daylight hours (07:00 – 18:00).

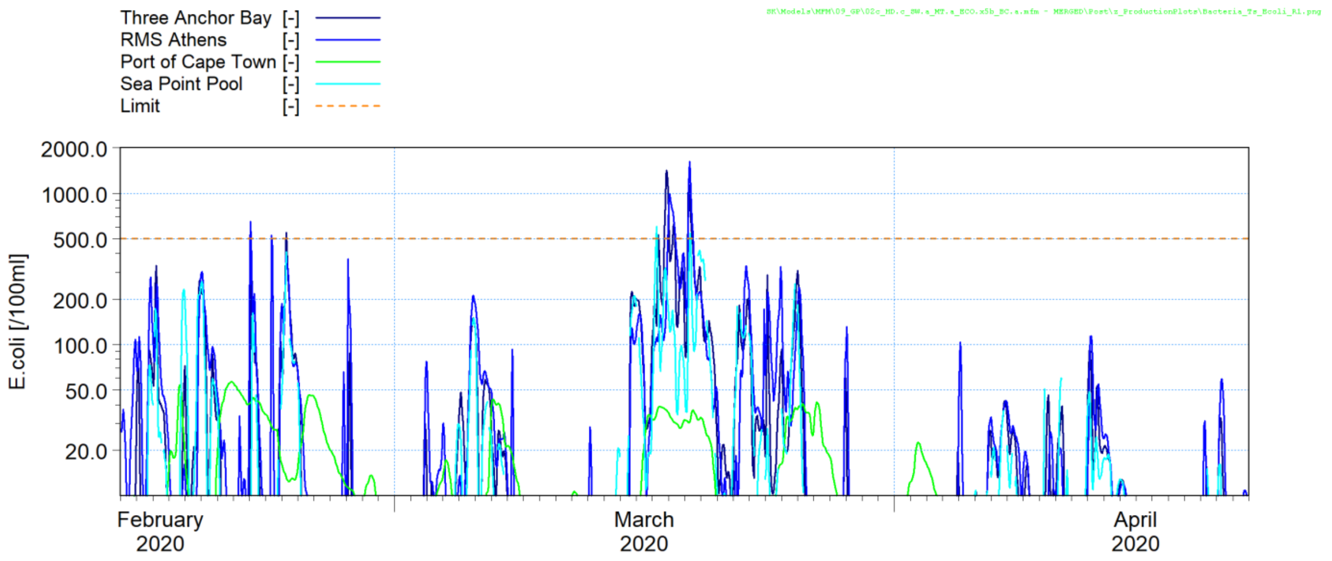

Figure 6-27: Summer/autumn: Time series of highest E.coli concentration at any depth at four key locations. The water quality guideline (500 CFU/100 ml 90th percentile in daylight) is also shown in orange.

A mixing zone distance of 6 600 m was required to meet the 90th percentile water quality guideline of 500 CFU/100 ml. The contour plots show that the 90th percentile E.coli concentrations were the highest at mid-depth and concentrations above the 500 CFU/100 ml guideline did not intersect with the shoreline. Locations such as Three Anchor Bay, RMS Athens (Thermopylae surf spot) and the Sea Point Pool were briefly exposed to E.coli concentrations above 500 CFU/100 ml on a number of occasions. Since the duration of these events was less than 10% of the daylight time these locations met the water quality guidelines.

6.2.3.2 Enterococci

Figure 6-28, Figure 6-29 and Figure 6-30 present the 90th percentile enterococci concentrations at the seabed, mid-depth and surface. Concentrations greater than 185 CFU/100 ml are shown in orange as this is the guideline for enterococci as discussed in Section 3.4.2. Concentrations less than 185 CFU/100 ml are shown in shades of blue. Although these are less than the guideline, they provide information on the far-field behaviour of the plume. A time series of enterococci concentrations at four key locations is shown in Figure 6-31.

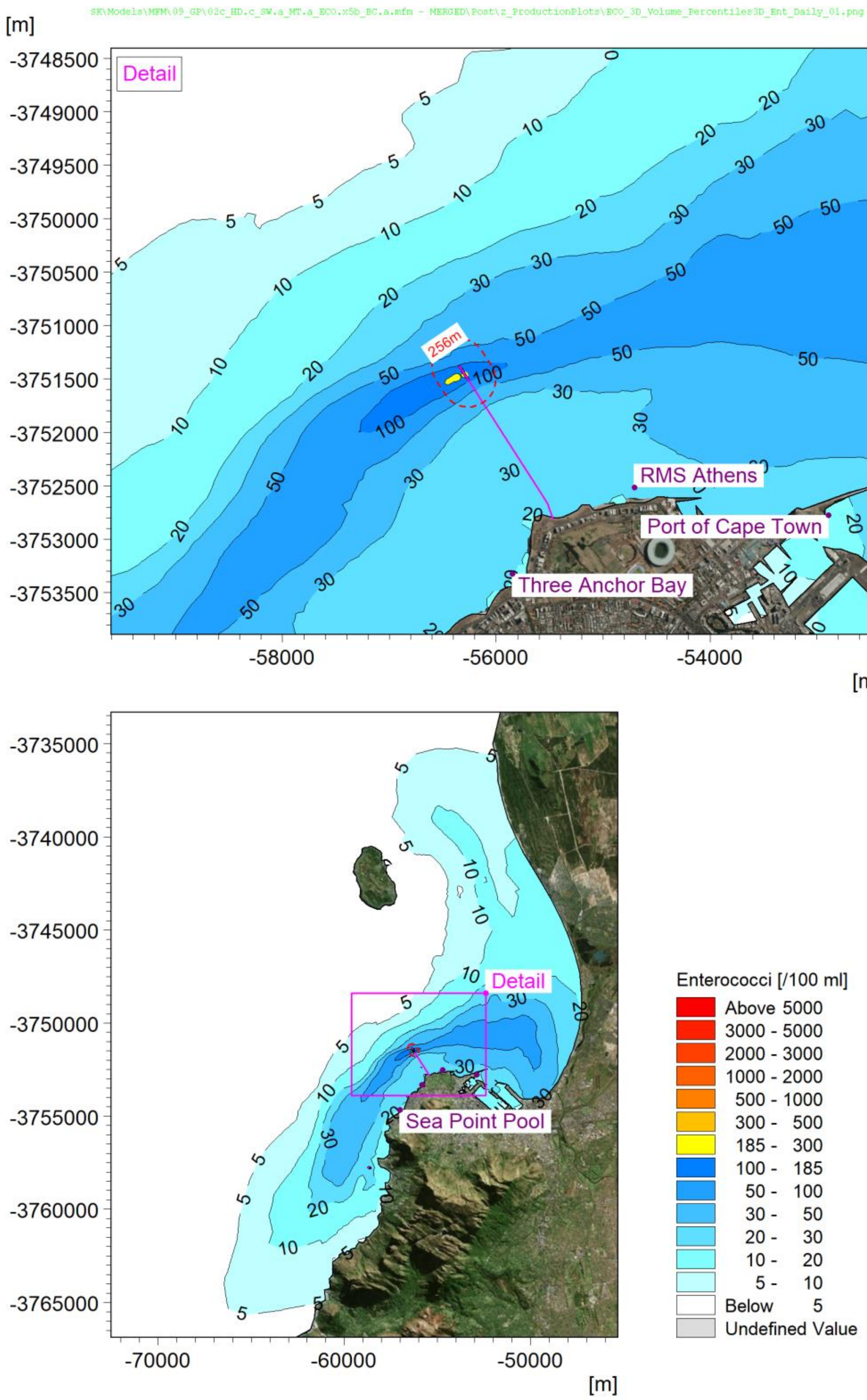

Figure 6-28: Summer/autumn: Enterococci concentration at the seabed, 90th percentile for daylight hours (07:00 – 18:00).

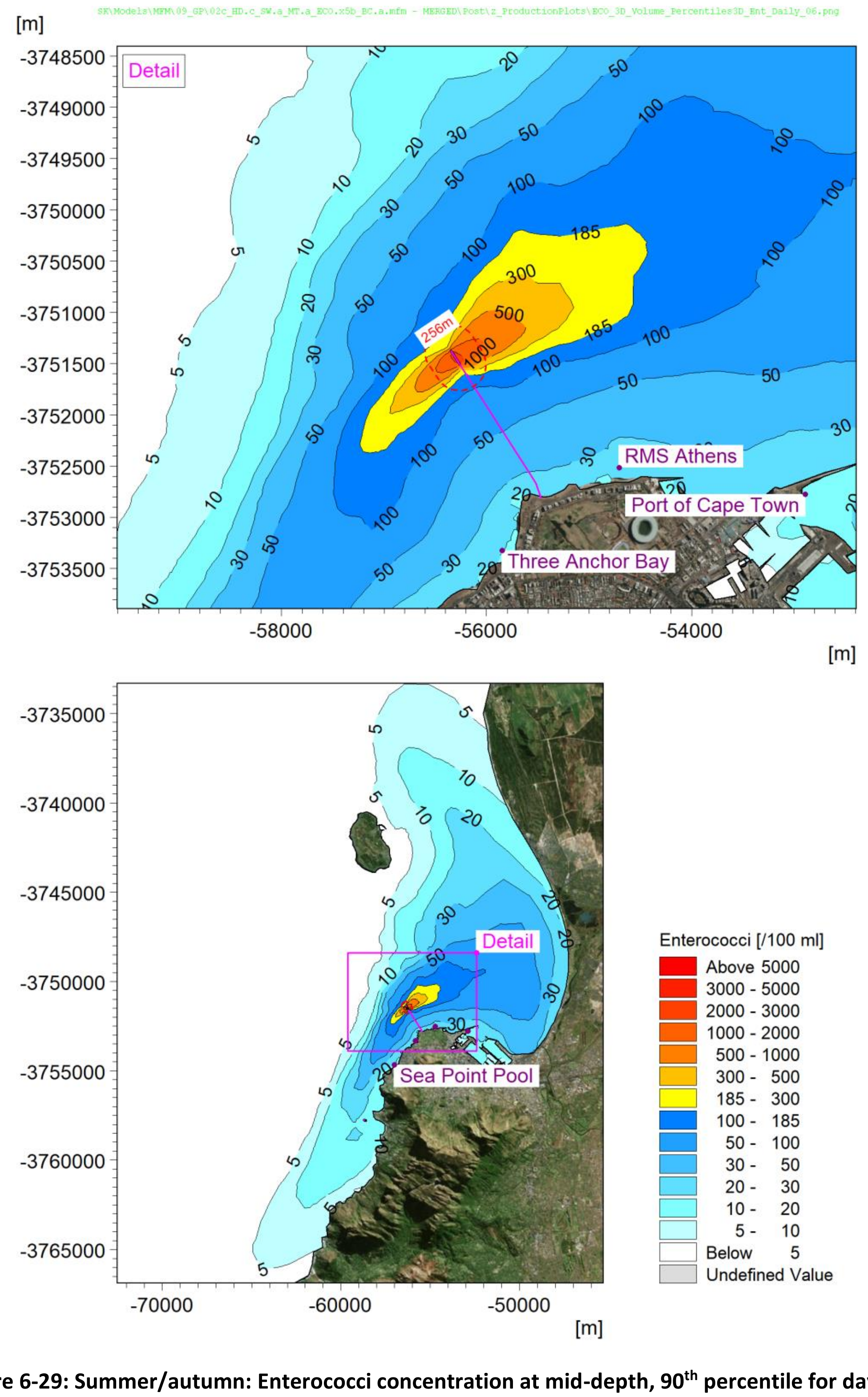

Figure 6-29: Summer/autumn: Enterococci concentration at mid-depth, 90th percentile for daylight hours (07:00 – 18:00).

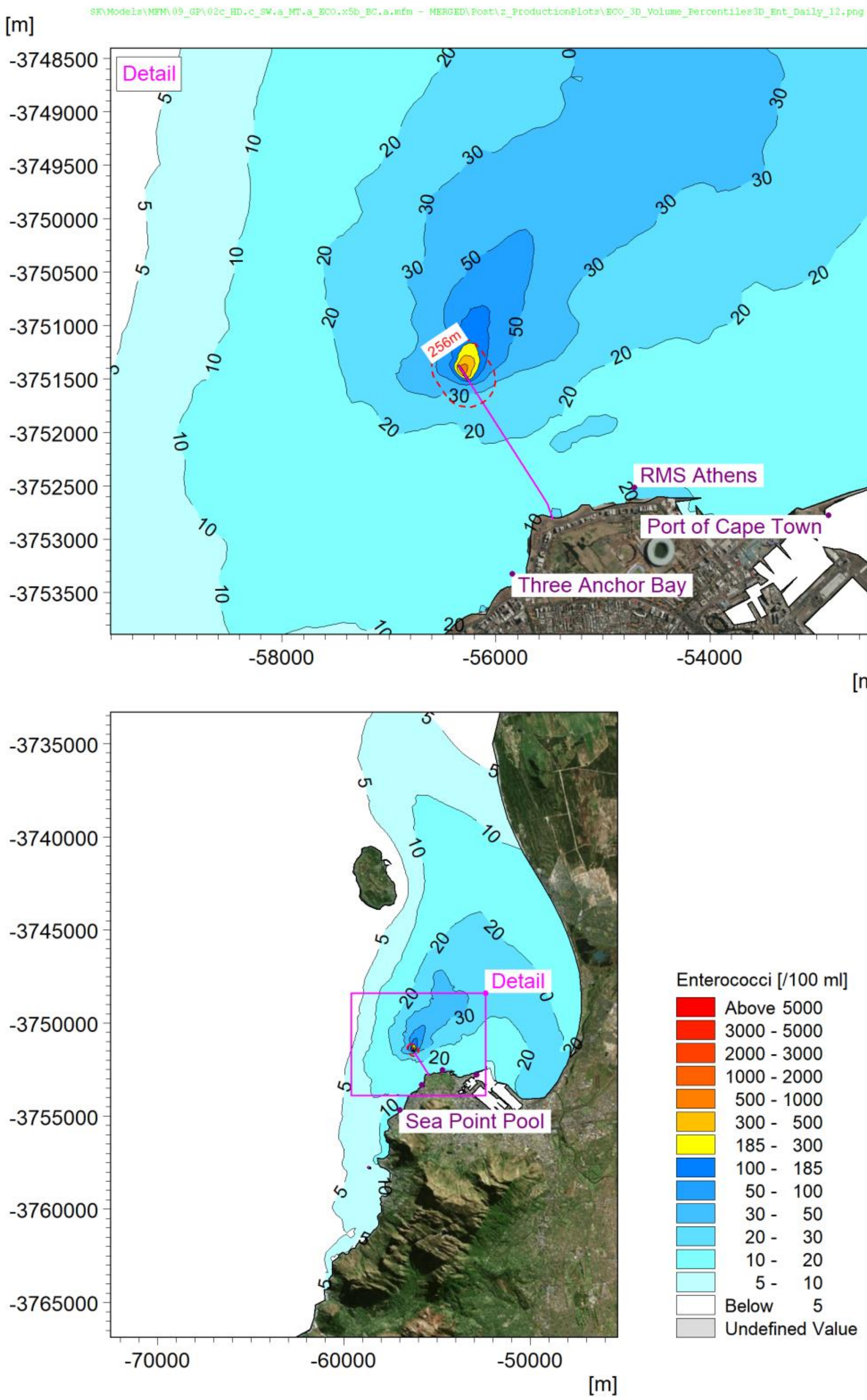

Figure 6-30; Summer/autumn: Enterococci concentration at the surface, 90th percentile for daylight hours (07:00 – 18:00).

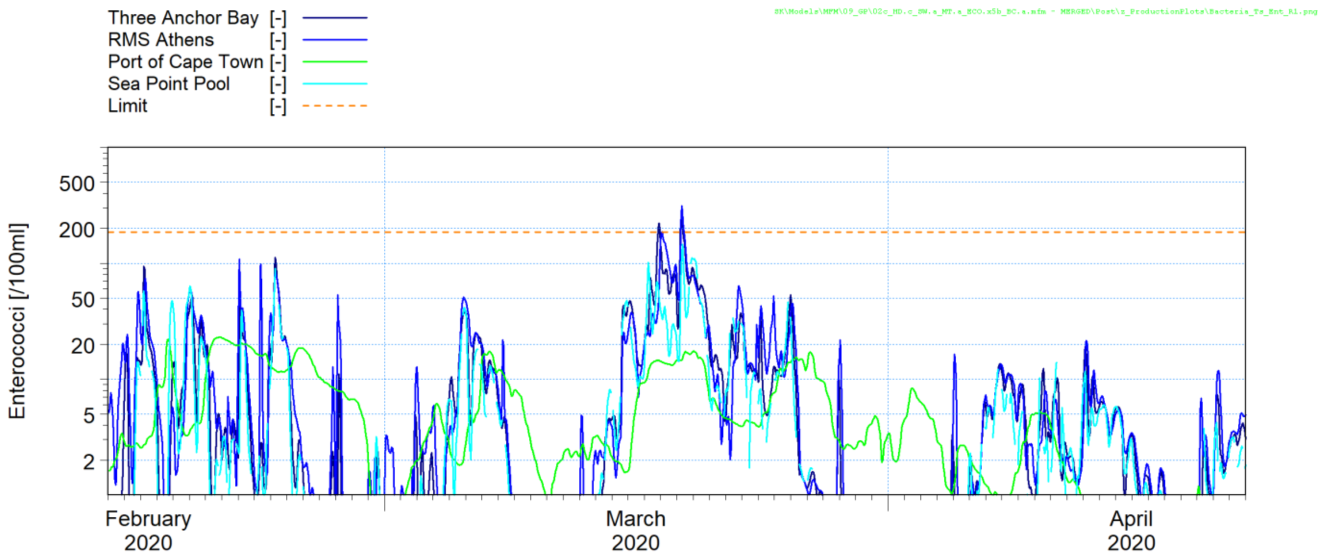

Figure 6-31: Summer/autumn: Time series of highest enterococci concentration at any depth at four key locations. The water quality guideline (185 CFU/100 ml 90th percentile in daylight) is also shown in orange.

A mixing zone distance of 2 300 m was required to meet the 90th percentile water quality guideline of 185 CFU/100 ml. The contour plots show that the 90th percentile enterococci concentrations were the highest at mid-depth and concentrations above the 185 CFU/100 ml guideline did not intersect with the shoreline. The enterococci concentrations at the key locations only exceeded 185 CFU/100 ml on two occasions in the 10-week summer/autumn period

6.2.3.3 Discussion

Based on the applicable water quality guidelines (discussed in Section 3.4.2), E.coli requires a greater mixing zone distance to meet the guidelines compared to enterococci.

The bacteria plumes have the highest concentrations at mid depth (the depth below the surface equal to 55% of the local water depth) where the plume usually becomes trapped. Solar radiation further reduces concentrations closer to the surface (illustrated in Figure 6-7).

During typical conditions the plume will be advected alongshore. South-westerly winds advects the bacteria plumes east into Table Bay but the processes of dispersion and bacteria die-off reduces the bacteria concentrations to below the applicable water quality guidelines before the plumes reach the shore in Table Bay. As discussed in Section 6.1.3.3, onshore movement usually occurs during certain north-westerly wind conditions or local upwelling events associated with south-westerly winds.

6.2.4 Total suspended solids

The concentrations of TSS were modelled in the water column and specifically where these were deposited on the seabed. This is a proxy for the fate of pollutants that adsorb to solid particles, e.g. heavy metals.

Figure 6-32 presents the bed mass of TSS at the end of the 10-week simulation. The deposited mass in the main depo-centres (demarcated in red) are summarised in Table 6-6. The table also includes the total mass of TSS that were advected outside of the model domain through the boundaries and TSS in suspension at the end of the run.

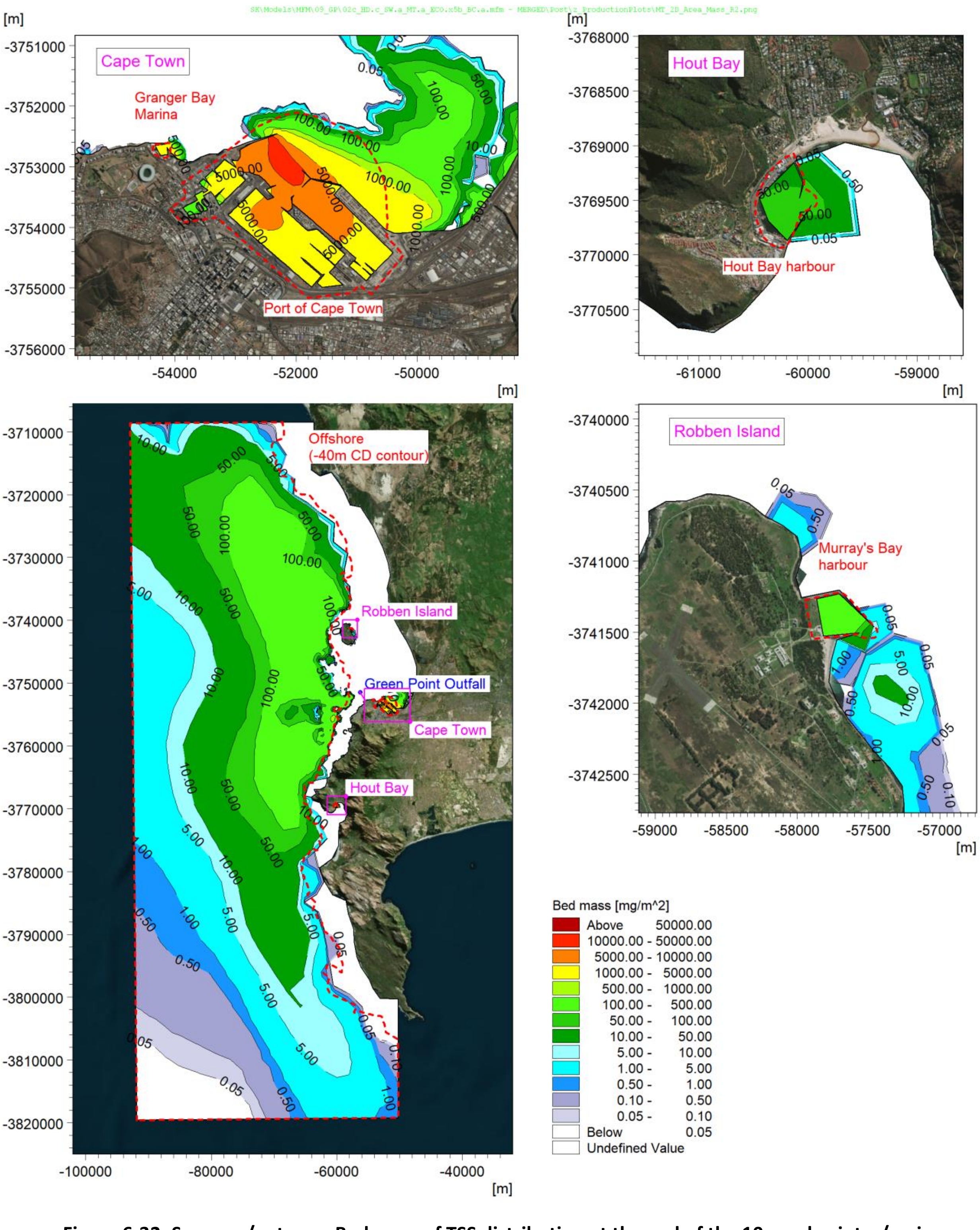

Figure 6-32: Summer/autumn: Bed mass of TSS distribution at the end of the 10-week winter/spring period.

Table 6-6: Summer/autumn: Integrated mass at the end of the 10-week simulation period.

Area	Mass [kg]	% released
Port of Cape Town	25 100	5.0%
Murray's Bay Harbour	23.6	< 0.1%
Granger Bay	107	< 0.1%
Hout Bay	11.8	< 0.1%
Offshore (-40 m CD contour)	141 000	28.1%
Out of domain	263 000	52.5%
Suspended	71 800	14.3%
Total mass released	**500 000**	**100%**

The highest concentrations are observed in the sheltered depo-centres, i.e. the Port of Cape Town, Granger Bay marina, Murray's Bay harbour and Hout Bay harbour where the bed shear stress due to waves and currents are sufficiently low to allow deposition. Accumulation also occurs in exposed areas where the water depth is greater than approximately 40 m due to the wave orbital velocities not exerting sufficient stress on the seabed to resuspend the sediment particles.

The largest depo-centre is the Port of Cape Town with approximately 5.0% of the TSS released from the Green Point outfall accumulating in the port. These results can be used in the design and interpretation of sediment quality sampling studies.

7. CONCLUSIONS

A 3D coupled near- and far-field hydrodynamic, water quality, suspended sediment and wave model has been set up for the Green Point outfall.

The model has been calibrated against wave, water level, current and seawater temperature measurements for a 6-week winter/spring period and a 10-week summer/autumn period.

The plume dispersion was then simulated for a 10-week winter/spring period and a 10-week summer/autumn period. The model results show the following:

- The plume has the lowest dilutions and highest bacteria concentrations at mid depth (the depth below the surface between 55% and 60% of the local water depth) where the plume usually becomes trapped.
- During typical conditions the plume will be advected alongshore. South-easterly winds, which are frequent in the summer, advect the bacteria plumes eastwards into Table Bay. Onshore movement can occur during certain north-westerly wind conditions (e.g. current direction reversal causing the plume to approach the coastline in the process) or during local upwelling events associated with south-westerly winds.
- The minimum number of dilutions achieved at the edge of the 256 m radius mixing zone is 528 in winter/spring and 687 in summer/autumn (5th percentile dilution).
- The required dilution of 1 753 for TSS is met at distance of 1 400 m from the diffuser in winter/spring and 940 m in summer/autumn (5th percentile dilution).
- E.coli requires a distance of 6 300 m to meet the applied guidelines in winter/spring and 6 600 m in summer/autumn (500 CFU/100 ml for the 90th percentile concentration during daylight hours).
- Locations such as Three Anchor Bay and the Sea Point Pool are briefly exposed to E.coli concentrations above 500 CFU/100 ml on two occasions in winter/spring. Three Anchor Bay, RMS Athens (Thermopylae surf spot) and the Sea Point Pool are briefly exposed to E.coli concentrations above 500 CFU/100 ml on a few occasions in summer/autumn. However, the cumulative duration of these events is less than 10% of the daylight time and the applied water quality guidelines are thus met at all locations along the shoreline (500 CFU/100 ml for the 90th percentile concentration during daylight hours).
- The applied guidelines for enterococci result in a smaller zone of impact compared to E.Coli.
- The largest depo-centre is the Port of Cape Town with approximately 3.0% of the Total Suspended Solids released from the Green Point outfall accumulating in the port in winter/spring and 5.0% in summer/autumn.

8. RECOMMENDATIONS

Based on the model results the following recommendations are made:

- Compared to Camps Bay and Hout Bay, the Green Point outfall has significantly lower dilutions due to the larger discharge rate. An assessment should be made on how future increases in discharge rate will further reduce the dilutions and increase the bacterial concentrations at Green Point.
- These results assume that the pipeline and diffusers are operating as designed and that there are no breakages, leaks or blockages. Regular underwater surveys are recommended to ensure that this is the case.
- Consideration should be given to operationalising the model to provide forecasts of bathing water quality, as is done in other countries including Denmark, Sweden and New Zealand, e.g. http://newkbh.badevand.dk. The forecast would identify one or two days in advance the occasions when the effluent plume is likely to reach specific bathing beaches or surf spots, which would facilitate mitigation of the associated risks to the public.

9. REFERENCES

Bellair, J. T., Parr-Smith, G. A. & Wallis, I. G., 1977. Significance of Diurnal Variations in Fecal Coliform Die-Off Rates in the Design of Ocean Outfalls. *Water Pollution Control Federation (Fiftieth Annual Conference),* 49(9), pp. 2022-2030.

Choi, K. & Lee, J., 2007. Distributed Entrainment Sink Approach for Modeling Mixing and Transport in the Intermediate Field.. *J. Hydraulic Eng.,* 133(7), pp. 805-815.

CSIR, 1992. *Guide for the Marine Disposal of Effluents through Pipelines,* Cape Town, South Africa: Council for Scientific and Industrial Research.

CSIR, 2017. *Cape Town Outfalls Monitoring Programme. Technical report for surveys made in 2015/2016.,* Cape Town, South Africa: Council for Scientific and Industrial Research.

DEA, 2012. *South African Water Quality Guidelines for Coastal Marine Waters. Volume 2: Guidelines for Recreational Use.,* Cape Town, South Africa: Departmet of Environmental Affairs: Republic of South Africa.

DHI, 2020a. *MIKE by DHI Flow Flexible Mesh Model, User Guide,* Copehagen, Denmark: Danish Hydraulics Institute.

DHI, 2020b. *MIKE by DHI Flow Flexible Mesh, Scientific Documentation,* Copenhagen, Denmark: Danish Hydraulics Institute.

DHI, 2020c. *MIKE by DHI ECOLAB, User Guide,* Copenhagen: Danish Hydraulics Institute.

DHI, 2020d. *MIKE by DHI ECOLAB, Scientific Documentation,* Copenhagen: Danish Hydraulics Institute.

DHI, 2020e. *MIKE 21 & MIKE 3 Flow Model FM, Mud Transport Module, User Guide,* Copenhagen, Denmark: Danish Hydraulics Institute.

DHI, 2020f. *MIKE 21 & MIKE 3 Flow Model FM, Mud Transport Module, Scientific Documentation,* Copenhagen, Denmark: Danish Hydraulics Institute.

DHI, 2020g. *MIKE 21, Spectral Waves FM Module, User Guide,* Copenhagen, Denmark: Danish Hydraulics Institute.

DHI, 2020h. *MIKE 21, Spectral Waves FM Module, Scientific Documentation,* Copenhagen, Denmark: Danishn Hydraulics Institute.

DHI, 2020i. *MIKE C-MAP, Extraction of World Wide Bathymetry Data and Tidal Information, User Guide,* Copenhagen, Denmark: Danish Hydraulics Institute..

DTU, 2010. *Improvement in global ocean tide model in shallow water regions,* Copenhagen, Denmark: Technical University of Denmark.

ECMWF, 2020. *European Centre for Medium-Range Weather Forecasts: ERA5.* [Online]
Available at: https://confluence.ecmwf.int/display/CKB/ERA5+data+documentation
[Accessed October 2020].

Erichsen, A. et al., 2006. *Implementation and description of different early warning systems for bathing water quality, Danish EPA, Miljøprojekt Nr. 1101 (in Danish),* Copenhagen, Denmark: Danish Hydraulic Institute.

HYCOM, 2020. *Hybrid Coordinate Ocean Model.* [Online]
Available at: https://tds.hycom.org/thredds/catalogs/GLBy0.08/expt_93.0.html
[Accessed 2020].

Jensen, M., 1990. *Estimation of E.coli decay from light, temperature and salinity. (in Danish),* s.l.: Isotopcentralen/ATV.

Jirka, G., 2004. Integral Model for Turbulent Buoyant Jets in Unbounded Stratified Flows. Part I: Single Round Jet.. *Environmental Fluid Mechanics,* Volume 4, pp. 1-56.

Kay, D. et al., 2008. Faecal indicator organism concentrations in sewage and treated effluents. *Water Research,* Volume 42, pp. 442-454.

Livingstone, D., Calder, M. & Connell, A., 1990. *Observations on the culturability of Coliforms and Escherichia coli I following exposure to natural seawater. WRC Report No. 214/1/90.,* s.l.: Water Research Commission.

NCEP, 2020. *National Weather Service Environmental Modeling Centre.* [Online]
Available at: http://polar.ncep.noaa.gov
[Accessed 2020].

PRDW, 2017. *Koeberg Nuclear Power Station: Coastal Processes Technical Information In Support Of The Coastal Waters Discharge Permit Application: Dispersion Modelling of Thermal, Chemical, Sediment and Radionuclide Discharges. Report No. S2015-RP-CE-001-R5,* Cape Town, South Africa: PRDW.

Sinton, L., Davies-Colley, R. & Bell, R., 1994. Inactivation of Enterococci and fecal coliforms from sewage and meatworks effluents in seawater chambers. *Applied and Environmental Microbiology,* 60(6), pp. 2040-2048.